Spring 2012

# Applying GIS Metrics to Determine Degree of Glacial Modification in Mountainous Landscapes

Carl Delbert Swanson II
*Central Washington University*

# APPLYING GIS METRICS TO DETERMINE DEGREE OF GLACIAL MODIFICATION IN MOUNTAINOUS LANDSCAPES

---

A Thesis

Presented to

The Graduate Faculty

Central Washington University

---

In Partial Fulfillment

of the Requirements for the Degree

Master of Science

Geology

---

by

Carl Delbert Swanson II

May 2012

CENTRAL WASHINGTON UNIVERSITY

Graduate Studies

We hereby approve the thesis of

Carl Delbert Swanson II

Candidate for the degree of Master of Science

APPROVED FOR THE GRADUATE FACULTY

______________ ______________________________
Dr. Audrey Huerta, Committee Chair

______________ ______________________________
Dr. J. Paul Winberry

______________ ______________________________
Dr. Robert Hickey

______________ ______________________________
Dean of Graduate Studies

# ABSTRACT

## APPLYING GIS METRICS TO DETERMINE DEGREE OF GLACIAL MODIFICATION IN MOUNTAINOUS LANDSCAPES

by

Carl Delbert Swanson II

May 2012

The ability to quantitatively assess the degree of glaciation in mountainous areas can be a powerful tool in unraveling the evolution of landscapes, and provide key insights in regions where field research is difficult. Here we determine, test, and apply metrics that assess the relative degree of past glacial modification in mountainous landscapes. Results show that slope results can be used to quantitatively assess the degree to which an area is modified by glaciation. In particular, analysis of basins using slope frequency distribution curves and slope vs. elevation plots capture steeper slopes, flatter valley bottoms, cirques, and arêtes of glaciated landscapes, and can be used to determine the relative impact of glacial vs. fluvial erosion on the development of the basin landscape.

ACKNOWLEDGMENTS

I would first like to thank my advisor, Dr. Audrey Huerta, for her support throughout the last two years. The success of this project is due to her insight and direction, which is greatly appreciated. I would also like to thank Dr. Paul Winberry and Dr. Robert Hickey for technical support working with Matlab and ArcGIS, respectively. Thanks are also in order for the rest of the CWU Geology department for being fantastic people, and making Lind Hall a great place to work. Special thanks go out to my fellow graduate students, in particular Meilani Kamaha'o, Andy Menking, and Zoe Futornick for coffee breaks, sci-fi, and general greatness, which made the last two years a lot more pleasant.

Big thanks go out to Molly Keogh, for being a great editor, motivational speaker, personal assistant, pastry chef, and friend. Her undying support during this project is a big reason for its success. I would also like to thank my wonderful family, who has always been there for me, even after I left the Midwest for more interesting topography. This research is made possible by a grant from the National Science Foundation (Grant # 22100600-0 to ADH). I would also like to thank Dr. Huerta, NSF, POLENET, and the United States Antarctic Program for giving me the incredible opportunity to spend a month working in Antarctica.

TABLE OF CONTENTS

TABLE OF CONTENTS (continued)

LIST OF TABLES

LIST OF FIGURES

LIST OF FIGURES (continued)

LIST OF FIGURES (continued)

Figure | Page

LIST OF FIGURES (continued)

# CHAPTER I

# INTRODUCTION

The shaping of mountainous topography is driven by climate fluctuations that drive erosional processes. Understanding the erosive processes that shape mountain ranges can help reveal the tectonic and climate conditions through which a landscape evolved. In particular, the ability to distinguish the degree to which a landscape has been affected by glacial vs. fluvial processes provides critical information towards unraveling past climate and tectonics, and increases our ability to predict future climate variations.

Recently, differences in the surficial expression of glacial vs. fluvial erosion have been a large focus of research in geomorphology (e.g. Montgomery, 2002; Naylor and Gabet, 2007; Amerson *et al*., 2008). Significant differences have been found between morphology (e.g. Kirkbride and Matthews, 1997; Montgomery, 2002; Naylor and Gabet, 2007; Amerson et al., 2008; Brook *et al*., 2008), erosion rates (e.g. Hicks *et al*., 1990; Oskin and Burbank, 2005), and erosional efficiency (e.g. Brozovic *et al*., 1997; Brocklehurst and Whipple, 2002; Mitchell and Montgomery, 2006; Foster *et al*., 2008; Stroeven *et al*., 2009) of glacial and fluvial processes in mountainous areas. These differences can be used to understand the fundamental effects of glaciation on a landscape, and how past glaciation has resulted in the landscapes we see today.

## Previous Work

To study the differences between glacial and fluvial processes, Montgomery (2002) analyzed glaciated, partially glaciated, and unglaciated basins on the western slope of the Olympic Peninsula in Washington State. Basins in this study were selected based on field observations and previously determined glacial extent in the area. The Olympic Peninsula is an extremely useful area for studying differences between morphology of glacial and fluvial landscapes, because of the occurrence of varying degrees of glacial influence within the same lithology, tectonic setting, and climate. Results show that glaciated valleys exhibit greater cross-sectional area and relief when compared to partially and unglaciated valleys, suggesting that glaciers remove more material than rivers, and are more effective at eroding and removing material from mountainous landscapes.

In a similar study in central Idaho (Amerson *et al*., 2008), quantitative comparisons were made to determine the differences in the morphometry of glacial and fluvial valleys. Like the Olympic Peninsula, the field area from this study exhibits varying degrees of glaciation within a region of relatively uniform lithology, tectonic setting, and climate. To determine past glaciation, a combination of previous work on the extent of glaciation in the area and field research was used to select 22 fluvial basins and 24 glacial basins for morphometric analysis. Results indicate that glacial valleys are up to 30% deeper than fluvial valleys, indicating that glaciers are more effective at removing material and generating relief, and therefore are more efficient at eroding mountainous landscapes.

In the Bitterroot Range, Montana, northern facing valley slopes show evidence of extensive glaciation, while the southern facing slopes show little to no glacial influence. Comparing north and south facing valleys, the Bitterroot Range was quantitatively analyzed for differences between glaciated and unglaciated areas (Naylor and Gabet, 2007). North and south facing slopes in this area show strong asymmetry and a 6° difference in mean slope angles. Besides showing morphometric differences between glacial and fluvial slopes, relief calculations were used to show that glaciers removed more than twice the amount of material from the Bitterroot Range than rivers, and that headwall retreat is the main geomorphic impact of glaciation.

A study in the Ben Oahu Range, New Zealand (Kirkbride and Matthews, 1997) used morphometrics on valleys formed by glaciers and rivers to look at the geomorphic effects of increasing glacial influence. In this study, hypsometric curves and distance-elevation plots were used to quantify geomorphic change resulting from glaciation. Kirkbride and Matthews (1997) found that increasing glacial influence results in more concave longitudinal valley profiles and higher proportionality of land area at low elevations, consistent with U-shaped valley geometry. Using tectonic transport rates, climate history, and reconstructed glacial extent limits, Kirkbride and Matthews (1997) concluded that typical glacial alpine topography requires ~200 kyr of temperate glacial erosion for formation.

Another morphometric study on the differences between glacial and fluvial erosion was performed in the Southern Alps, New Zealand (Brook *et al*., 2008). This study used uplift and tectonic transport rates along with oxygen isotope ratios to approximate time constraints to the development of alpine topography. These time constraints allow for estimates of the duration of glacial occupancy required to create classic "U-shaped" glacial valley geometry. In the Two Thumb Range, alpine topography (and therefore glacial influence) increases northward along the mountain range. Results from this study estimate that valley glaciers require 400-600 kyr of occupancy to create U-shaped cross-sections, and that the ability of glaciers to flatten valley profiles and create U-shaped cross-sections from V-shaped cross-sections show that glaciers are more capable at eroding large volumes of rock than rivers in mountainous areas.

Brocklehurst and Whipple (2006) used simulated fluvial landscapes to explore the possible effects of glaciation on landscape evolution. By re-creating fluvial landscapes in valleys modified by glaciers, they were able to determine where glacial erosion focused in a valley, and the effects of glaciation on basins of various sizes. Simulations show that erosional modification by large valley glaciers is much more effective than erosion by smaller valley glaciers. Large glaciers incise and widen valleys more effectively, and much faster than smaller glaciers, particularly in the ablation zone. In contrast, small glaciers are somewhat effective at widening valley walls, but not at producing relief. Large valley glaciers also widen valleys, but lower valley bottoms and produce relief significantly more than smaller valley glaciers.

Brocklehurst and Whipple (2004) applied hypsometric curves to assess the degree of glacial modification in neighboring drainage basins. To do this, they used three previously studied landscapes with varying degrees of glacial modification: the Owens Valley in California, the Sangre de Cristo Range in Colorado, and the Ben Oahu Range in

New Zealand. Using individual drainage basins, the following four hypotheses were tested: 1) that hypsometry can assess the degree of glaciation of a landscape, 2) that the position of the equilibrium line altitude (ELA) has a major effect on hypsometric curves, 3) that hypsometric curves of large areas do not exhibit the variation and detail shown by smaller-scale individual basins, and 4) that unique landforms such as hanging valleys and icefields will significantly effect hypsometric curves. From the results of this study, Brocklehurst and Whipple (2004) were able to show how different types of glacial erosion change the shape of hypsometric curves, and how the onset and continual evolution of glaciation will affect hypsometry. They show that as glaciation begins in fluvial valleys, the middle section of the hypsometric curve moves toward higher elevation, and continual modification by long-term valley glaciers moves the middle section of the curve the other direction, towards lower elevations. These conclusions allow for assessment of glacial modification based on a hypsometric curve in each individual landscape studied, but results are inconsistent between different study areas, showing the limitations in using hypsometry in assessing the impact of glaciation on evolution of the landscape.

Hypsometry and a new morphometric parameter from the hypsometric curve gradient named the “hypsokyrtome” were used in a recent study (Sternai *et al*., 2011) to look at the spatial variation of glacial erosion, and its modification of landscapes. The usefulness of hypsometric integrals and the hypsokyrtome are evaluated in the Ben Oahu Range in the Southern Alps of New Zealand. Sternai and others (2011) found that different landscapes can result in similar hypsometric integrals, but the hypsokyrtome (gradient of hypsometric curve) gives a better assessment of landscape modification by glacial processes. The hypsometric integral and gradient were also applied to the European Alps and the Apennines, and results suggest that climate can effectively limit topography, a phenomenon named "glacial buzzsaw."

The "glacial buzzsaw" hypothesis has recently been a hot topic in glacial research (e.g. Brozovic *et al*., 1997; Mitchell and Montgomery, 2006; Foster *et al*., 2008). This hypothesis states that in mountainous terrain, elevations are effectively limited by glacial and periglacial processes. A study in the northwest Himalayas (Brozovic *et al*., 1997) concluded that glacial processes can impose a limit on topography at the snowline of mountainous terrain. This result was based on patterns of elevation, hypsometry, and slope distribution that are strongly related to the extent of glacial erosion, and that landscape form is not dependent on tectonic processes and uplift rates. Simply put, the equilibrium line altitude (ELA) defines the limit of alpine topography instead of exhumation rates.

Another study (Mitchell and Montgomery, 2006) used hypsometric analysis of cirques in the western Cascades in Washington State to test the validity of the glacial buzzsaw hypothesis. Topographic evidence cited for the glacial buzzsaw in the western Cascades is that there is very little topography above the ELA. Another line of evidence used to support the glacial buzzsaw hypothesis is that uplift rates do not correlate with maximum elevation values, indicating that tectonics do not control the altitudes of a mountain range. This supports the idea that the formation of cirques by mountain glaciers at and above the ELA is extremely effective at limiting height of mountain ranges, and is the major limiting factor on altitude.

Contrary to the glacial buzzsaw hypothesis, Foster *et al*. (2008) showed that in some areas, crystalline rocks form peaks high above the ELA, and that the glacial buzzsaw is ineffective at limiting elevations in certain areas. In the western United States, Grand Teton and Mt. Moran are high above the ELA, and are referred to by the authors as “teflon peaks”, which are not significantly modified by glacial erosion. While not entirely rejecting the ability of mountain glaciers to limit topography, Foster *et al*. (2008) instead present exceptions to the glacial buzzsaw hypothesis and warn that while there is a significant trend between ELA and topography, it is not always the case.

While studying morphometric differences between glacial and fluvial landscapes is a very useful approach to understanding the character of glacial erosion, assessment of relative erosion rates of glacial and fluvial erosion may also be used. Oskin and Burbank (2005) used a large surface unconformity as a datum to analyze glacial erosion in the Kyrgyz Range in central Asia. They were able to show that glaciers in the Kyrgyz Range have highest incision rates in cirque headwalls. Cirque headwall retreat due to incision in the Kyrgyz Range is two to three times greater than valley incision rates, suggesting that when glaciers occupy valleys, initial erosion is dominated by headwall erosion of cirques.

Brocklehurst and Whipple (2002) studied basins in the eastern Sierra Nevada Range of California that exhibit varying degrees of glaciation to investigate the effect of glaciation on previously unglaciated terrain. They looked at the distribution of relief of 28 different basins, and used a one-dimensional model to simulate topography of glaciated valleys if glacial erosion had never occurred there. Results from this study show that glacial erosion rates are highest in cirque headwalls, and that glaciers are most effective at changing the relief structure of a basin where headwalls cut into low-relief topography. Brocklehurst and Whipple (2002) also noticed differences in spatial relief distribution and concavity of the longitudinal profiles of glacial and fluvial valleys, and results suggest that glaciers are more effective at downward erosion above the ELA in the Sierra Nevada Range.

Stroeven *et al*. (2009) mapped an area on the Tibetan Plateau using satellite imagery to look for patterns and distribution of the geomorphology of glacial and fluvial valleys, investigating the erosional history of a plateau remnant. They found that the glacial valleys in the plateau remnant were wider and deeper than adjacent fluvial valleys, indicating that glacial erosional processes in the area erode more material than fluvial erosional processes.

Hicks *et al*. (1990) used bathymetric surveys performed over a ten-year period to estimate sediment yields in Ivory Lake, located in the New Zealand Southern Alps. Ivory Lake is located in a cirque, and was formed as the glacier occupying this valley retreated. Hicks *et al*. (1990) found that precipitation in the area of Ivory Lake causes greater variation in sediment yield than glaciation, and that ~60% of the sediment in Ivory Lake originates from the steep valley walls of the cirque basin. Although this does show an important caveat to glacial processes being more effective at moving material than rivers, the fluvial processes in this area are working on formerly glaciated terrain, and high rates could be the result of post-glacial processes returning the valley to equilibrium.

Overall, research on differences between glacial and fluvial erosion have shown that when compared to unglaciated valleys, glaciated valleys exhibit steeper slopes, higher relief, flatter longitudinal profiles, wider and deeper valleys, and greater cross-sectional area (Amerson *et al*., 2008; Montgomery, 2002; Brocklehurst and Whipple, 2006; MacGregor *et al*., 2000; Stroeven *et al*., 2009). Glaciers have also been shown to exhibit consistently higher erosional capacity than rivers (Montgomery, 2002; Amerson *et al*., 2008; Naylor and Gabet, 2007; Brook *et al*., 2008; Stroeven *et al*., 2009) and in many cases, limit topography at and above the ELA (Brozovic *et al*., 1997; Sternai *et al*., 2011; Mitchell and Montgomery, 2006; Foster *et al*., 2008).

# CHAPTER II

# PROJECT DESCRIPTION

## Purpose of Research

In this study, we focus on developing morphometrics that capture varying degrees of glacial influence on shaping mountainous landscapes. Visually, glacial landscapes are distinguished from fluvial landscapes by steeper slopes, U-shaped geometry, and characteristic landforms such as cirques, hanging valleys, and arêtes. If glacial influence can be recognized qualitatively, there must be a way that glacial influence can be quantified.

Typically, the effect of glacial and fluvial processes on mountainous landscapes is assessed through field research and identification of landforms. While field research is an effective way to document the impact of glaciation, remote analysis techniques can provide key techniques to assess glacial impact where field work is difficult. Given that glaciated valleys typically have steeper side slopes, flatter long valley profiles, and exhibit characteristic landforms such as cirques and arêtes, we explore the use of standard GIS metrics of slope, curvature, and relative elevation on DEMs of mountainous landscapes dominated by glacial erosion and landscapes dominated by fluvial erosion. This quantitative approach is important in that it allows for mathematical interpretation of glacial and fluvial landforms.

### *Questions to Address*

By exploring the use of slope, curvature, and relief on landscapes dominated by glacial and fluvial processes, we hope to answer the following questions:

1. Are there morphometrics that quantitatively capture the differences between glaciated and nonglaciated basins?

2. Can we use these morphometrics to assess the relative impact of glacial vs fluvial processes where degree of glaciation is unknown?

## Study Area: Sawtooth Range, Idaho

Previous work in the Sawtooth Range and South Fork Payette River basin, Idaho (Amerson *et al*., 2008) selected 22 fluvial basins and 24 glacial basins of varying sizes and shapes to study morphometric differences between glacial and fluvial valleys (figure 2.1). Basins were chosen based on reconstructed equilibrium-line altitude (ELA) levels from the Sawtooth Range (Meyer *et al*., 2004). Using the basins from Amerson *et al*., we look for quantitative differences between specific GIS metrics in glacial, transitional, and fluvial valleys. In addition to the 46 valleys previously studied, 24 valleys are added between the glacial and fluvial areas, in search of a transitional signal between areas dominated by glacial erosion and areas dominated by fluvial erosion (figure 2.2).

Transitional valleys are chosen based on visual evidence such as flat valley bottoms, hanging valleys, cirques, and proximity to fully glaciated terrain.

Lithology of the Sawtooth Range consists of Eocene and Cretaceous granitic rocks of the Idaho Batholith (Hyndman, 1983). The climate of this region is temperate, with average annual precipitation in the Sawtooth Mountains ranging from ~0.3 to ~1.3 m/yr (source: www.worldatlas.gov). Uplift rates due to isostatic rebound from past glaciation (Pelletier, 2004) are generally low.

The Sawtooth Range has experienced extensive glaciation throughout several glacial cycles, most recently in the late Pleistocene (e.g. Stanford, 1982; Meyer *et al*., 2004; Thackray *et al*., 2004). Reconstructed ELA levels (Meyer *et al*., 2004) show extensive glaciation of the Sawtooth Range during the last glacial maximum, which diminishes westward.

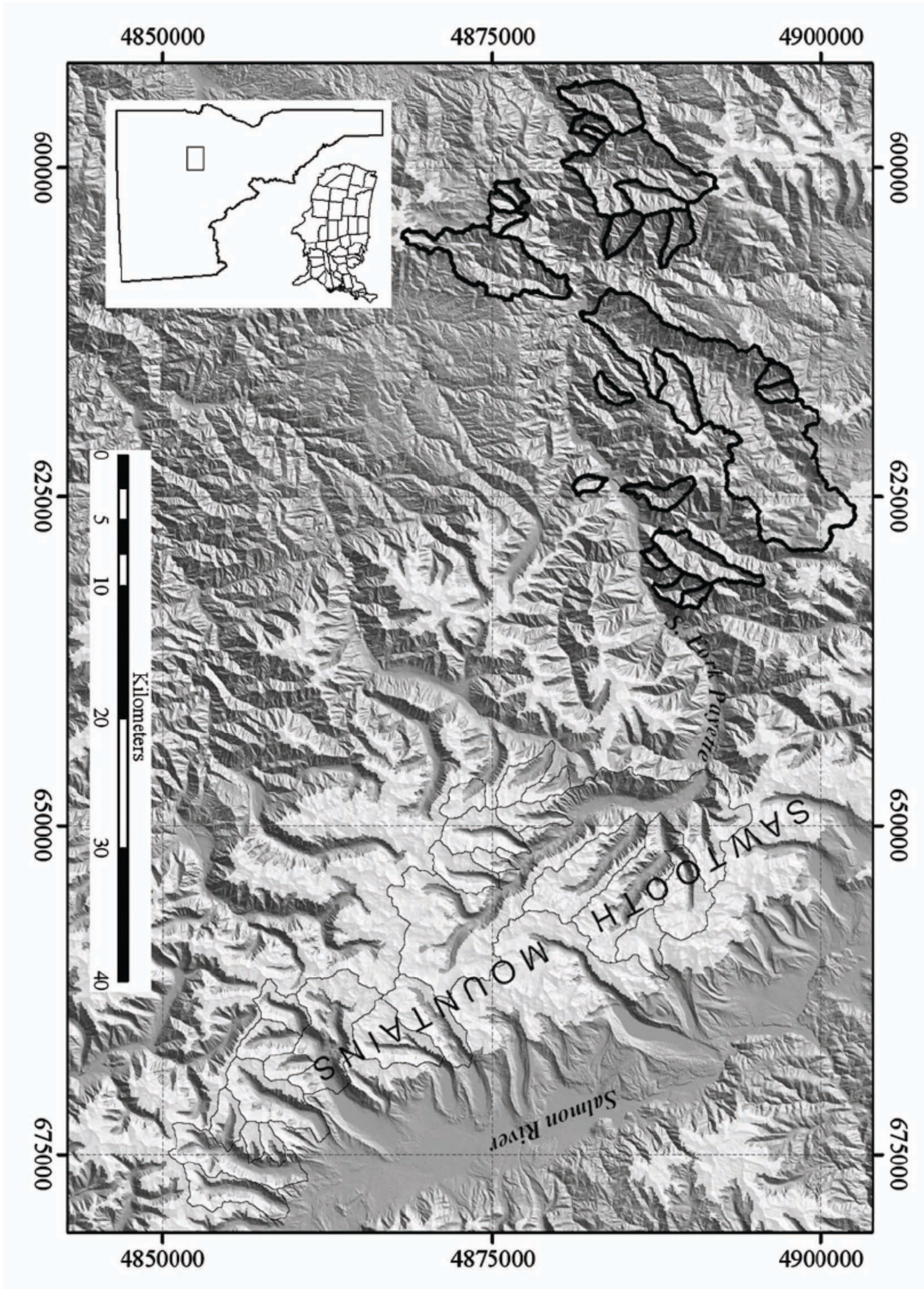


Figure 2.1: Study area map modified from Amerson *et al*., 2008. Glacial valleys are outlined with thin black lines, and fluvial valleys are outlined with heavy black lines. White shaded area denotes elevations that lie above the ELA.

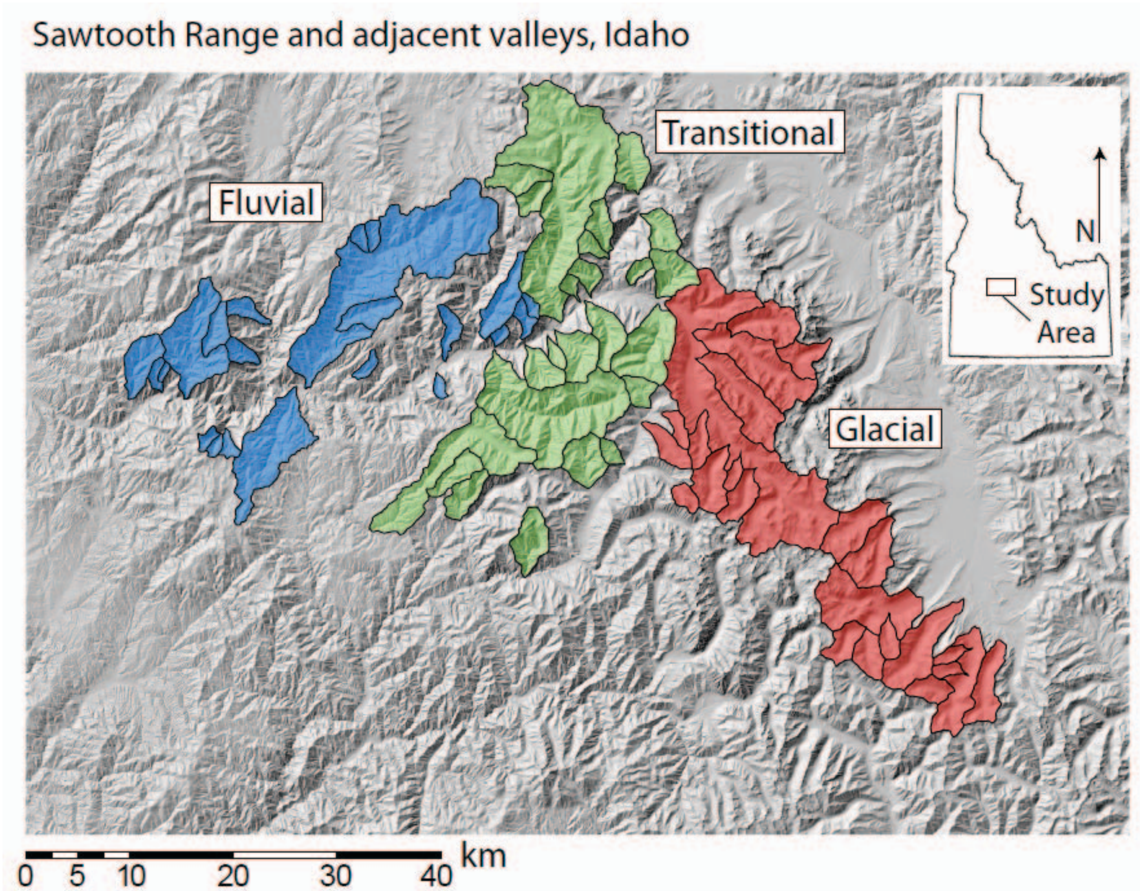


Figure 2.2: Study area, Sawtooth Range and adjacent fluvial basins, central Idaho showing glacial (red), transitional (green), and fluvial (blue) basins used for analysis. Basins selected based on previous work (Amerson *et al*., 2008).

# CHAPTER III

# METHODS

To calculate slope and curvature using digital elevation models (DEMs), we use ESRI's geospatial analysis software ArcGIS. This software allows for calculations on a cell-by-cell basis and creates grids that are easily converted to other formats for analysis.

In ArcGIS, slope is calculated as the maximum change between the cell in which slope is being calculated and the 8 adjacent cells. The slope function fits a plane to a 3 x 3 cell neighborhood in a DEM, calculates the slope for that plane, and assigns the value of the plane to the cell. One important thing to consider in regards to DEM resolution is that this method of slope calculation effectively decreases the resolution from 10 $m^2$ per cell to 30 $m^2$ per cell.

Curvature is the rate of change of slope (or the slope of the slope), in units of (1/100) $m^{-1}$. Two types of curvature are used in this analysis: planform curvature and profile curvature. Planform curvature is measured perpendicular to the maximum slope direction (i.e., curvature of a line of constant elevation), and profile curvature is measured parallel to the maximum slope direction (i.e., curvature down a slope). ArcGIS calculates curvature by numerically estimating the 2$^{nd}$ derivative of a 3 x 3 cell window in a DEM. A positive planform curvature corresponds with a surface that is convex (i.e., extruding ridge), and a negative value corresponds with a concave surface (i.e., cirque). For profile curvature, a positive value corresponds with a concave up surface, and a negative value corresponds with a convex up surface. For both types of curvature, a value of 0 corresponds with a flat surface.

## Basin Delineation

To explore the morphometrics of mountainous landscapes, we first separate the landscape into individual basins. U.S. Geologic Survey 10-m resolution DEMs in the Sawtooth Range are used for basin delineation and extraction of point data using ESRI's ArcGIS 10. The first step in our analysis process is removing pits and sinks from the DEM. Pits and sinks are anomalously high or low data values, which can be smoothed using elevation values of surrounding cells by using the ArcGIS "fill" function. A DEM that is free of pits and sinks is necessary for delineation of individual drainage basins. Using the continuous raster, the ArcGIS "flow direction" function defines the theoretical direction of flow for all cells in the DEM. The flow direction raster is then used as input for the ArcGIS "flow accumulation" function, creating a raster that shows concentration of flow into certain cells, defining the stream network throughout the DEM. Using the flow accumulation raster, pour points are then set manually by creating a point layer and digitizing points at the mouth of each drainage basin we wish to delineate. A raster of individual basins is created with the ArcGIS "watershed" function, which uses the digitized pour points and the flow direction raster as inputs to delineate drainage basins. The output from the watershed function is a raster delineating the drainage basins, assigning each cell within a basin a unique value. Using the ArcGIS "extract by attributes" function, unique values for each basin are used to create an individual raster layer for each basin to be used as masks to extract data from the original DEM.

Using the ArcGIS "slope" and "curvature" functions from the spatial analyst toolbox, raster layers of slope, profile curvature, and planform curvature are created from the modified DEM raster. The individual basin masks are used to extract point data for each basin, using the ArcGIS "extract by mask" function. Layers are created for elevation, slope, profile curvature, and planform curvature for each basin in the study area. Data from each layer is converted to ASCII format using the ArcGIS "raster to ASCII" function, and exported as "*.txt" files for quantitative analysis in Mathworks' numerical analysis software Matlab.

## Quantitative Analysis

Analysis of the slope, elevation, and curvature data for each basin is performed by constructing frequency distribution plots for each individual basin. Plots of weighted mean values are then constructed for all basins. Frequency distribution plots of mean values of all fluvial, transitional, and glacial basins in a given area use weighted means, weighting each basin equally. A bin size of 50 is used for frequency distribution plots of slope and curvature, as well as for elevation distribution plots.

Investigation of differences in relative elevation values between glacial and fluvial basins is performed by constructing plots of elevation distribution (or elevation vs.

area), giving us a quantitative way to look at how land mass is distributed as a function of elevation throughout an individual basin.

To investigate slope as a function of elevation (Katsube and Oguchi, 1999), we use box and whisker plots (figures 5.9 to 5.12) to show the distribution of slope values throughout different elevations. Box and whisker plots are constructed for each 10 percent elevation range. In each elevation range, box and whisker plots show the median slope value (red line), the 25$^{th}$ and 75$^{th}$ percentile (edges of box), and the range of data outside the 25$^{th}$ and 75$^{th}$ percentile (whiskers) at that elevation range.

# CHAPTER IV

# RESULTS

Plots of slope, elevation, and curvature of basins in the Sawtooth Range in central Idaho show distinct differences between glacial, partially glaciated (transitional), and fluvial landscapes.

## Slope Analysis

Slope Frequency distribution curves of individual glacial basins exhibit a measurable proportion of low slope values, slope values above 50°, and low peak frequency (figure 4.1). Frequency distribution curves of fluvial basins, however, exhibit an extremely small proportion of low slope values, no slope values above 50°, and a high proportion of slope values at peak frequency (30°) (figure 4.2).

Visual inspection of DEMs of glacial basins reveal that these basins are characterized by a large proportion of high and low slope values capturing the slopes from steep valley walls, cirques, arêtes, and flat valley bottoms (figure 4.3). Fluvial landscapes exhibit more gentle slopes with V-shaped valley cross-sectional geometry when compared to glacial landscapes (figure 4.4).

Comparison of weighted mean slope frequency distribution curves for glacial, transitional, and fluvial basins show that as glaciation increases, basins exhibit systematically higher range of values and higher standard deviation (figure 4.5, table 4.1).

## Planform and Profile Curvature Analysis

Planform and profile frequency distribution curves of glacial basins exhibit a majority of curvature values at 0, and a wide range of non-zero curvature values (figures 4.6, 4.11). Frequency distribution curves of fluvial basins also exhibit a majority of curvature values at 0, however, non-zero curvature values exhibit a narrow range of planform and profile curvature values (figures 4.7, 4.12).

Visual inspection of DEMs of glacial basins reveal that for these basins the extreme (less than -5, greater than 5) planform and profile curvature values are primarily found in rilled valley walls, arêtes, and cirque headwalls (figures 4.8, 4.13), while rare extreme curvature values in fluvial landscapes are found in hilltops and gullies (figures 4.9, 4.14). While there are distinct differences in planform and profile curvature values between glacial and fluvial basins, curvature analysis does not capture entire cirques and arêtes as expected, due to the 10-meter resolution of the DEMs. Extreme curvature values within cirques, at arête peaks, and within the rilled landscape seem to be a signal unique to glacial landscapes, but exactly where the signal is coming from is unknown.

Comparison of planform and profile frequency distribution curves for glacial, transitional, and fluvial basins show that as glaciation increases, basins systematically exhibit more extreme curvature values (figure 4.10, 4.15, table 4.2, 4.3).

## Elevation Analysis

Elevation distribution curves for glacial basins exhibit a low proportion of land area at high elevations (figure 4.16), in comparison to fluvial basins (figure 4.17).

Visual inspection of DEMs of glacial basins reveal little land area at high elevations, a result of cirque erosion and large areas at the valley bottom (figure 4.18). Fluvial basins, however, exhibit a comparatively high proportion of land area at high elevations (figure 4.19).

Comparison of weighted mean elevation distribution curves of weighted means for glacial, transitional, and fluvial basins show that as influence of glaciation increases, basins yield systematically less land area at high elevations (figure 4.20).

## Slope vs. Elevation

Slope vs. elevation plots for glacial basins in central Idaho exhibit a high range of slope values at each elevation, and high variation of median slope values between elevations (figure 4.21). Slope vs. elevation plots for fluvial basins, however, exhibit a lower range of slope values at each elevation, and more consistent median slope values at each elevation when compared to glacial basins (figure 4.22).

An easy way to see differences between glacial and fluvial basins is to plot curves that show the distribution of mean values as a function of elevation for each basin (figure 4.23). Mean values for each basin show that glacial basins exhibit low slope values in the bottom of basins (flat valley bottoms) and high slope values in the upper elevations of basins (arêtes). To get a better idea of the shape of each glacial mean slope curve vs. the shape of each fluvial mean slope curve, we use the weighted mean of all slope values at each elevation for glacial and fluvial basins (figure 4.24). The mean slope distribution curves for all glacial basins show distribution curves exhibiting a “S” shape, while mean slope distribution curves for all fluvial basins exhibit a “bow” shape. Consistency of the shapes of slope distribution curves for all individual glacial basins and all individual fluvial basins is shown by separating each mean slope distribution curve for each individual basin (figures 4.25, 4.26).

## Patterns of Glacial vs. Fluvial Erosion

In the Sawtooth Range, Idaho, morphometrics of slope, slope distribution, elevation distribution, and curvature reveal distinctive differences between glacial and fluvial basins. The steep walls of cirques and arêtes, and the flat valley bottoms characteristic of glacial basins yield distinctive frequency distribution curves of slope, and distinctive curves of slope as a function of elevation. Curvature results yield more extreme planform and profile curvature values with increasing glaciation, however the source of extreme curvature values is difficult to determine. Elevation distribution yields a systematically lower proportion of land area at high elevations with increasing glaciation, due to cirque erosion and valley bottom flattening.

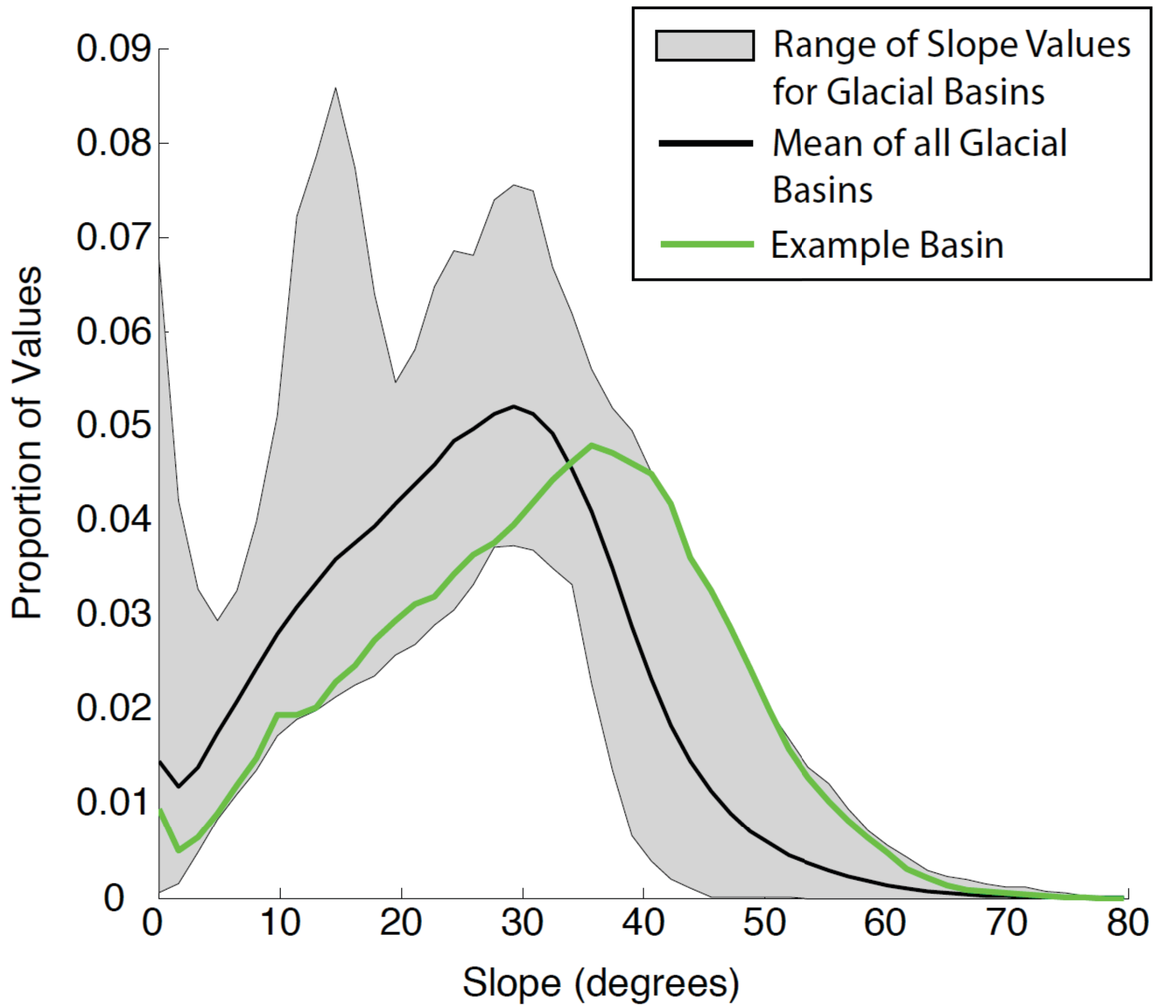


Figure 4.1: Frequency distribution plot for slope values of glacial basins in the central Idaho study area, with the weighted mean of all glacial basins (black line), frequency distribution curve of an example basin (green line), and the envelope that includes frequency distribution curves for all glacial basins (shaded gray area).

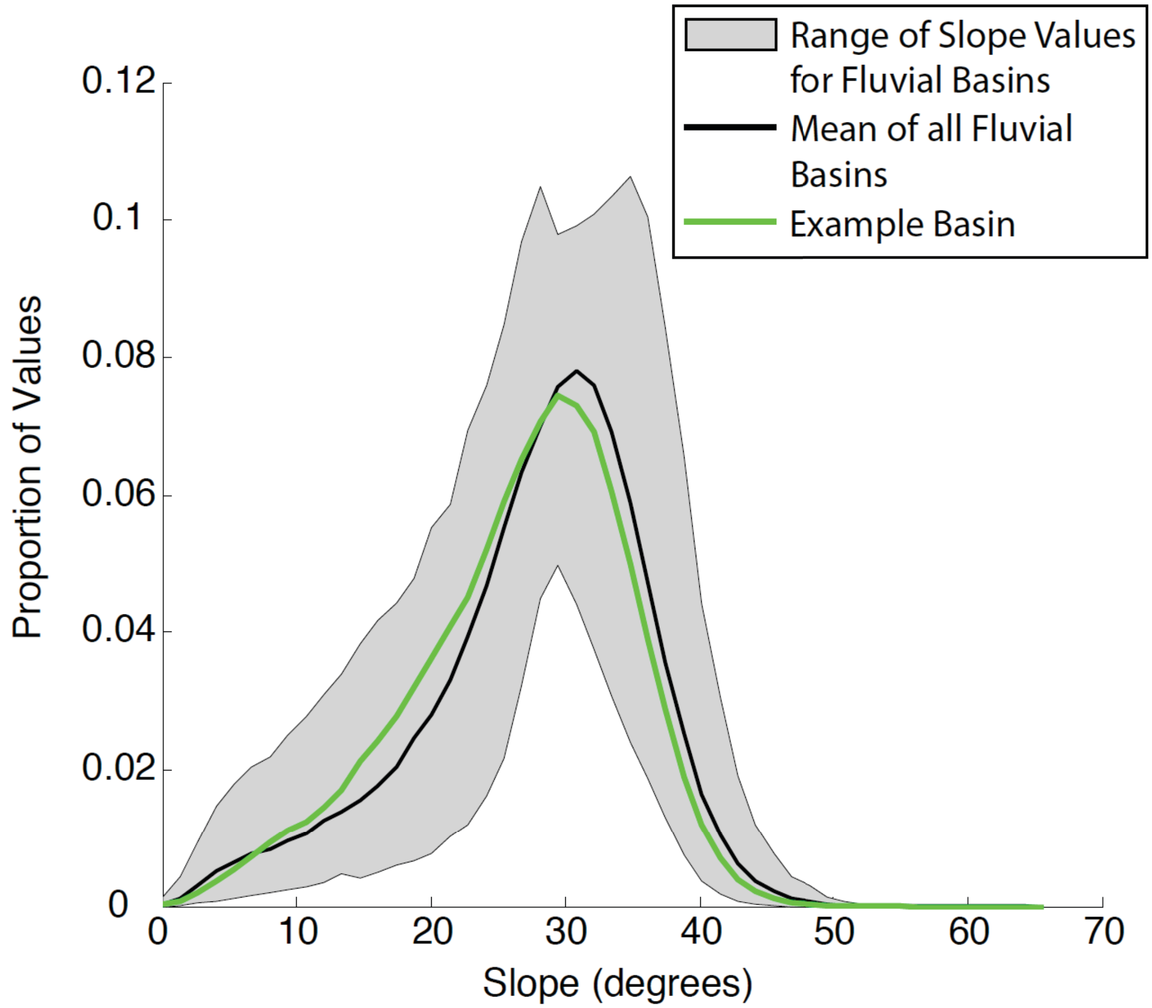


Figure 4.2: Frequency distribution plot for slope values of fluvial basins in the central Idaho study area, with the weighted mean of all fluvial basins (black line), frequency distribution curve of an example basin (green line), and the envelope that includes frequency distribution curves for all fluvial basins (shaded gray area).

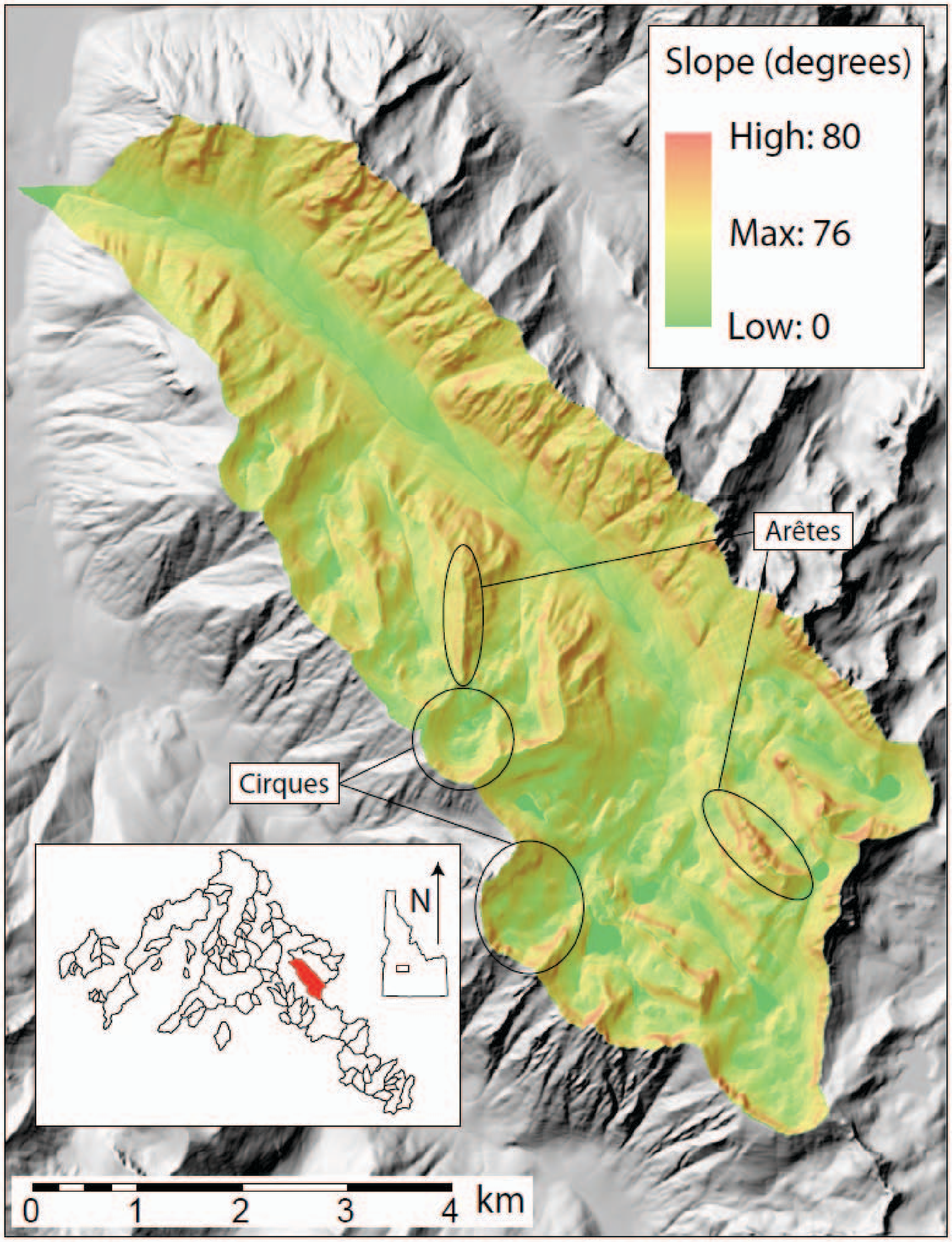


Figure 4.3: Slope map of an example glacial basin, Sawtooth Range, Idaho.

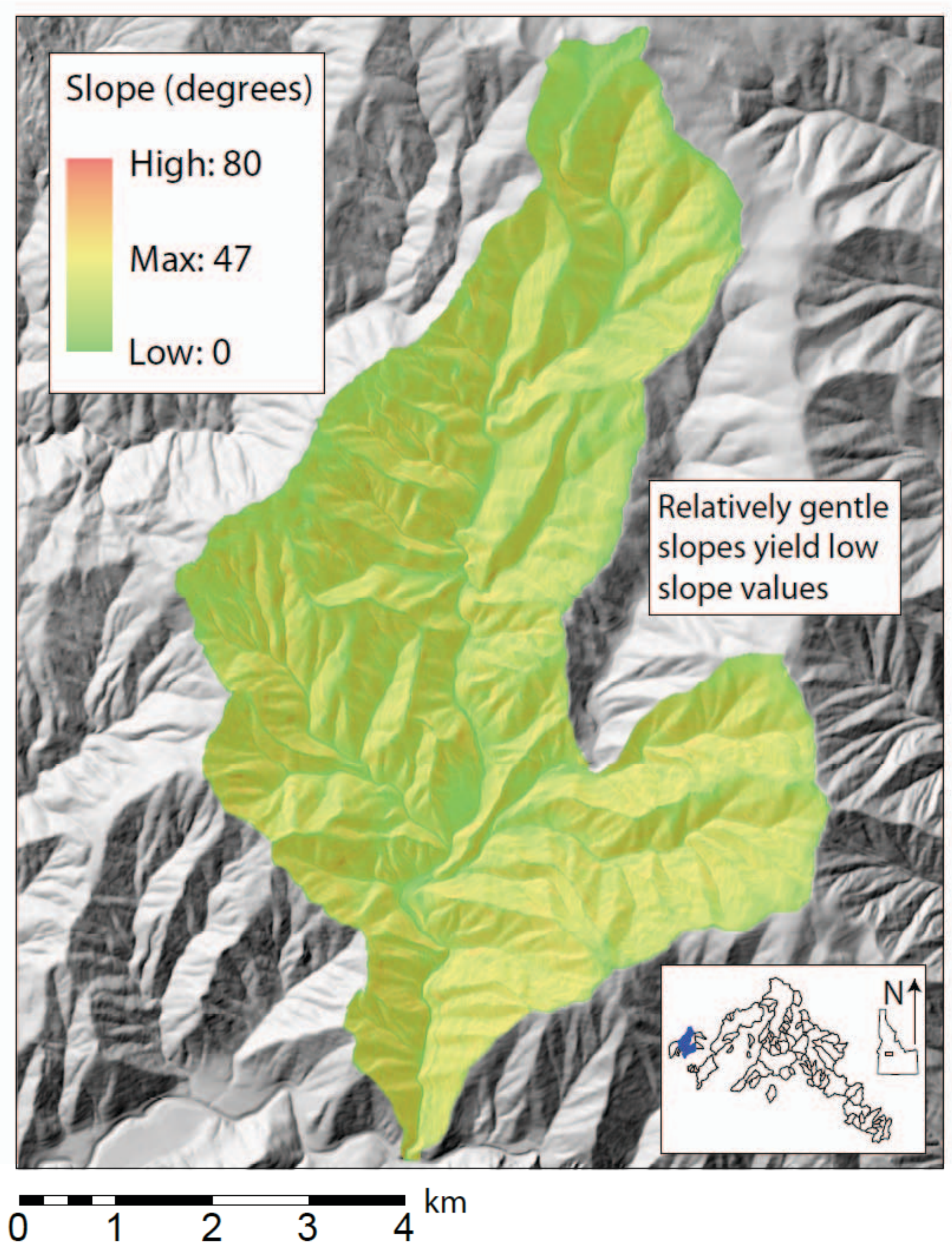


Figure 4.4: Slope map of an example fluvial valley, Sawtooth Range, Idaho.

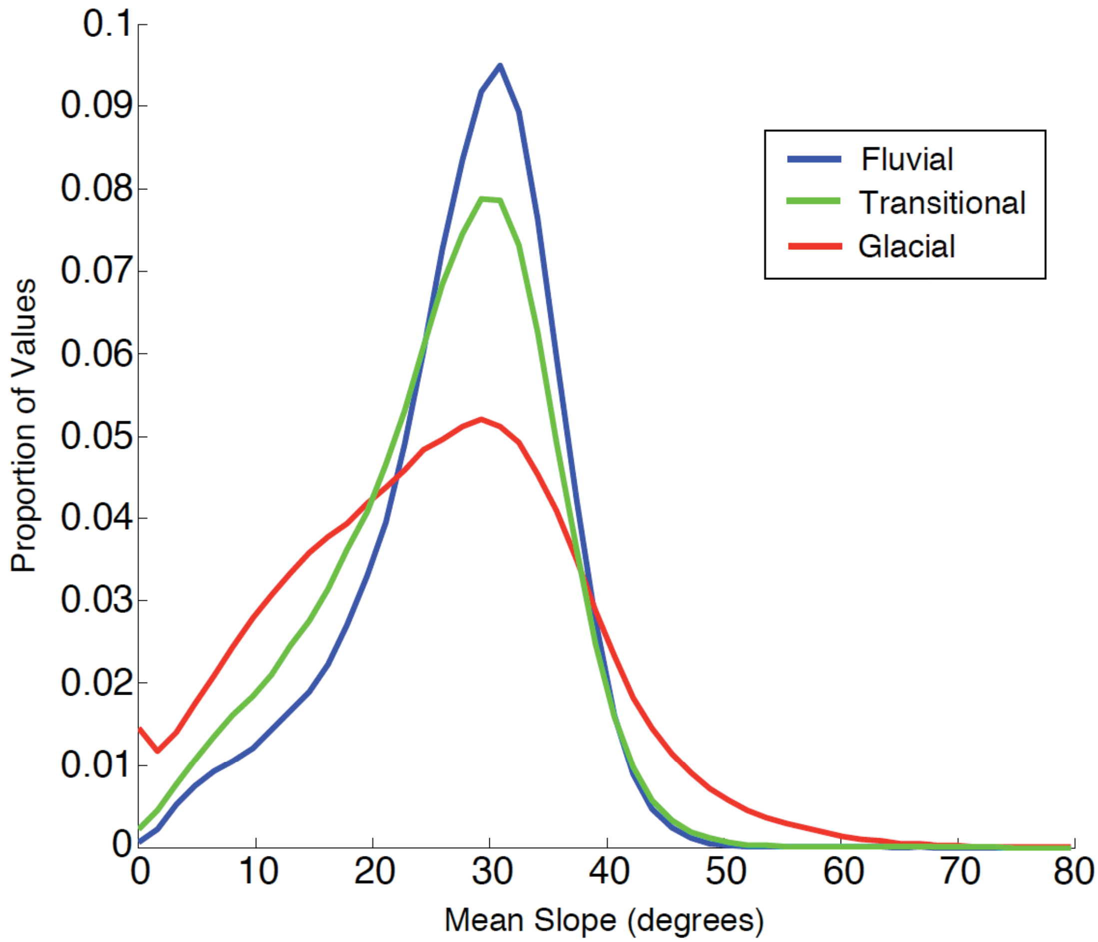


Figure 4.5: Mean slope results for central Idaho, using weighted means of all fluvial, transitional, and glacial basins in the Sawtooth Range study area.

Table 4.1: Slope values for central Idaho.

| Sawtooth Range and South Fork Payette River Basin, Idaho: Slope | | | | | | |
|---|---|---|---|---|---|---|
| Basin Type | Min | Max | Mean | Mode | Median | Std Dev |
| Glacial | 0 | 79.7 | 25.6 | 35.88 | 26.11 | 11.47 |
| Transitional | 0 | 73.0 | 26.2 | 29.91 | 27.01 | 8.23 |
| Fluvial | 0 | 65.6 | 27.7 | 32.14 | 28.77 | 7.59 |

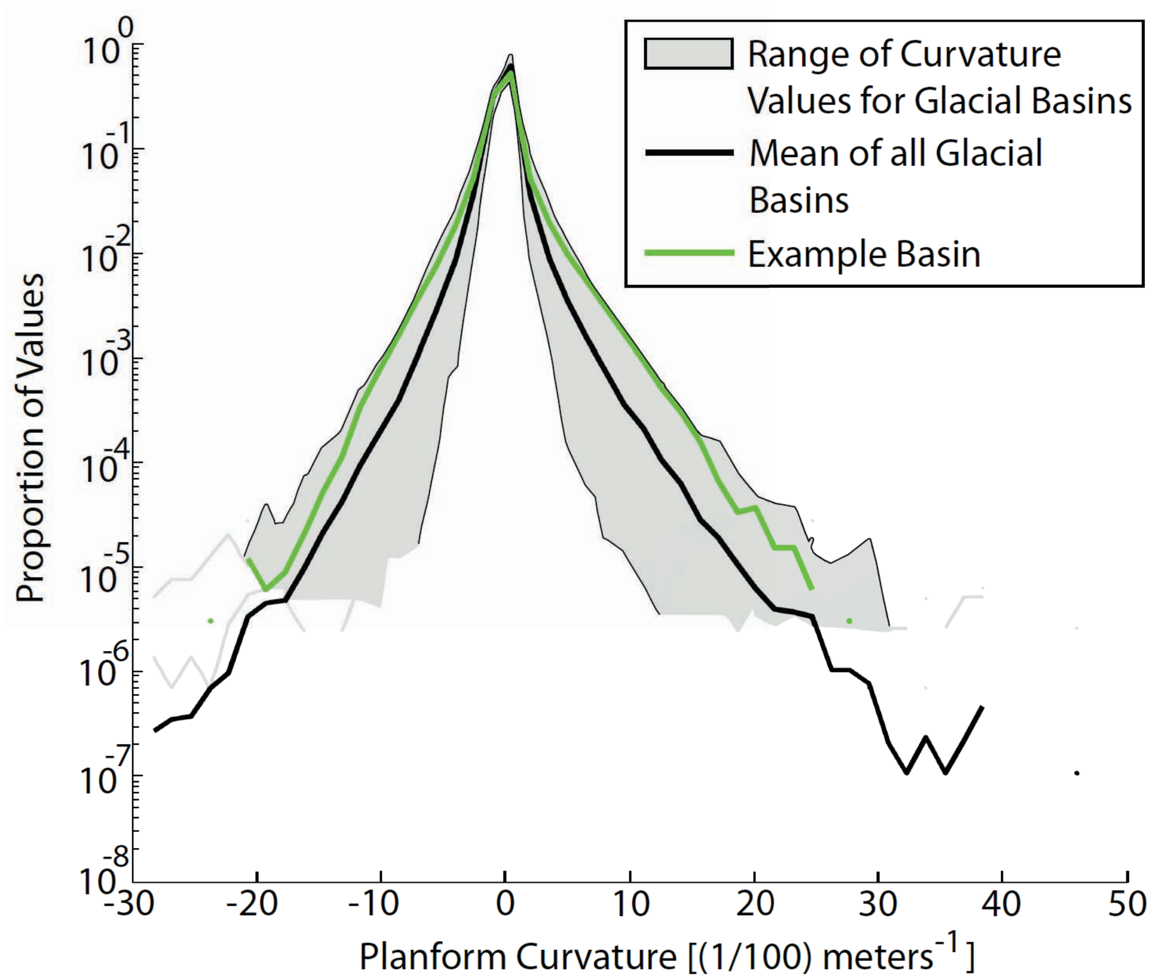


Figure 4.6: Frequency distribution plot for planform curvature values of glacial basins in the central Idaho study area, with the weighted mean of all glacial basins (black line), frequency distribution curve of an example basin (green line), and the envelope that includes frequency distribution curves for all glacial basins (shaded gray area).

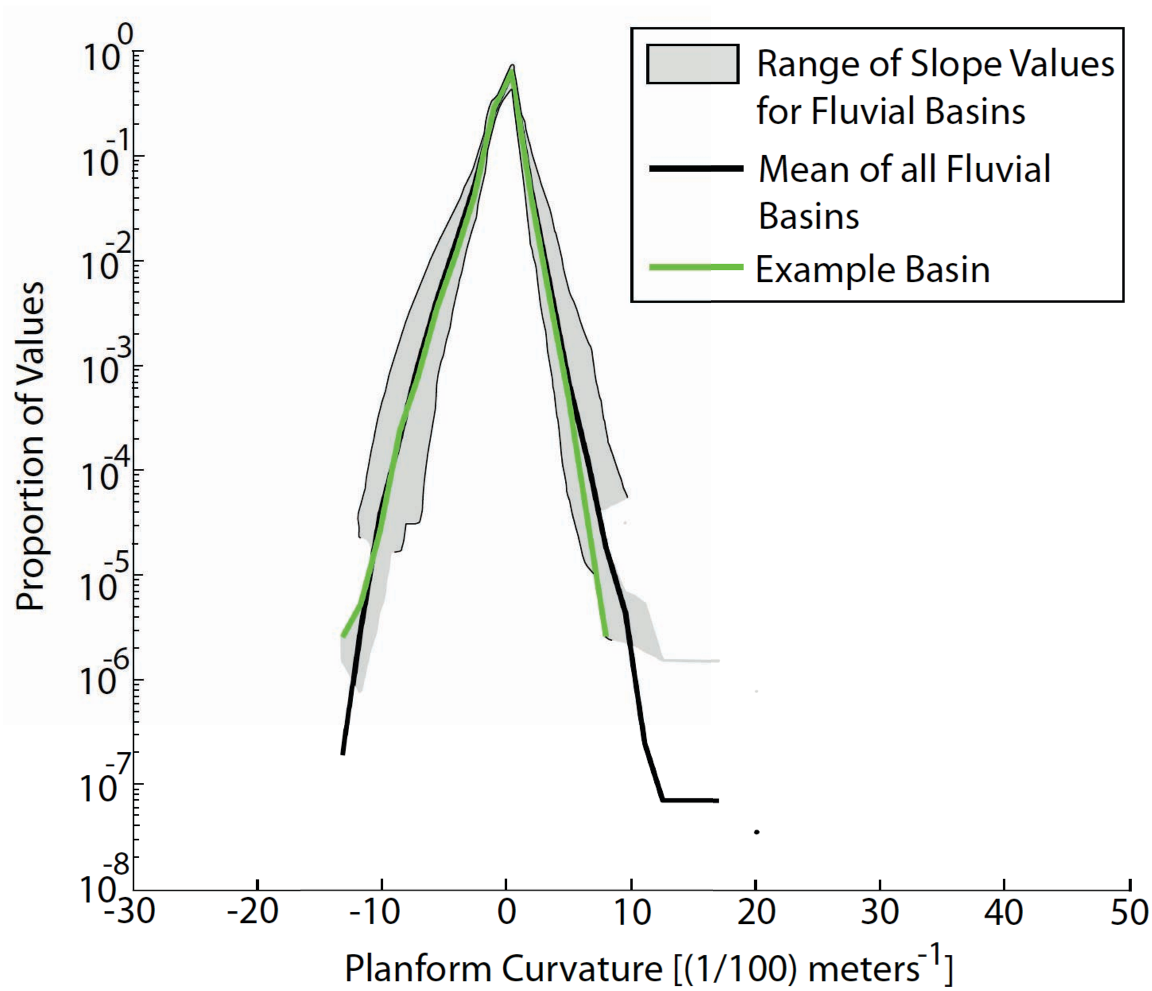


Figure 4.7: Frequency distribution plot for planform curvature values of fluvial basins in the central Idaho study area, with the weighted mean of all fluvial basins (black line), frequency distribution curve of an example basin (green line), and the envelope that includes frequency distribution curves for all fluvial basins (shaded gray area).

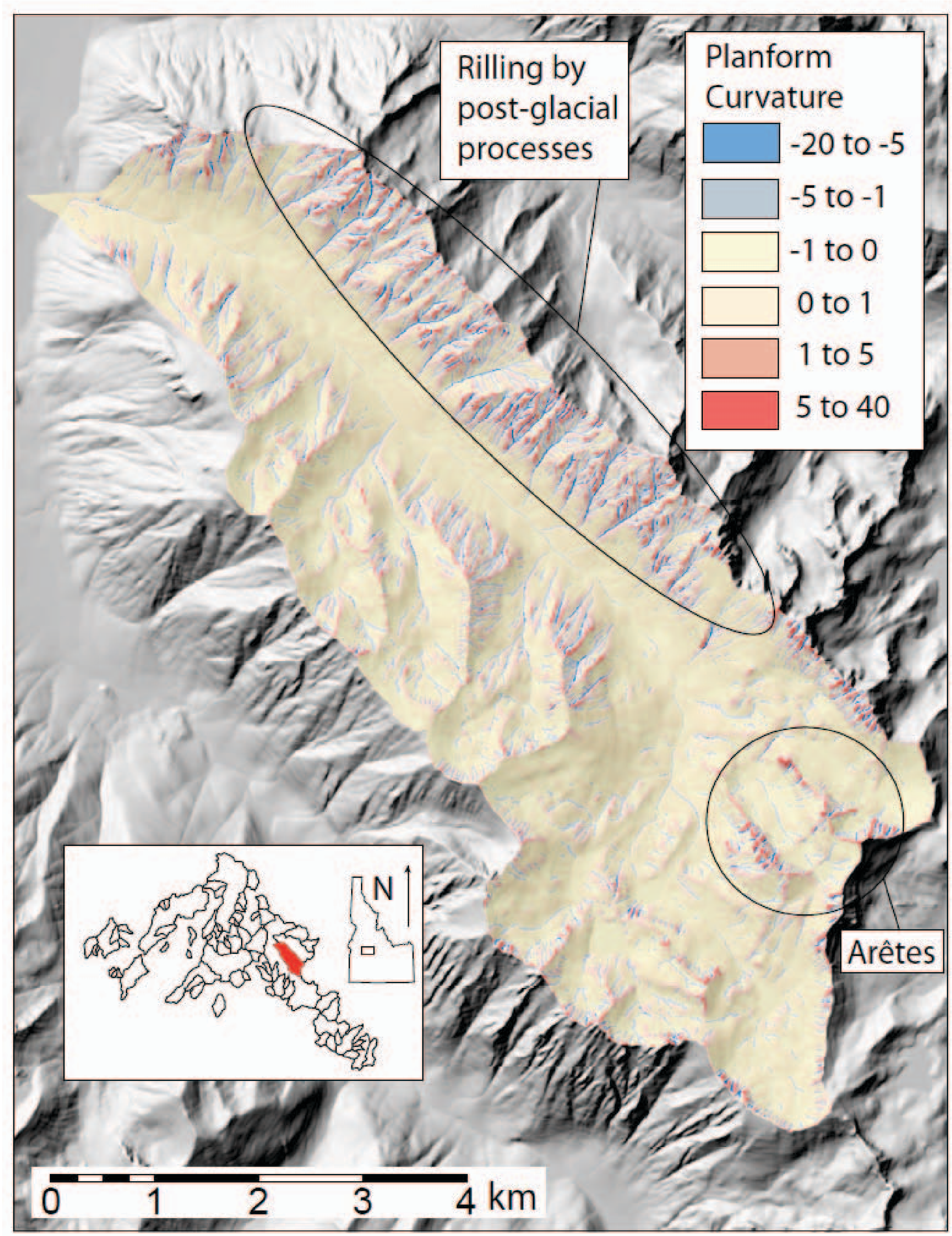


Figure 4.8: Planform curvature map of an example glacial valley, Sawtooth Range, Idaho.

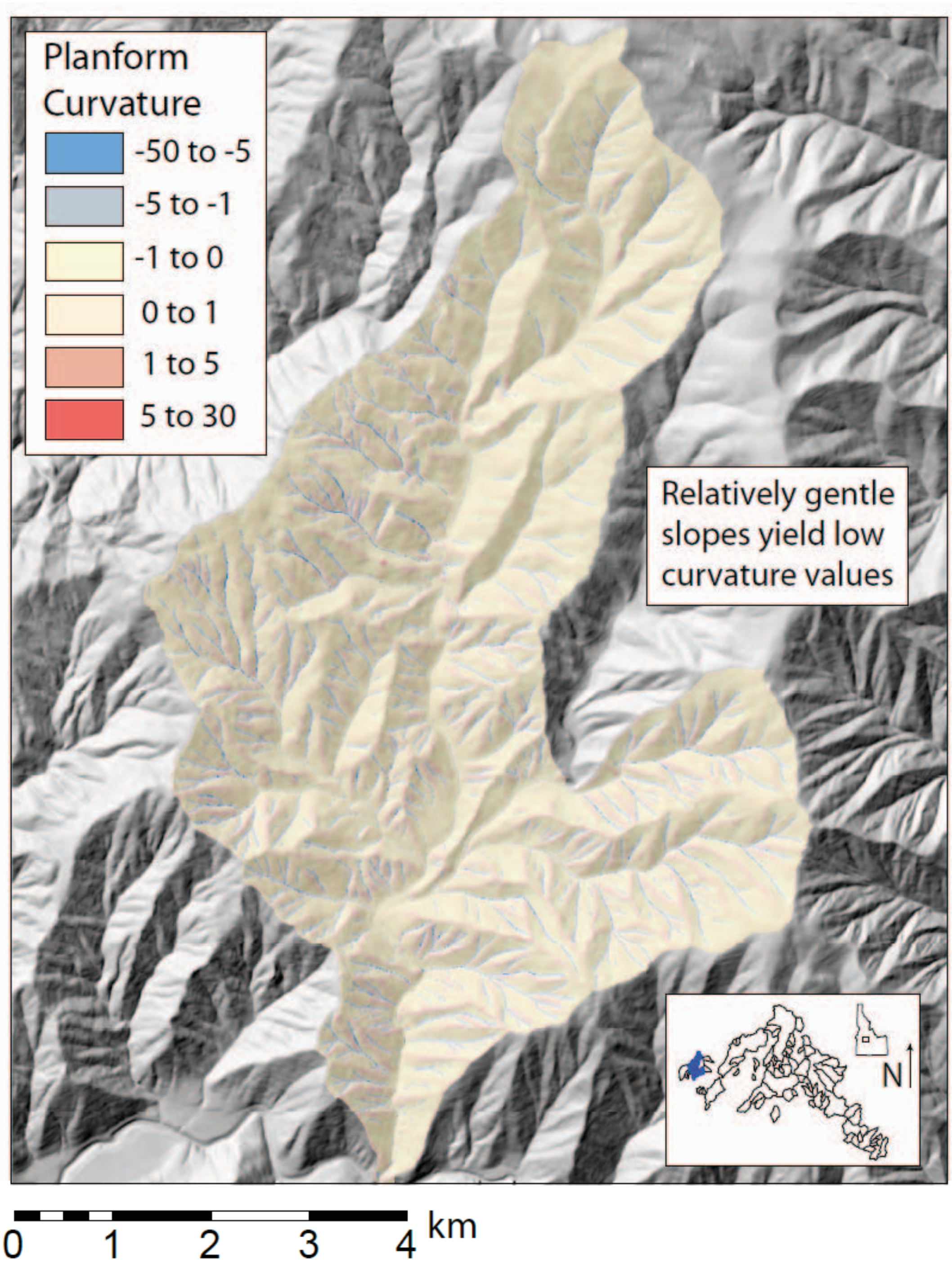


Figure 4.9: Planform curvature map of an example fluvial valley, Sawtooth Range, Idaho.

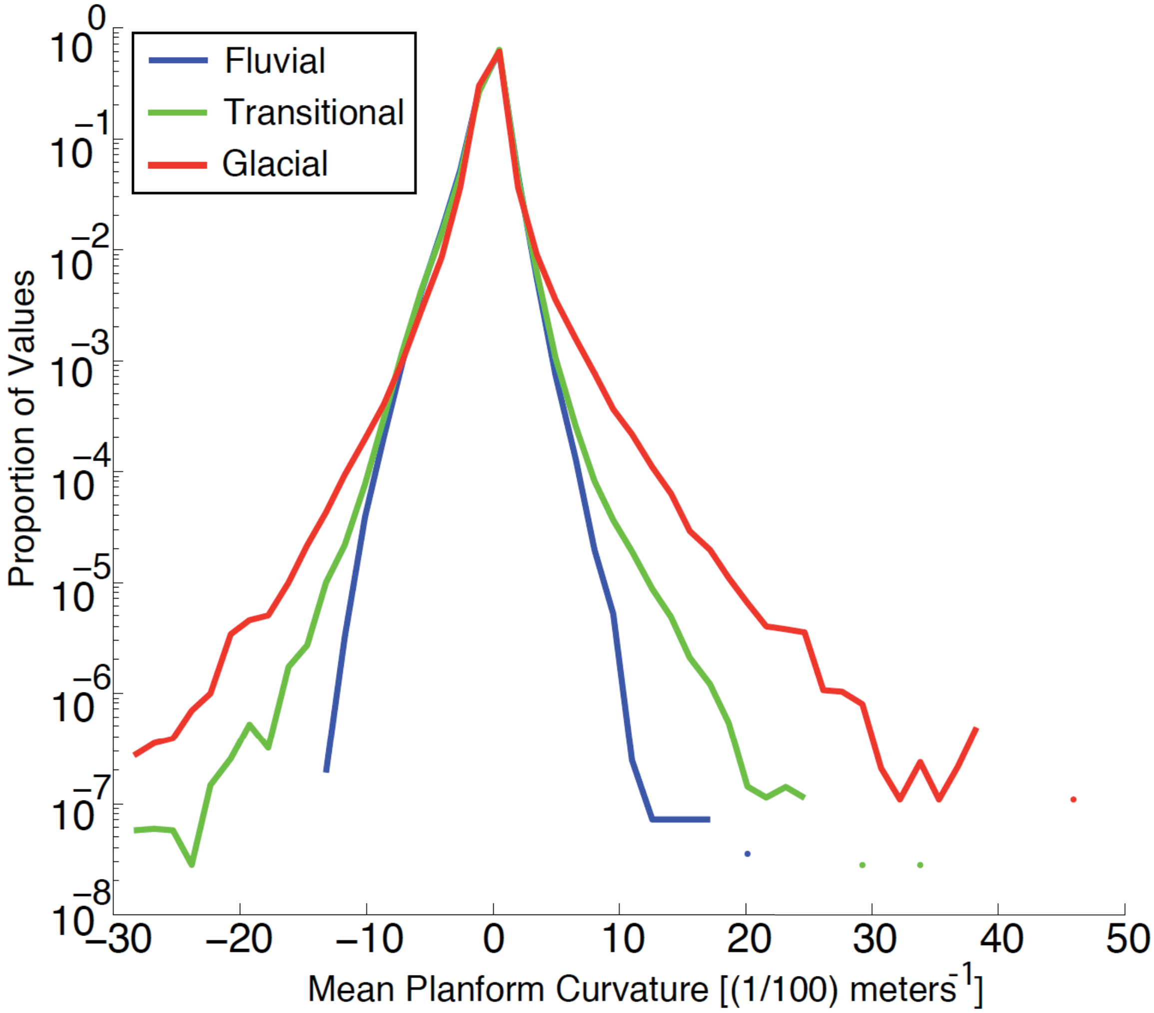


Figure 4.10: Mean planform curvature results for central Idaho, using weighted means of all fluvial, transitional, and glacial basins in the Sawtooth Range study area.

Table 4.2: Planform Curvature Values for central Idaho

| Sawtooth Range and South Fork Payette River Basin, Idaho: Planform Curvature | | | | | | |
|---|---|---|---|---|---|---|
| Basin Type | Min | Max | Mean | Mode | Median | Std Dev |
| Glacial | -28.3 | 45.9 | 0.0301 | 0.6628 | 0.0369 | 1.075 |
| Transitional | -26.2 | 17.1 | 0.0096 | 0.2365 | 0.1014 | 1.063 |
| Fluvial | -12.6 | 19.3 | 0.0022 | 0.4695 | 0.1108 | 1.060 |

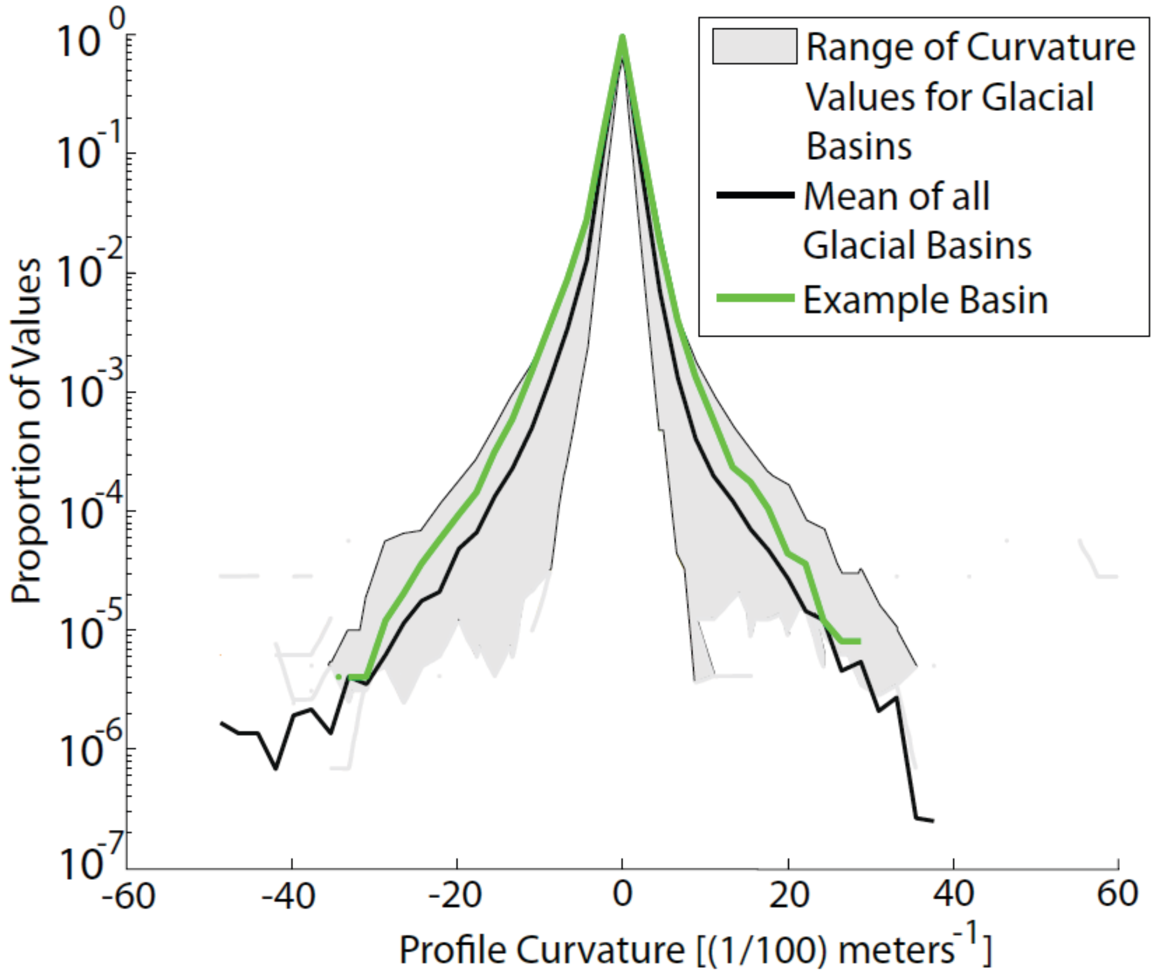


Figure 4.11: Frequency distribution plot for profile curvature values of glacial basins in the central Idaho study area, with the weighted mean of all glacial basins (black line), frequency distribution curve of an example basin (green line), and the envelope that includes frequency distribution curves for all glacial basins (shaded gray area).

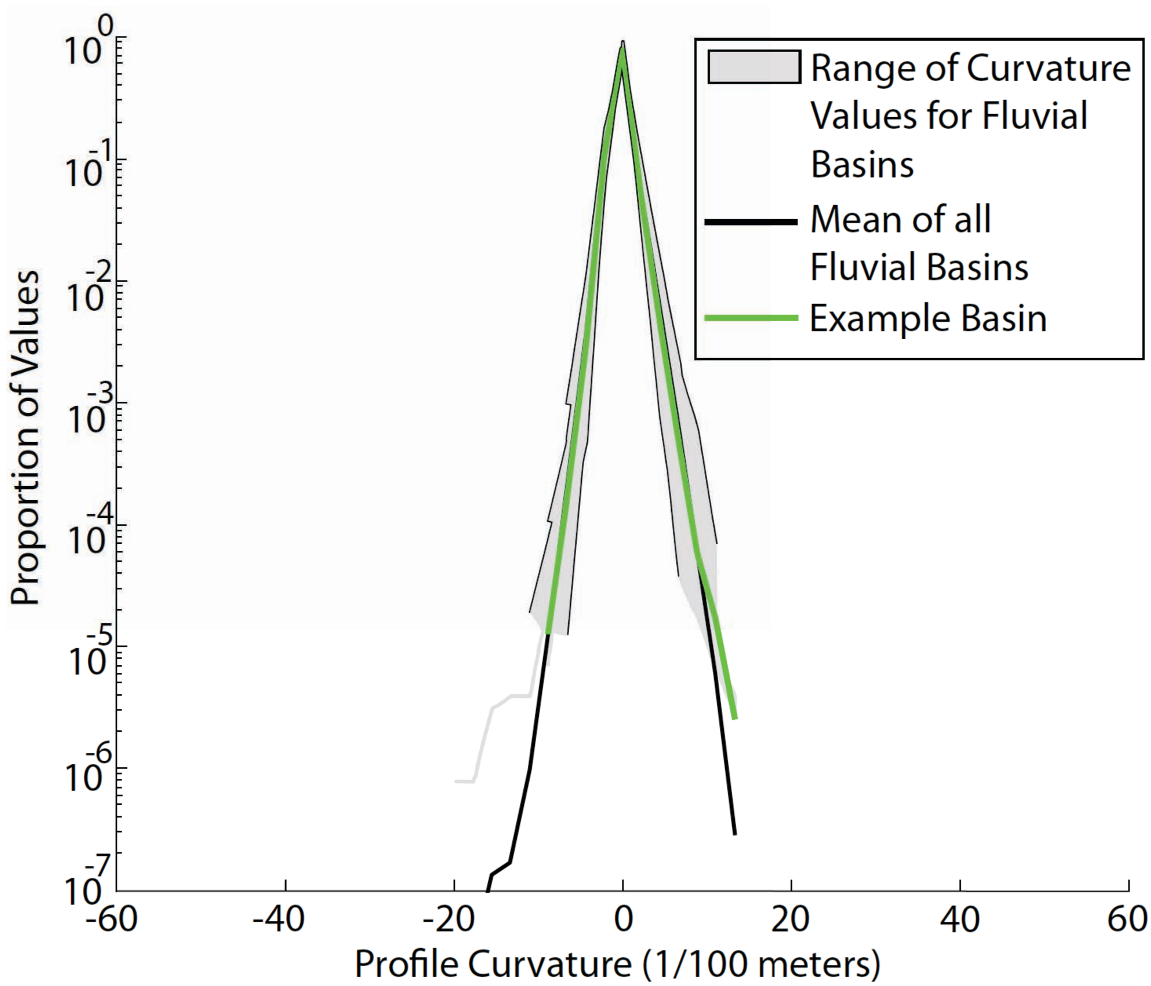


Figure 4.12: Frequency distribution plot for profile curvature values of fluvial basins in the central Idaho study area, with the weighted mean of all fluvial basins (black line), frequency distribution curve of an example basin (green line), and the envelope that includes frequency distribution curves for all fluvial basins (shaded gray area).

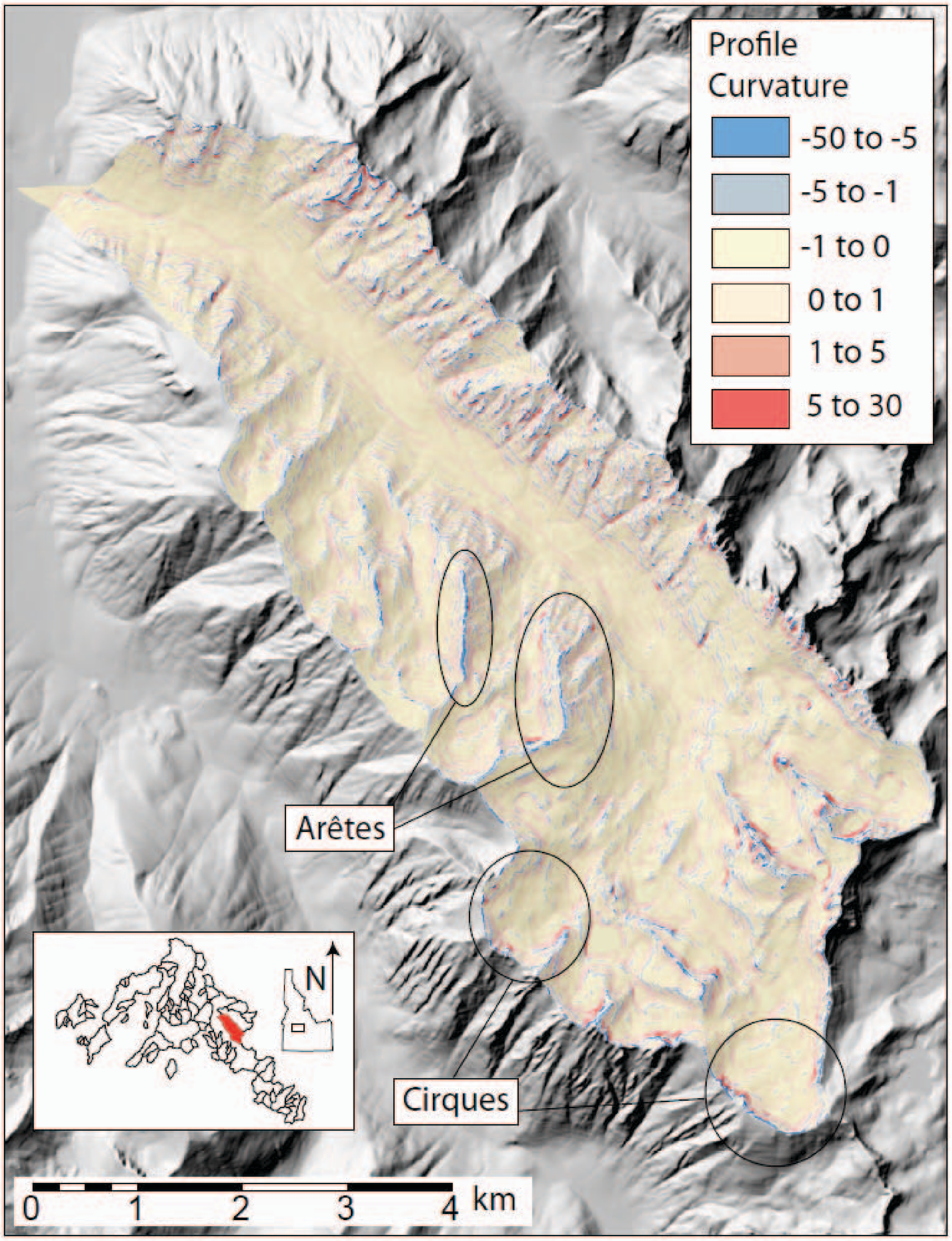


Figure 4.13: Profile curvature map of an example glacial valley, Sawtooth Range, Idaho.

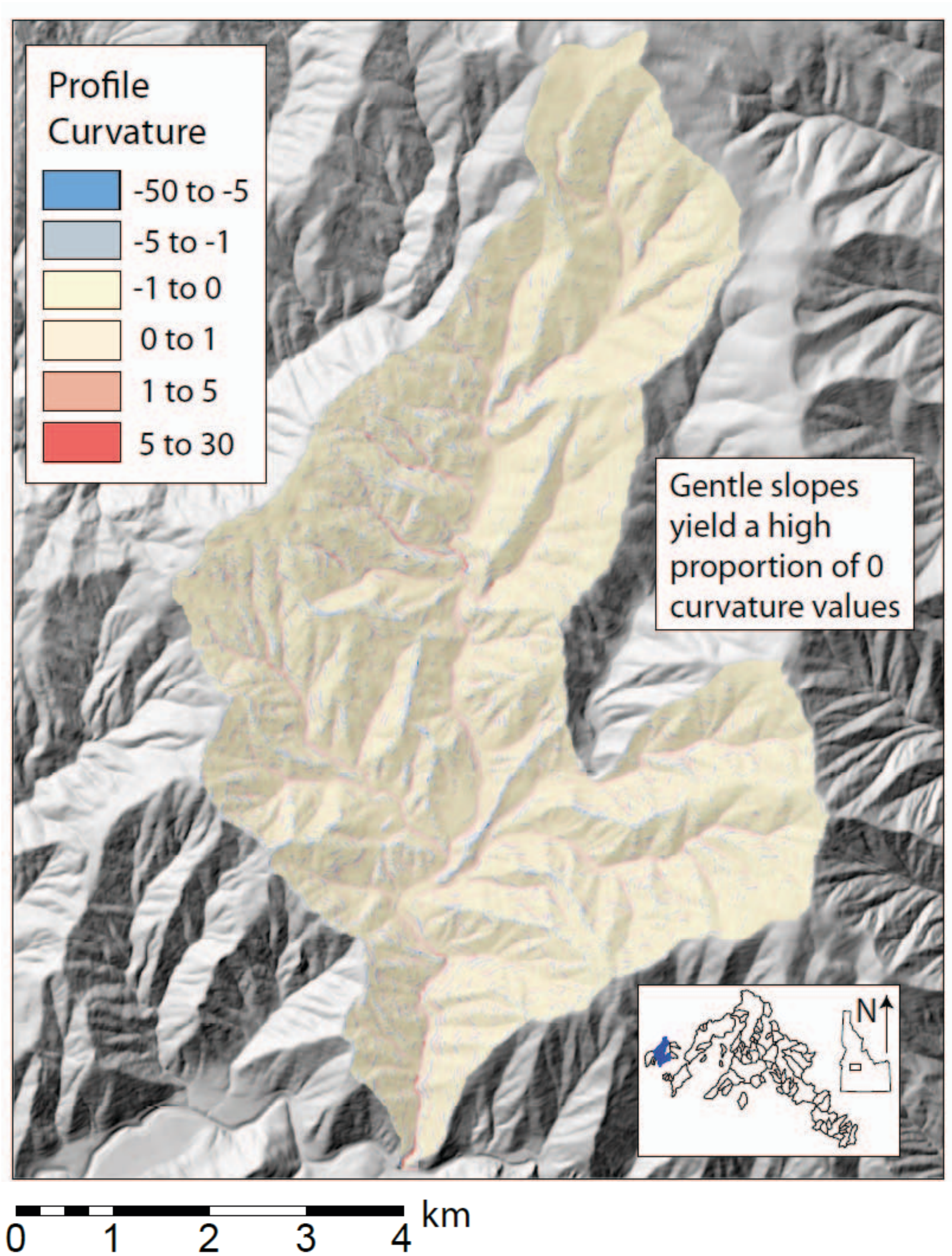


Figure 4.14: Profile curvature map of an example fluvial valley, Sawtooth Range, Idaho.

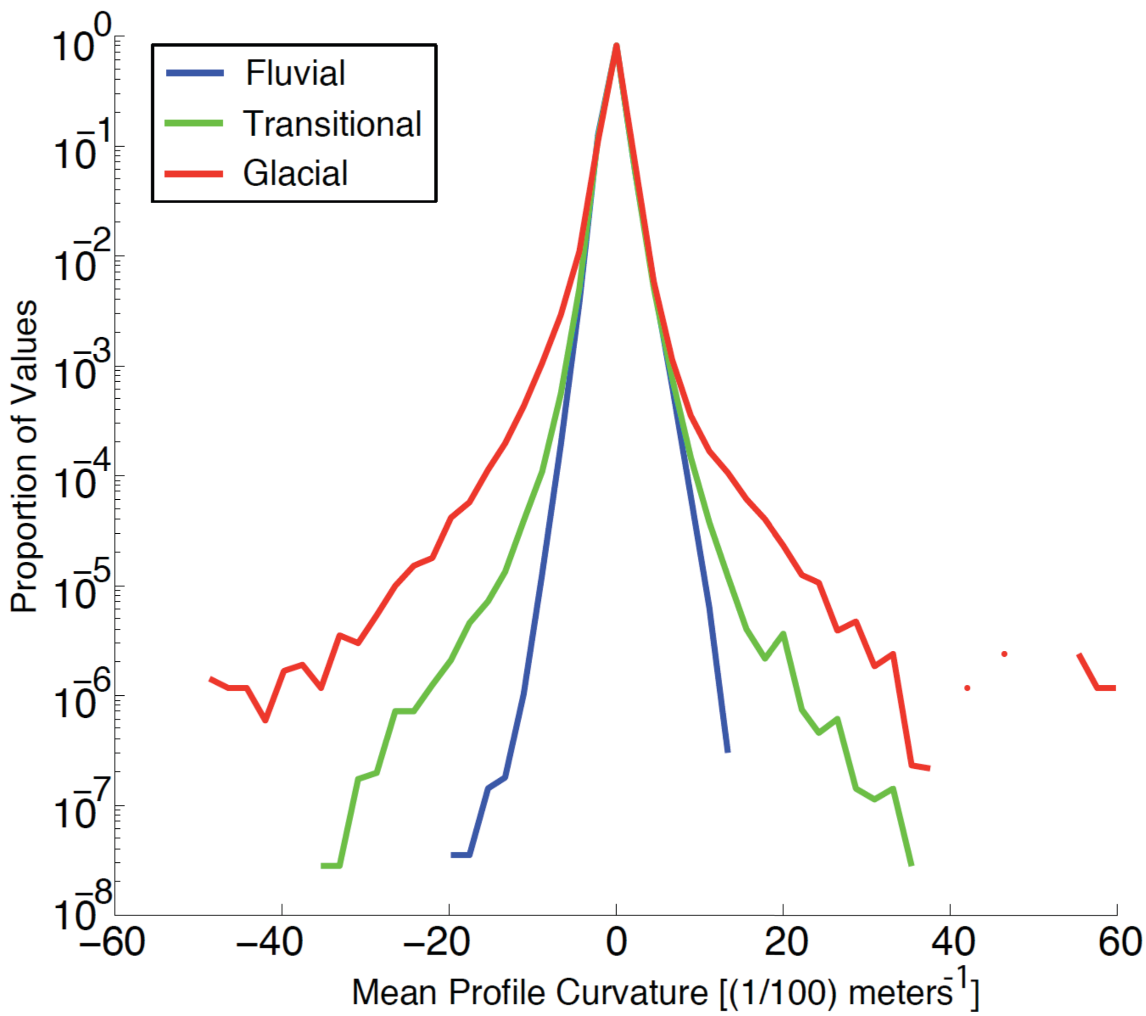


Figure 4.15: Mean profile curvature results for central Idaho, using weighted means of all fluvial, transitional, and glacial basins in the Sawtooth Range study area.

Table 4.3: Profile Curvature Values for central Idaho

| Sawtooth Range and South Fork Payette River Basin, Idaho: Profile Curvature | | | | | | |
|---|---|---|---|---|---|---|
| Basin Type | Min | Max | Mean | Mode | Median | Std Dev |
| Glacial | -48.5 | 59.8 | 0.0301 | 0.2218 | 0.05010 | 1.200 |
| Transitional | -24.9 | 25.9 | 0.0100 | -0.0320 | -0.00297 | 0.944 |
| Fluvial | -18.7 | 14.0 | 0.0025 | -0.0557 | -0.02220 | 0.933 |

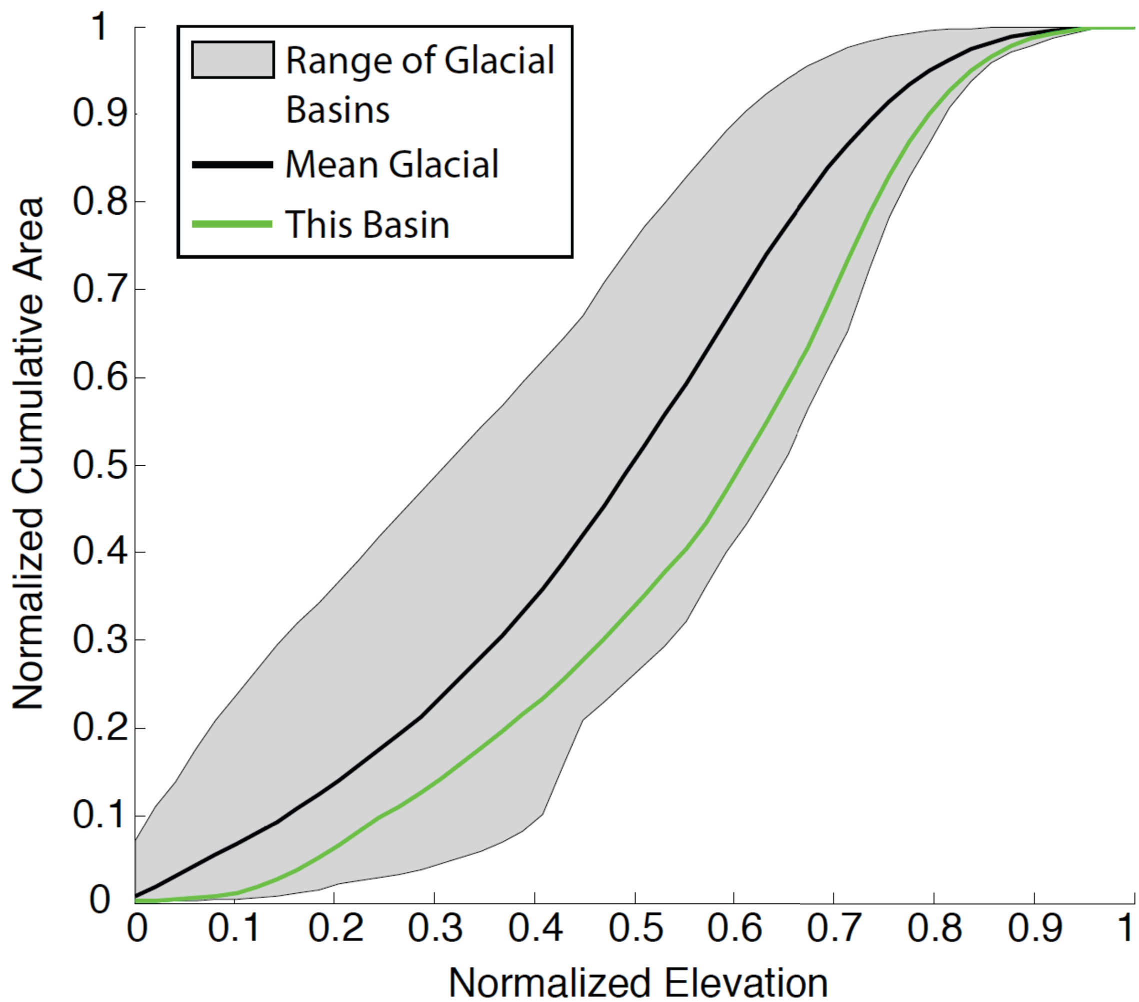


Figure 4.16: Elevation distribution plot for glacial basins in the central Idaho study area, with the weighted mean of all glacial basins (black line), elevation distribution curve of an example basin (green line), and the envelope that includes elevation distribution curves for all glacial basins (shaded gray area).

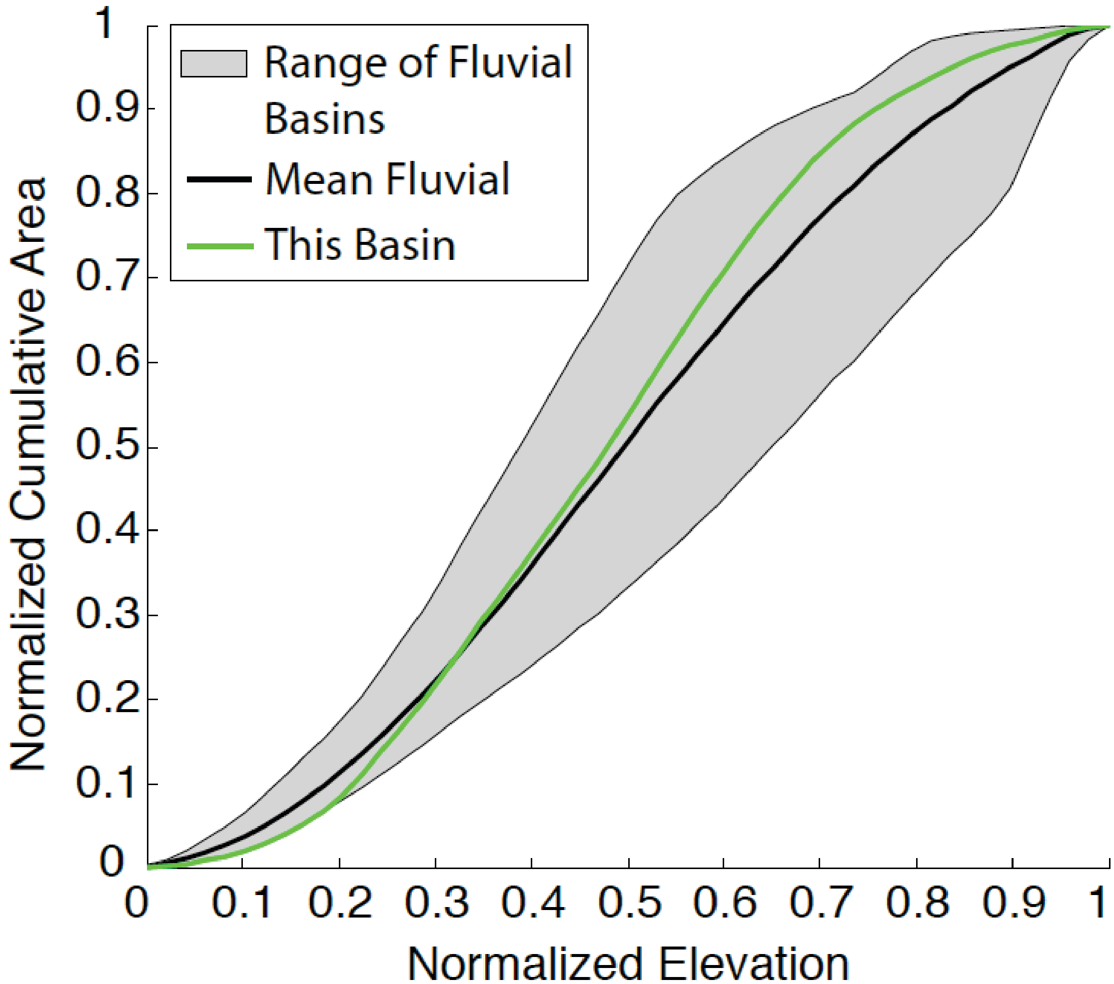


Figure 4.17: Elevation distribution plot for fluvial basins in the central Idaho study area, with the weighted mean of all fluvial basins (black line), elevation distribution curve of an example basin (green line), and the envelope that includes elevation distribution curves for all fluvial basins (shaded gray area).

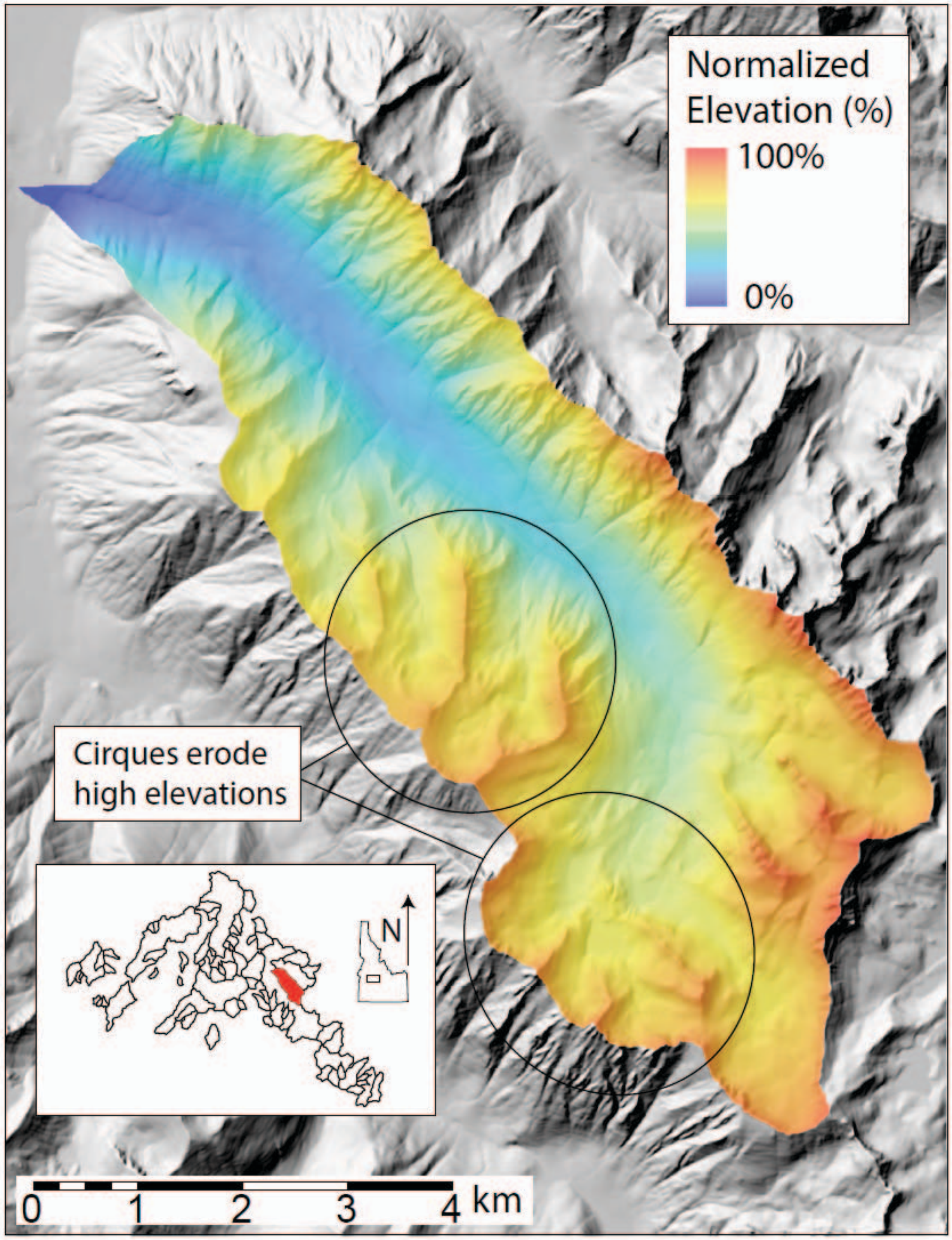


Figure 4.18: Elevation distribution map of an example glacial valley, Sawtooth Range, Idaho.

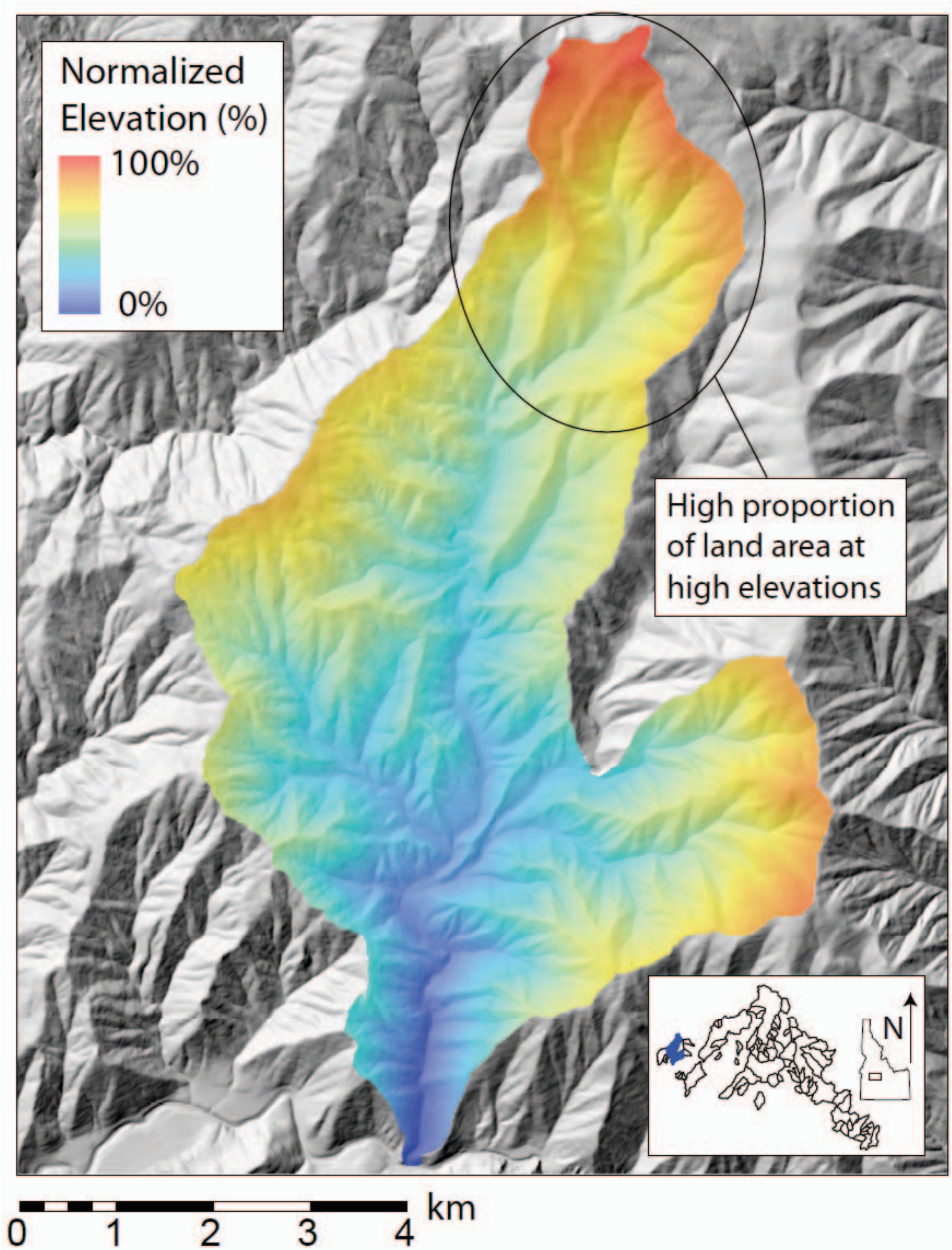


Figure 4.19: Elevation distribution map of an example fluvial valley, Sawtooth Range, Idaho.

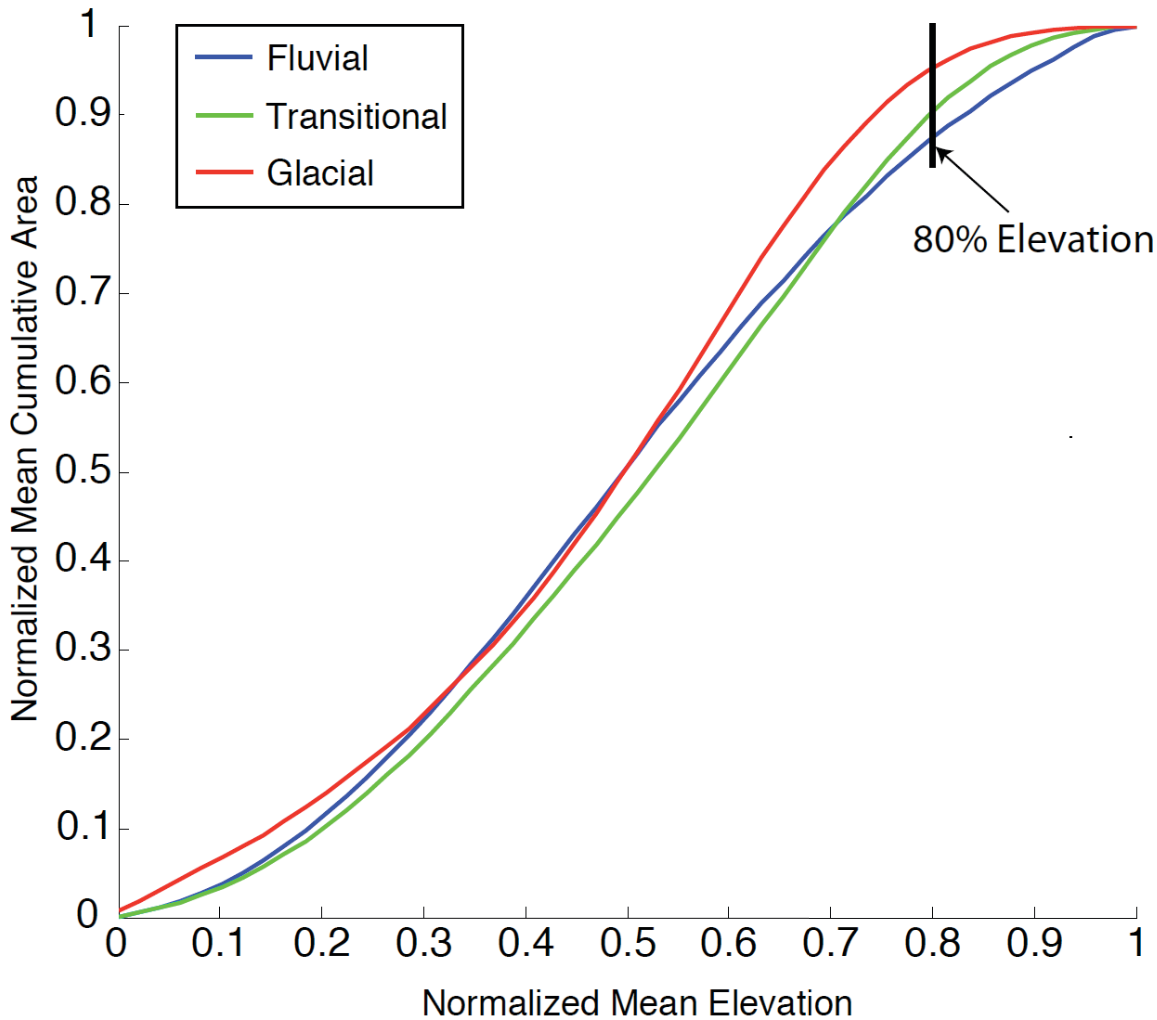


Figure 4.20: Hypsometric results for central Idaho. The line added at the 80% elevation line highlights a systematic decrease in land area at high elevations for glacial, transitional, and fluvial basins.

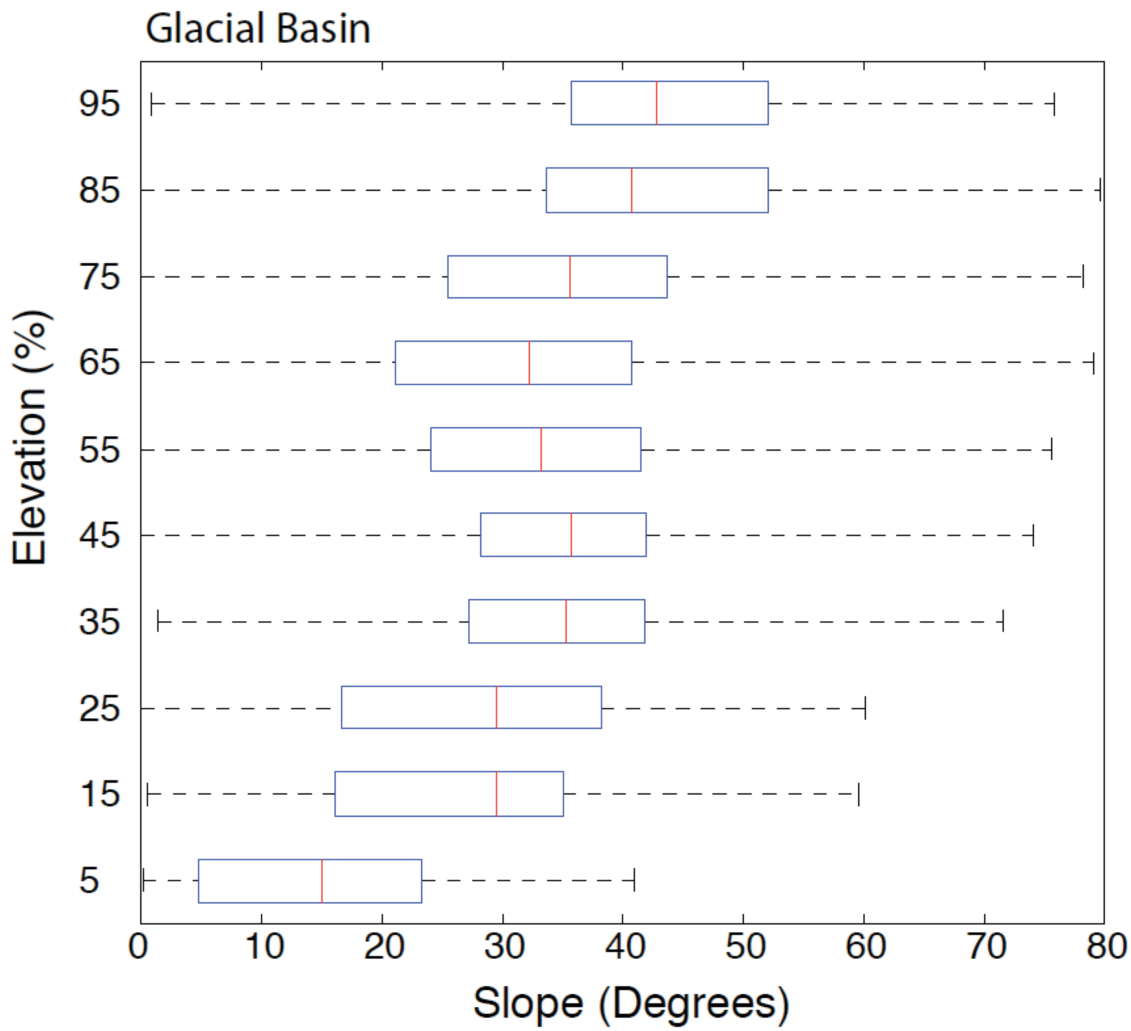


Figure 4.21: Slope vs. elevation plot of a typical glacial valley, Sawtooth Range, Idaho.

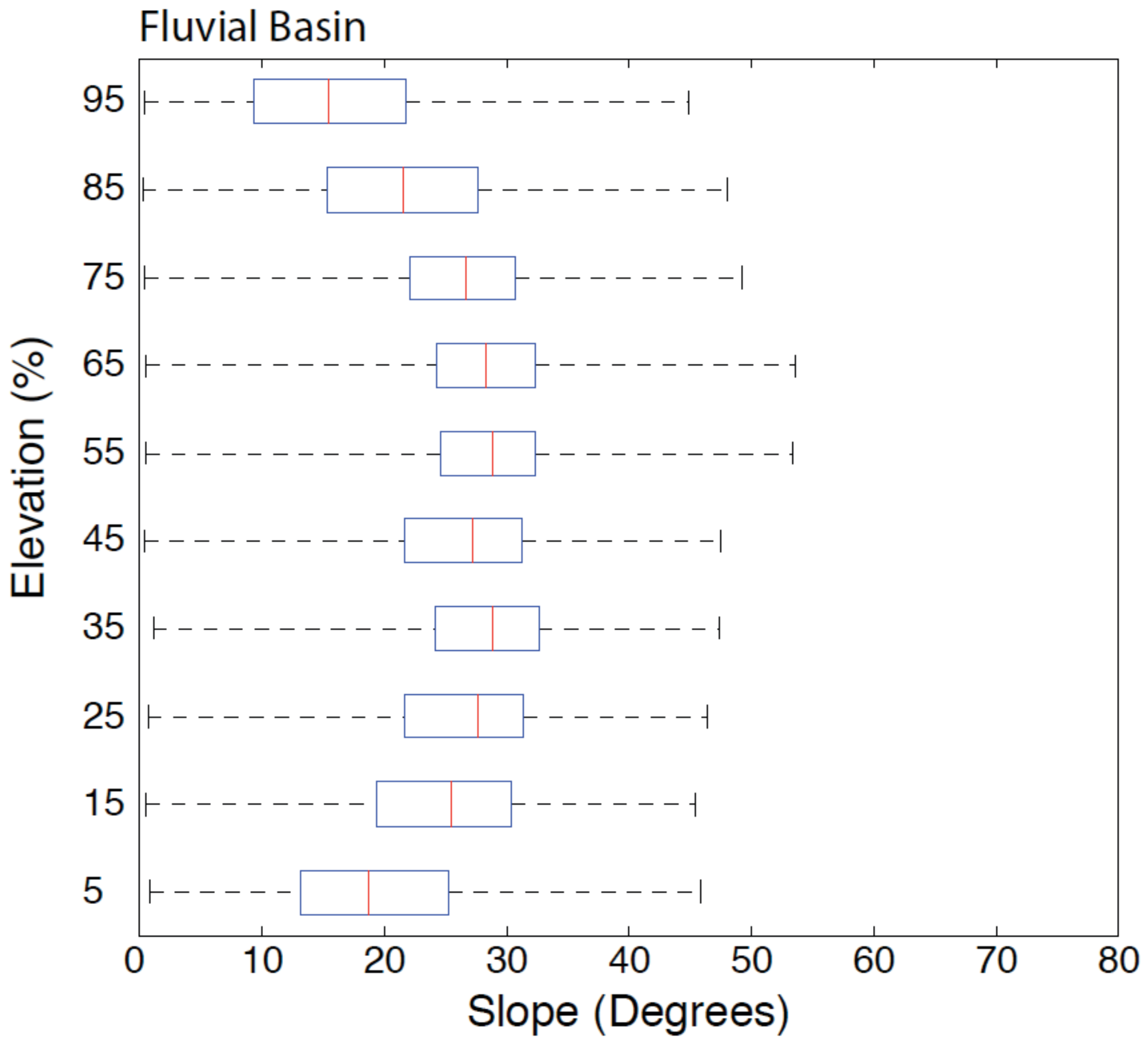


Figure 4.22: Slope vs. elevation plot of a typical fluvial valley, Sawtooth Range, Idaho.

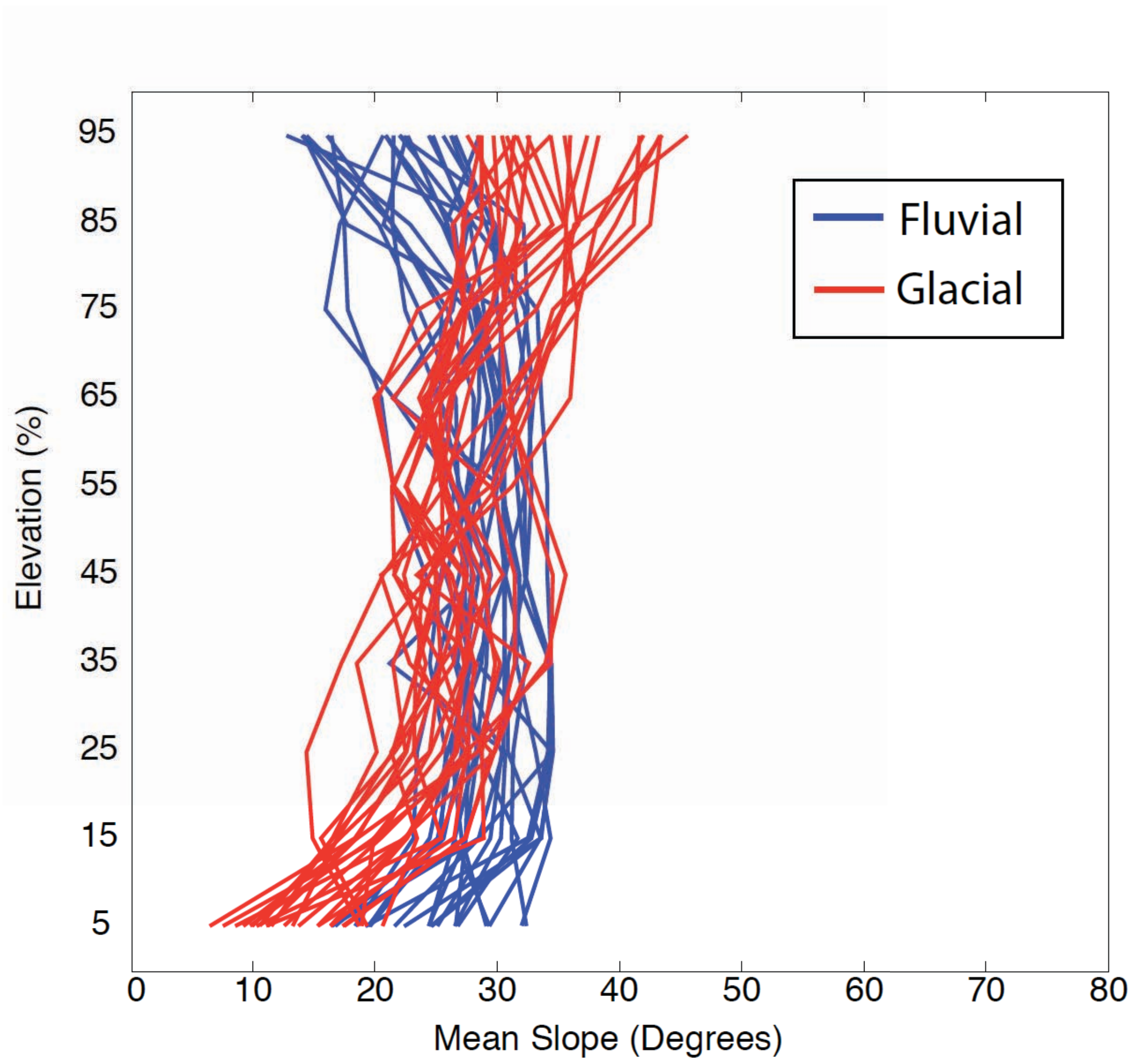


Figure 4.23**:** Slope vs. elevation plot showing the mean slope values for each basin at different elevations for glacial and fluvial basins in central Idaho.

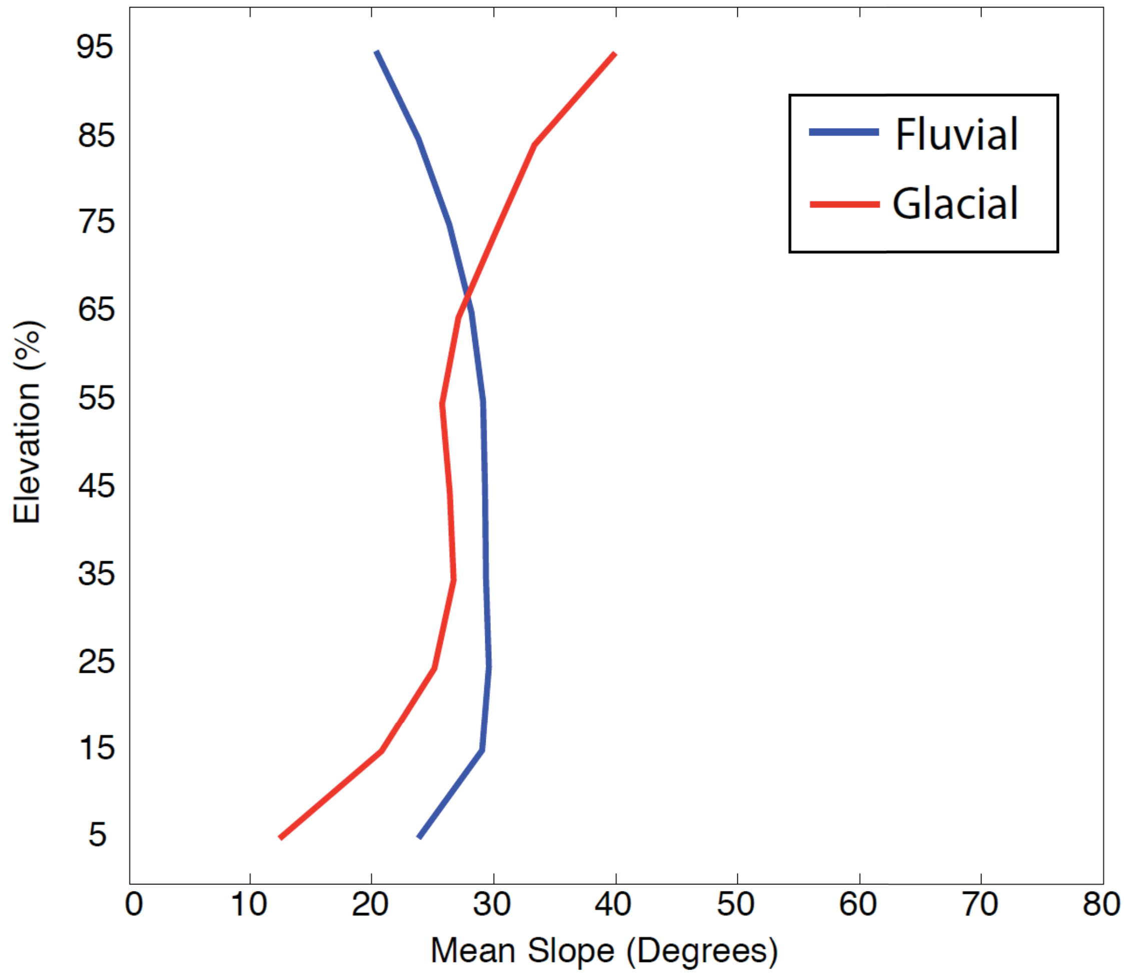


Figure 4.24**:** Slope vs. elevation plot showing the mean of all slope values at different elevations for glacial and fluvial basins in central Idaho.

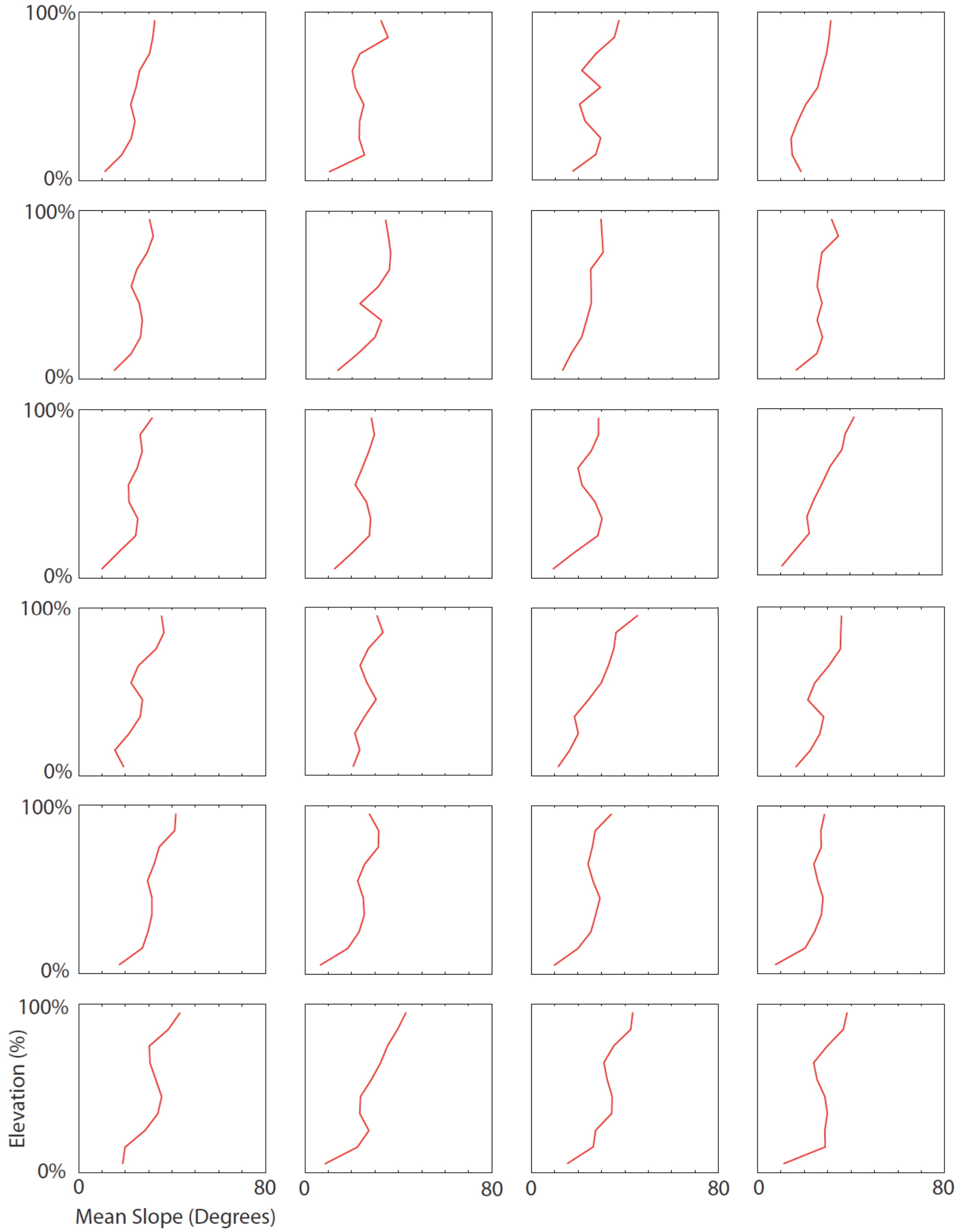


Figure 4.25: The curves of distribution of mean slope values across different elevations, showing the distinctive shape of mean slope curves for glacial basins. Each plot is set to the same scale, shown at bottom left.

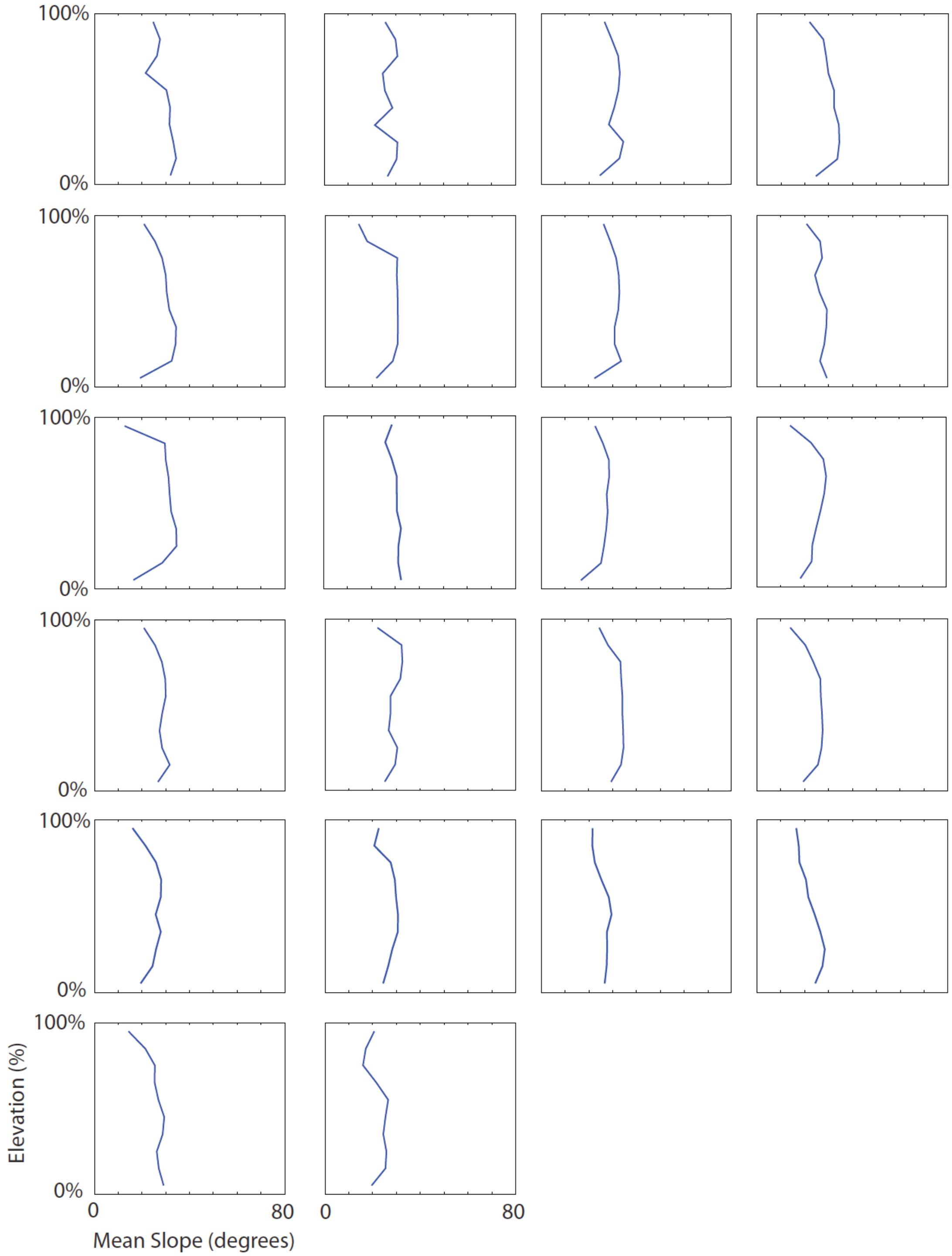


Figure 4.26: The curves of distribution of mean slope values across different elevations, showing the distinctive shape of mean slope curves for fluvial basins. Each plot is set to the same scale, shown at bottom left.

# CHAPTER V

# TESTING THE ROBUSTNESS OF GLACIAL METRICS

The reliability of metrics determined in the Sawtooth Range to assess degree of glacial modification are tested in the Olympic Mountains in Washington State. Glacial influence and extent has previously been studied in the Olympics (Montgomery, 2002). The Olympics have markedly different tectonics, lithology, and climate compared to central Idaho, allowing for not only verification of the reliability of metrics from central Idaho, but can also give us a sense of how other factors such as uplift rate and precipitation affect glaciated landscapes.

## Olympic Mountains, Washington

Quantitative analysis of valleys with varying degrees of glaciation is performed using U.S. Geologic Survey 10-meter resolution DEMs in the western Olympic Mountains in Washington State. We use previous classification (Montgomery, 2002) of glaciated, partially glaciated, and unglaciated basins in the Olympics.

The Olympic Range differs from the central Idaho field area in 3 key ways: less cohesive rocks, higher uplift rates, and higher precipitation. Rocks of the Olympic Range consists of late Miocene sediments and basalts accreted from the seafloor during the convergence of North America and the Juan de Fuca plate (Tabor and Cady, 1978). Uplift rates have remained constant in the western Olympic Mountains since ~14 Ma, at ~0.75

mm/yr (Brandon *et al*., 1998). Precipitation rates range from ~2.5 m/yr in the western section of the Olympic Mountains, to over 4.5 m/yr at higher elevations (source: www.wamaps.com).

Using the glacial extent presented in Montgomery, 2002, 3 glacial, 3 transitional, and 4 fluvial basins were chosen for analysis (figure 5.1). For our analysis, we chose basins not currently occupied by glaciers.

## Comparison of Results between the Olympic Range and Central Idaho

Comparison of slope values in the Olympics to values from central Idaho show consistent results between the two areas. Slope values show a systematic increase in standard deviation and range with increasing glacial influence. Direct comparison of slope frequency distribution curves from glacial, transitional, and fluvial basins between the Olympics and central Idaho show similar shapes between the two areas: glacial slope frequency distribution curves are characterized by a wider range of values, lower proportion of values at the peak of the curve, higher maximum values, and a high proportion of values below 10° compared to fluvial slope frequency distribution curves (figure 5.2). Glacial basins in the Olympics exhibit a higher proportion of 0° slope values compared to Idaho, due to wider and flatter valleys.

Comparison of planform and profile curvature values in the Olympics to values from central Idaho show consist results between the two areas. Curvature values show a systematic increase in standard deviation and range with increasing glacial influence.

Direct comparison of glacial and fluvial frequency distribution curves between the Olympics and central Idaho show similar shapes of distribution curves between the two areas: glacial curvature frequency distribution curves are characterized by a wider range of values compared to fluvial curvature frequency distribution curves (figures 5.3, 5.4).

Comparison of elevation distribution in the Olympics to elevation distribution curves from central Idaho show consistent results between the two areas: elevation distribution curves show a systematic decrease of land area at high elevations with increasing glacial influence. However, direct comparison of glacial and fluvial hypsometric curves between the Olympics and central Idaho show inconsistencies of the shapes of curves between the two areas (figure 5.5). Elevation distribution curves are useful for analyzing glacial landscapes within an area, but are not useful between different mountain ranges, consistent with past research (Brocklehurst and Whipple, 2004).

Slope vs. elevation plots for the Olympic Mountains, Washington show a similar pattern to slope vs. elevation plots in central Idaho: mean slope values at low elevations in glacial basins are lower compared to fluvial basins, and mean slope values at high elevations of glacial basins are high compared to fluvial basins (figures 5.6, 5.7). In both the Olympics and central Idaho, mean slope vs. elevation curves for glacial basins exhibit minimum values in the lower 10% of elevations, and maximum values in the upper 20%, giving the curves characteristic “S” shapes. Fluvial slope vs. elevation mean curves, however, exhibit low values in both the bottom 10% and top 10% of elevations, giving the curves a characteristic “bow” shape.

## Selection of Preferred Metrics for Identifying Glacial Erosion

The exceptional consistencies between the Olympics and central Idaho for slope and slope vs. elevation results allow us to select preferred metrics for assessing glacial influence in mountainous landscapes. Slope results show a lower peak frequency of slope values, higher variation, and a higher proportion of 50° slope values between glacial and fluvial basins. Slope vs. elevation results show a higher range of values, maximum values at higher elevations, and higher mean slope values between glacial and fluvial basins. While curvature results show differences in variation for glacial, transitional, and fluvial basins, specific metrics remain elusive between different field areas. Elevation distribution curves show a systematic decrease in amount of land area at high elevations with increasing glacial influence; however, results are inconsistent between field areas.

Consistencies between the Olympics and central Idaho allow for determination of "type curves": criteria for classifying the degree of glaciation in a basin. Glacial basins exhibit slope frequency distribution plots with:

1. A proportion of slope values above 50°
2. Peak frequency of curves below 0.06
3. Range of proportion of values at 0.01 greater than 45° (figure 5.8).

For slope vs. elevation plots, glacial basins exhibit:

1. Maximum slope values above 80% elevation
2. Mean slope values greater than 30°
3. Range of slope values greater than 20° (figure 5.9).

For each type curve, classification of glacial influence is based on how many of the preceding criteria are met. Results for the two type curves applied to a basin are added together to create a classification based on 6 total criteria. If 5-6 out of 6 criteria are met, the basin is considered “high glacial,” if 3-4 out of 6 criteria are met the basin is considered “mid glacial,” if 1-2 out of 6 criteria are met the basin is considered “low glacial,” and if 0 out of 6 criteria are met the basin is considered fluvial.

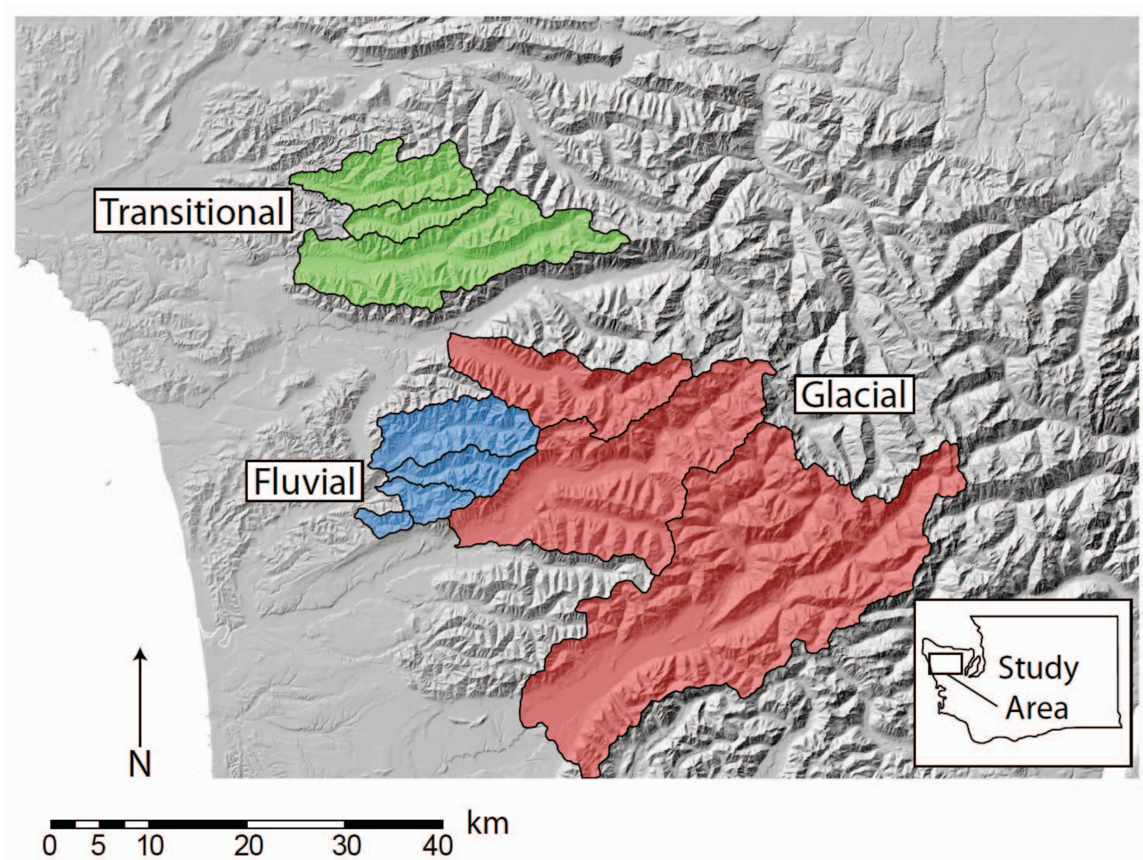


Figure 5.1: Study area in the Olympic Mountains, Washington showing glacial (red), transitional (green), and fluvial (blue) basins used for analysis. Basins area selected based on previous work (Montgomery, 2002).

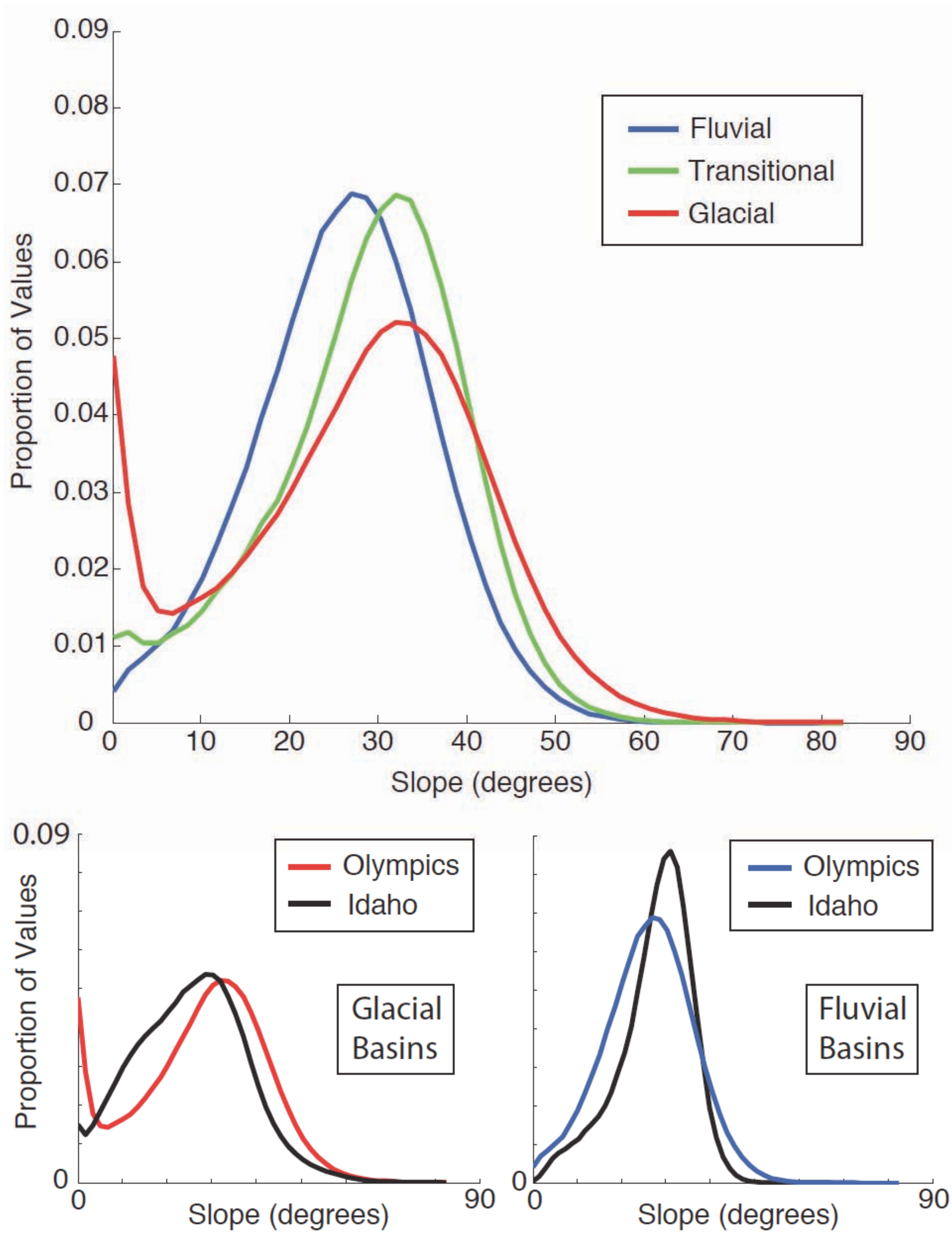


Figure 5.2: Frequency distribution plots of weighted mean slope values for glacial, transitional, and fluvial basins in the Olympic Range (top), comparison of glacial slope values between the Olympics and Idaho (bottom left), and comparison of fluvial slope values between the Olympics and Idaho (bottom right).

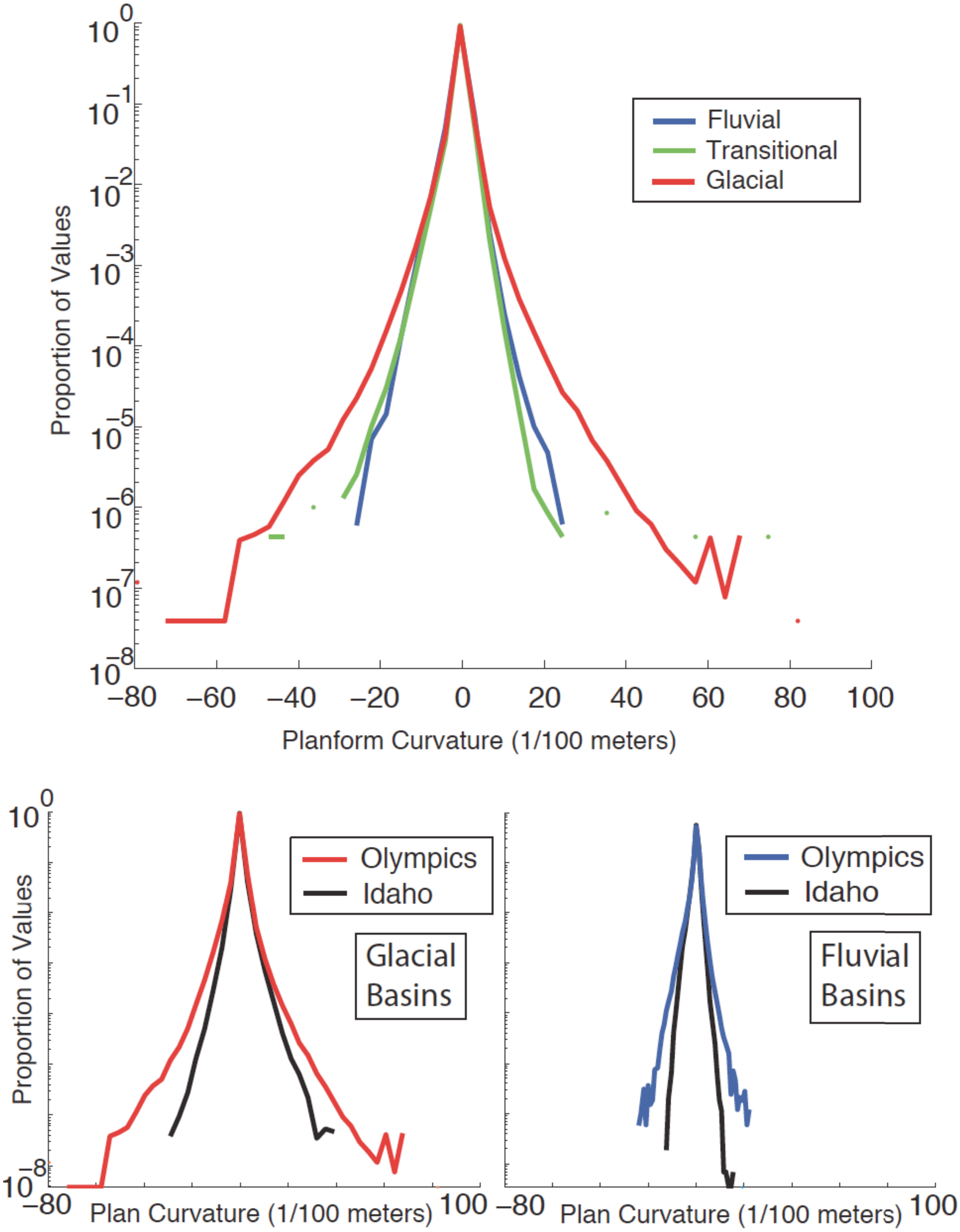


Figure 5.3: Frequency distribution plots of weighted mean planform curvature values for glacial, transitional, and fluvial basins in the Olympic Range (top), comparison of glacial planform curvature values between the Olympics and Idaho (bottom left), and comparison of fluvial planform curvature values between the Olympics and Idaho (bottom right).

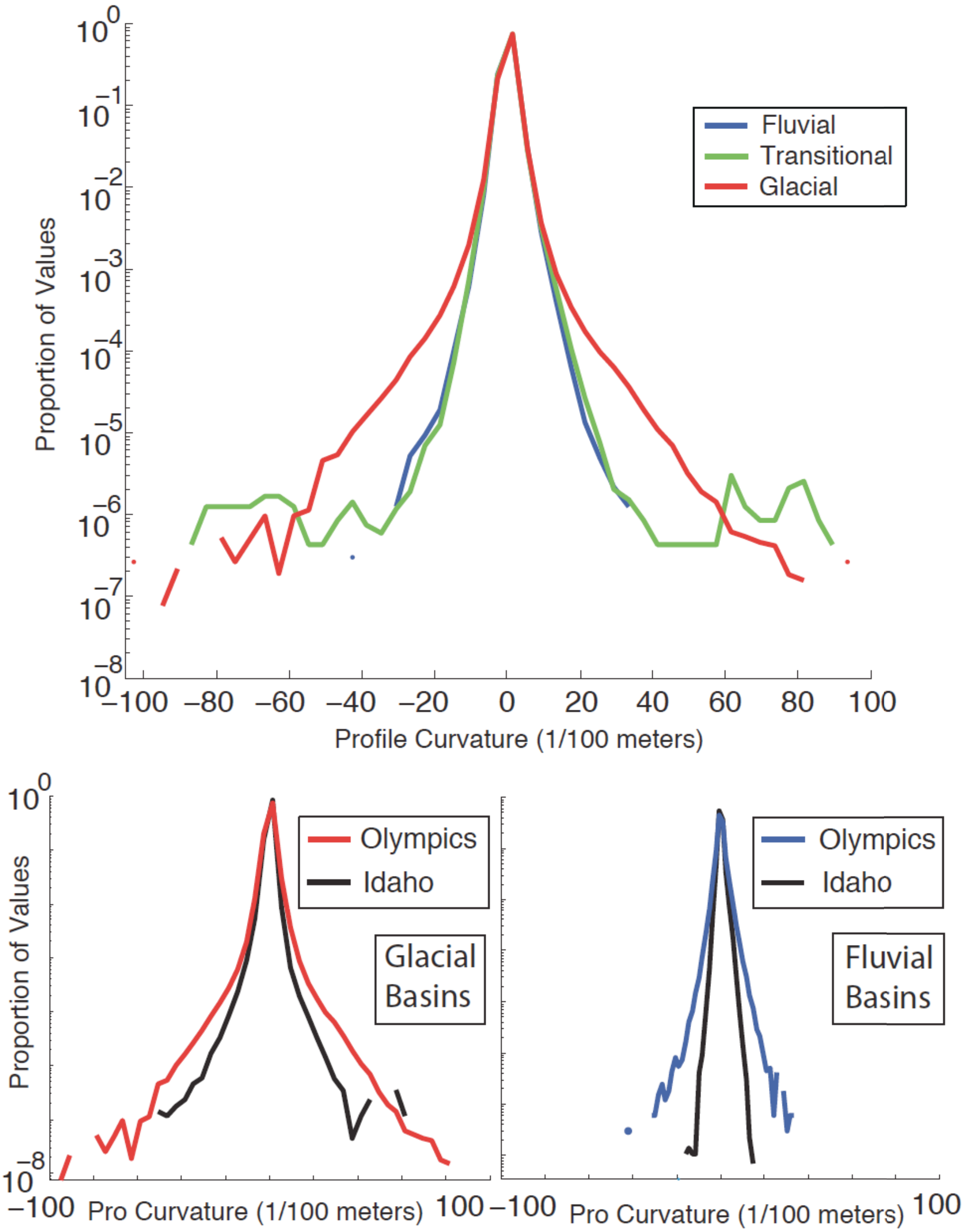


Figure 5.4: Frequency distribution plots of weighted mean profile curvature values for glacial, transitional, and fluvial basins in the Olympic Range (top), comparison of glacial profile curvature values between the Olympics and Idaho (bottom left), and comparison of fluvial profile curvature values between the Olympics and Idaho (bottom right).

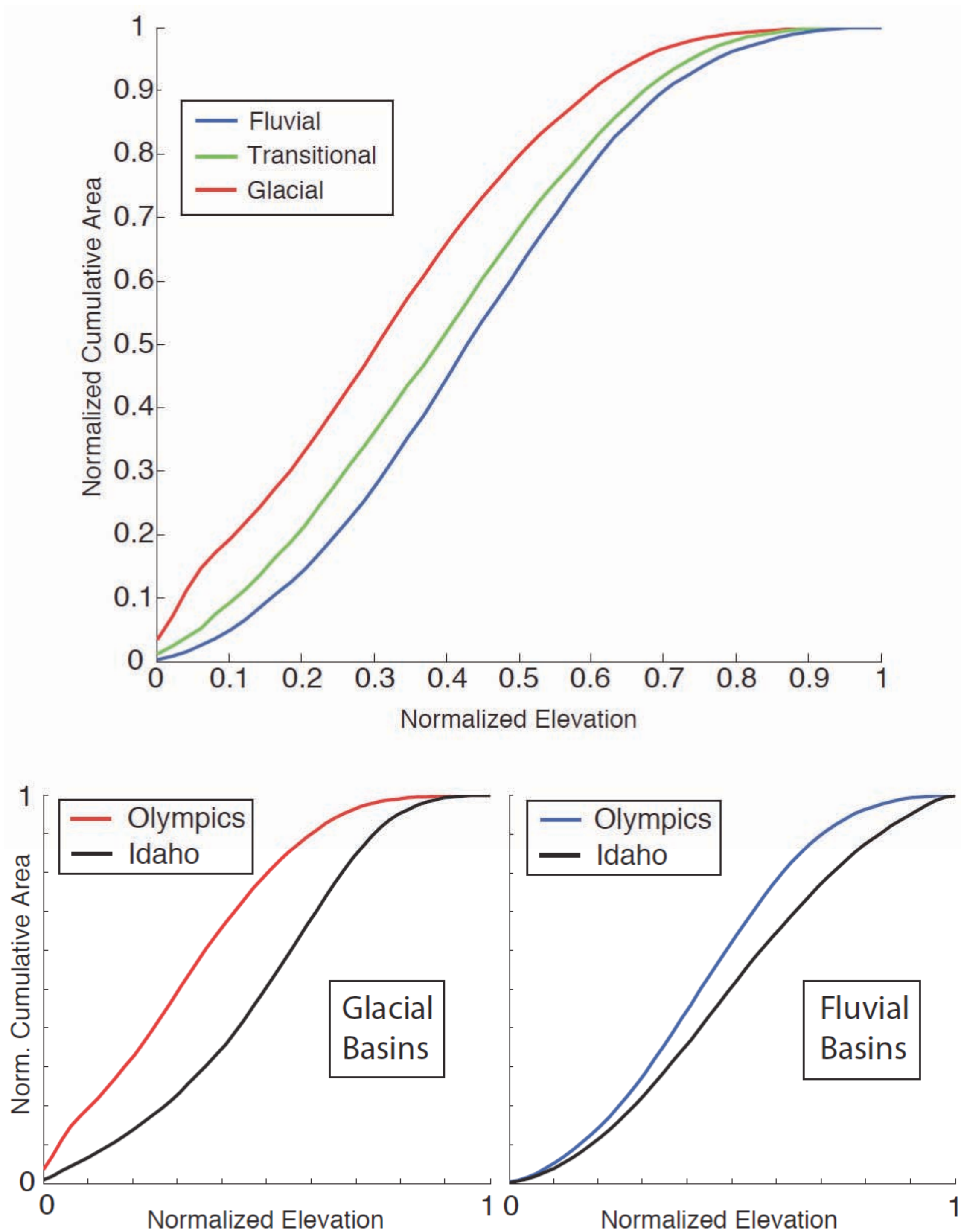


Figure 5.5: Elevation distribution curves for glacial, transitional, and fluvial basins in the Olympic Range (top), comparison of glacial elevation distribution curves between the Olympics and Idaho (bottom left), and comparison of fluvial elevation distribution curves between the Olympics and Idaho (bottom right). All plots set to the same scale.

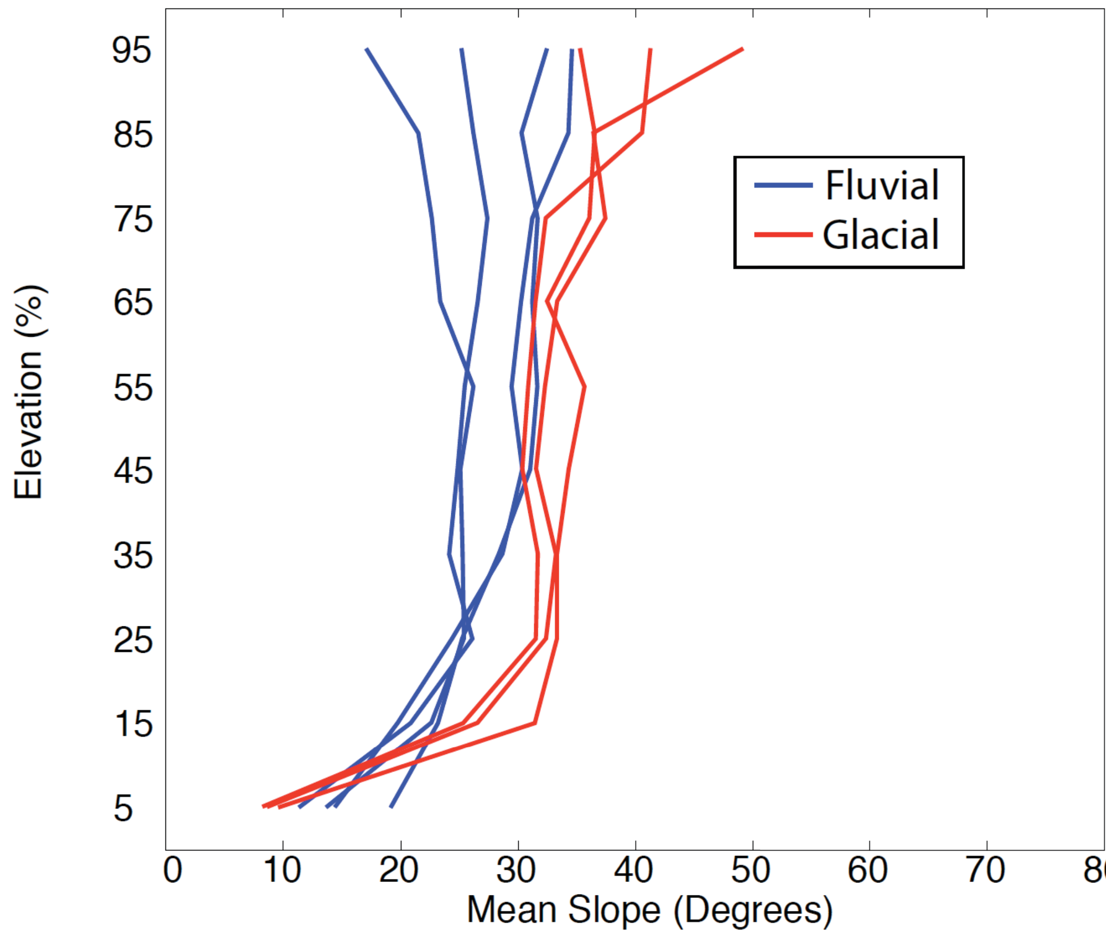


Figure 5.6: Slope vs elevation plot showing mean slope values at different elevations for glacial and fluvial basins in the Olympic Mountains, Washington. Glacial valleys exhibit low mean slope values in lower elevations (flat valley bottoms) and high mean slope values at higher elevations (arêtes).

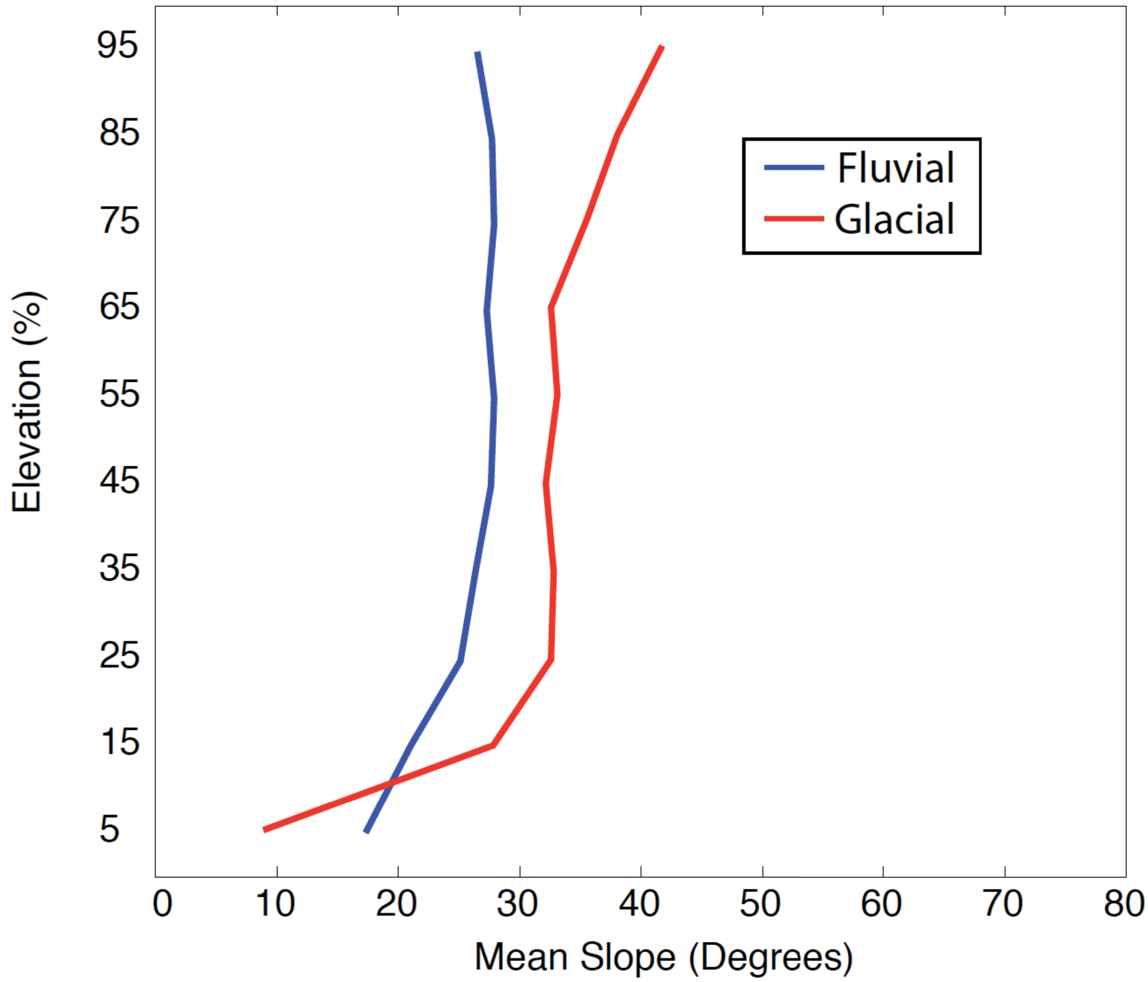


Figure 5.7: Slope vs elevation plot showing the mean slope values at different elevations for glacial and fluvial basins in the Olympic Mountains, Washington.

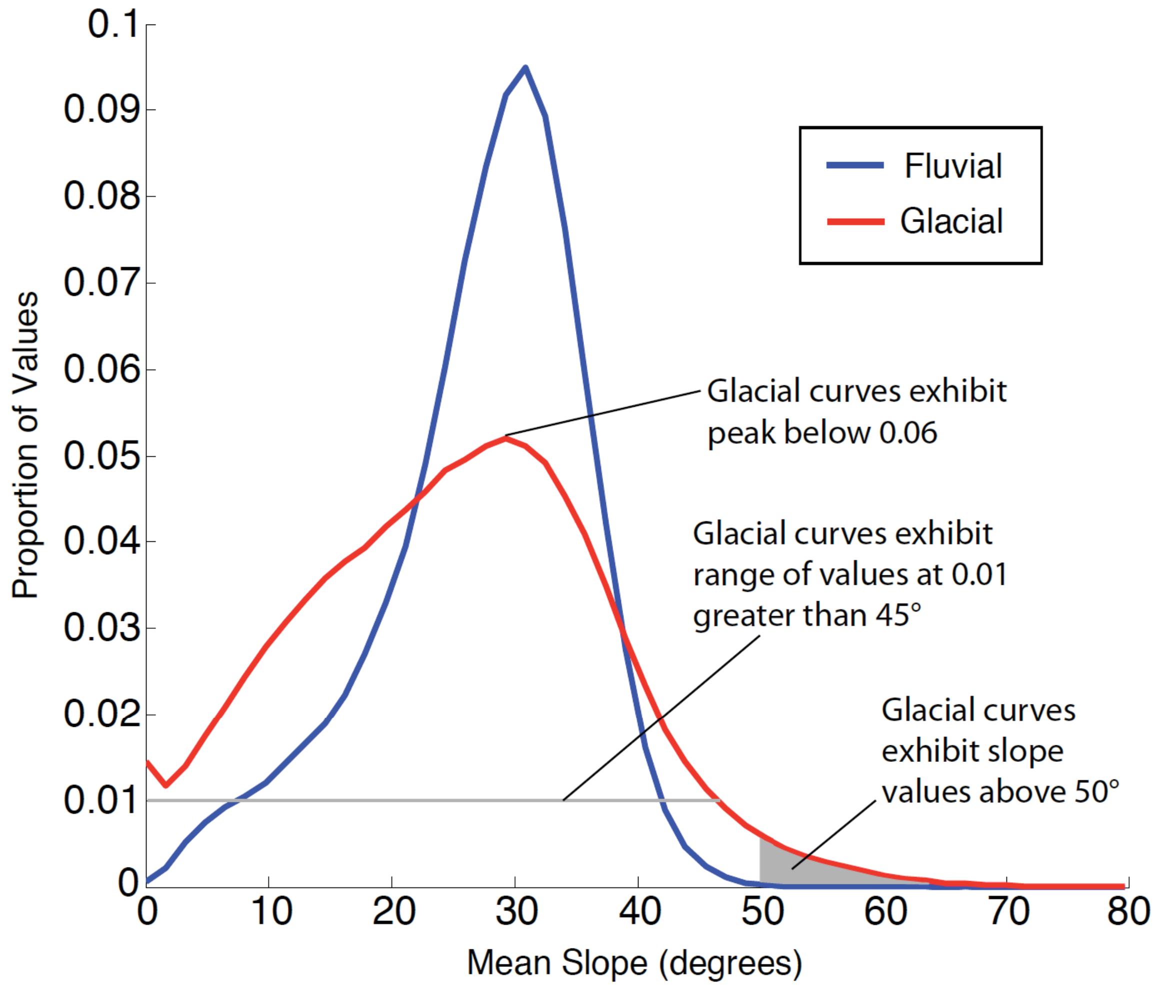


Figure 5.8: Attributes of frequency distribution type curves identified between the Olympics and central Idaho that indicate glacial modification.

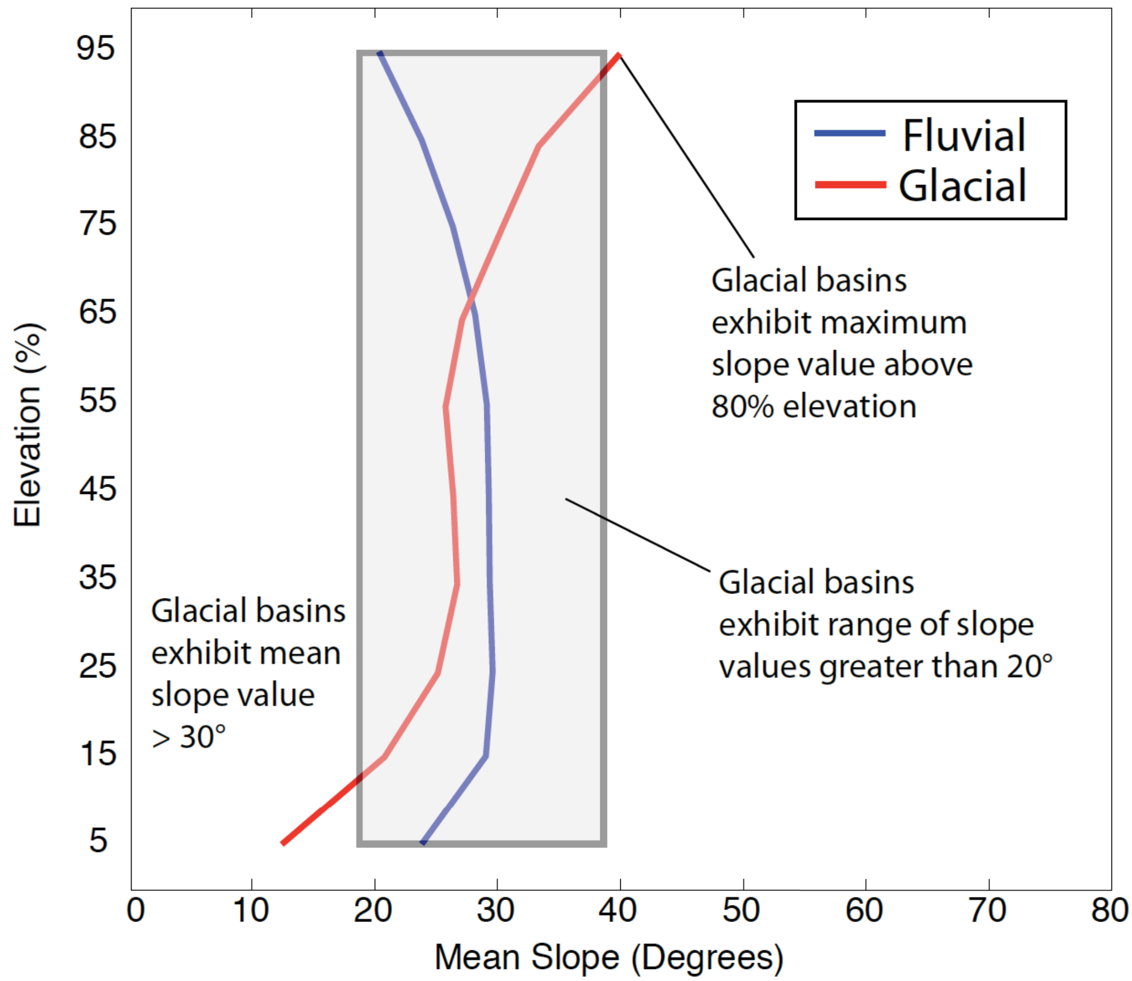


Figure 5.9: Attributes of frequency distribution type curves identified between the Olympic Range and central Idaho that indicate glacial modification.

# CHAPTER VI

# APPLICATION OF GLACIAL METRICS TO A TEST AREA

To test our glacial metrics, we go to the Two Thumb Range, New Zealand. The Two Thumb Range consists of granitic bedrock (Brook *et al*., 2008) that is very uniform throughout the range, and highly resistant to glacial erosion (Augustinus, 1992). Uplift rates in the region are high at ~1-5 mm/yr (Tippet and Kamp, 1995; Upton *et al*., 2004), and precipitation rates range from ~0.6 m/yr in the south to ~5 m/yr in the north (McGowan and Sturman, 1997). Previous work (Brook *et al*., 2008) determined that degree of glacial modification increases northward along the Two Thumb Range, which allows for an opportunity to test our metrics at determining degree of glaciation in individual basins. Using a New Zealand National 25-meter resolution DEM in the Two Thumb Range, 15 basins were chosen to test the robustness of our metrics in determining degree of glaciation. For each basin, we use the 2 type curves with 3 criteria each (6 total criteria) to determine the relative degree of glaciation in a basin.

In general, peak frequency decreases northward, the occurrence of 50° slope values increases northward, and the range of values at 0.01 proportion increases northward, indicating increasing glacial erosion (figure 6.1). Slope distribution plots exhibit increasing mean slope values, maximum values in the upper 80% of basin elevation, and increasing range of slope values northward, indicating increasing glacial erosion (figure 6.2).

Classification of basins ranges from fluvial to high glacial, generally from south to north along the Two Thumb Range (figure 6.3). Classification based on type curves is consistent with Brook *et al*., 2008: degree of glaciation increases northward along the Two Thumb Range with the exception of one basin in the southern reach classified as mid glacial (figures 6.1 - 6.3, table 6.1). The basin in the southern reach that is classified as mid glacial barely meets a few of the criteria, yet shows the limitation of a technique that uses strict guidelines to classify the amount of glacial influence that has occurred in a basin. Overall, our results show that quantitative metrics can be used to not only select glacial and fluvial basins, but also to determine relative degree of glaciation in mountainous landscapes.

To verify classification of glacial influence, we look at features in the landscape that indicate past glacial erosion such as flat bottomed U-shaped valleys, cirques and arêtes.

In the basins classified as high glacial, we see visual evidence consistent with glaciation: steep valley walls, flat valley bottoms, arêtes, horns, and cirques (figures 6.4, 6.5). Basins classified as mid glacial, however, yield steep slopes and arêtes, but lack cirques (figure 6.6).

Visually, the basin classified as mid glacial in the southern part of the Two Thumb Range appears fluvial (figure 6.7), however steeper peaks in the upper elevations of the range may be the cause of its classification.

The basins classified as low glacial exhibit limited arêtes, but show dendritic, V-shaped valleys consistent with fluvial basins (figure 6.8).

The basins in the southern Two Thumb Range classified as fluvial exhibit flat drainages where sediment has accumulated, indicative of past glacial erosion, but overall show gentle slopes and dendritic patterns and rounded hilltops consistent with fluvially dominate landscapes (figure 6.9).

Basins in the Two Thumb Range show visual evidence of increasing glaciation northward along the Two Thumb Range: more flat valley bottoms, steeper valley sides, more cirques and arêtes, which supports our analysis and is consistent with results from Brook *et al*., (2008). Despite the basin in the southern extent of the Two Thumb Range classified as mid glacial, our metrics work extremely well at classifying basins in mountainous areas into different degrees of glaciation.

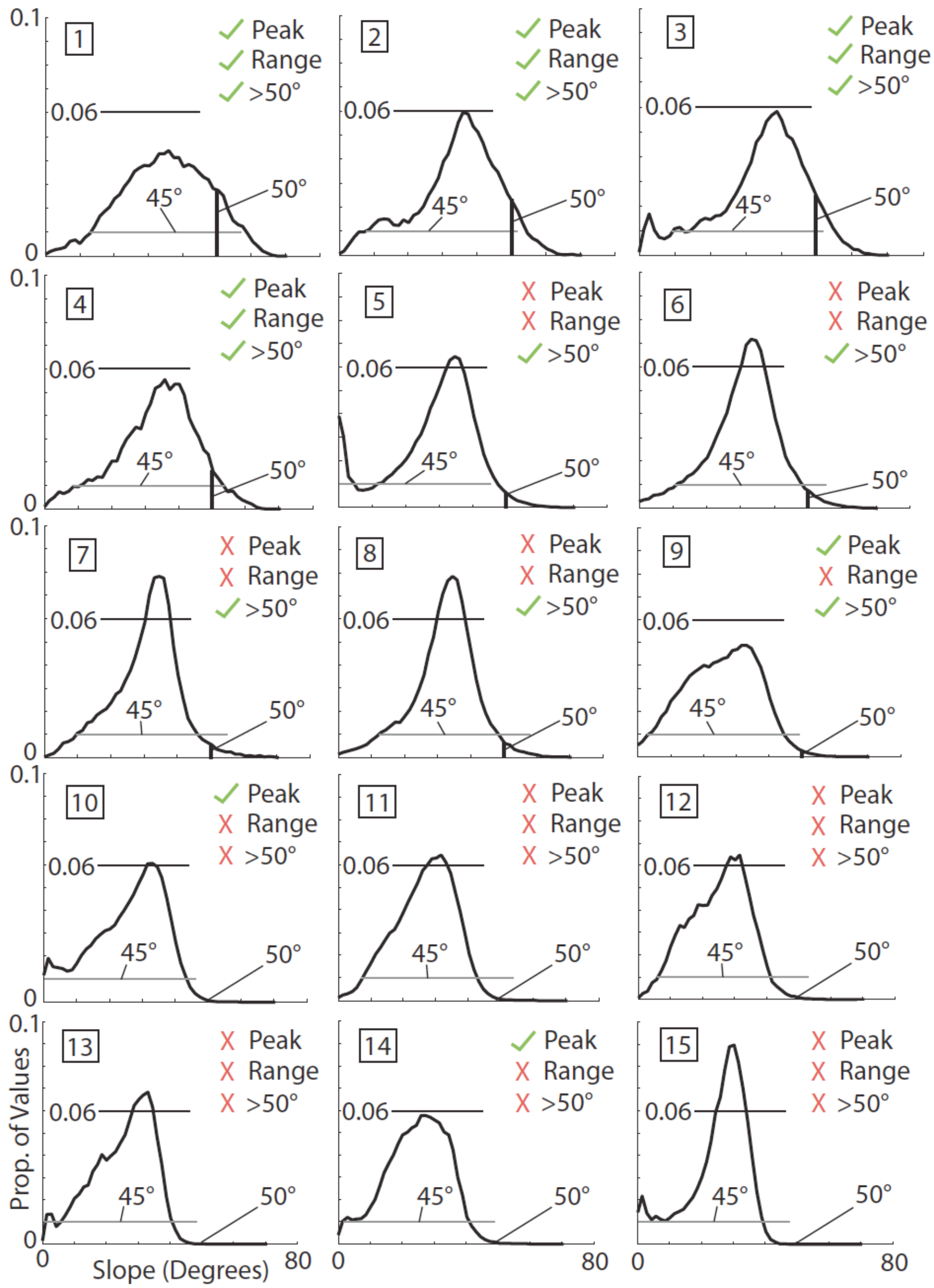


Figure 6.1: Classifications based on slope frequency distribution type curves for each basin in the Two Thumb Range. The 3 criteria used to determine glacial influence are: peak frequency below 0.06 proportion of values, range of slope values greater than 45° at 0.10 proportion of values, slope values above 50°. Basins are numbered based on glacial influence determined in Brook *et al*., 2008 with 1 being most glaciated, and 15 being the least glaciated.

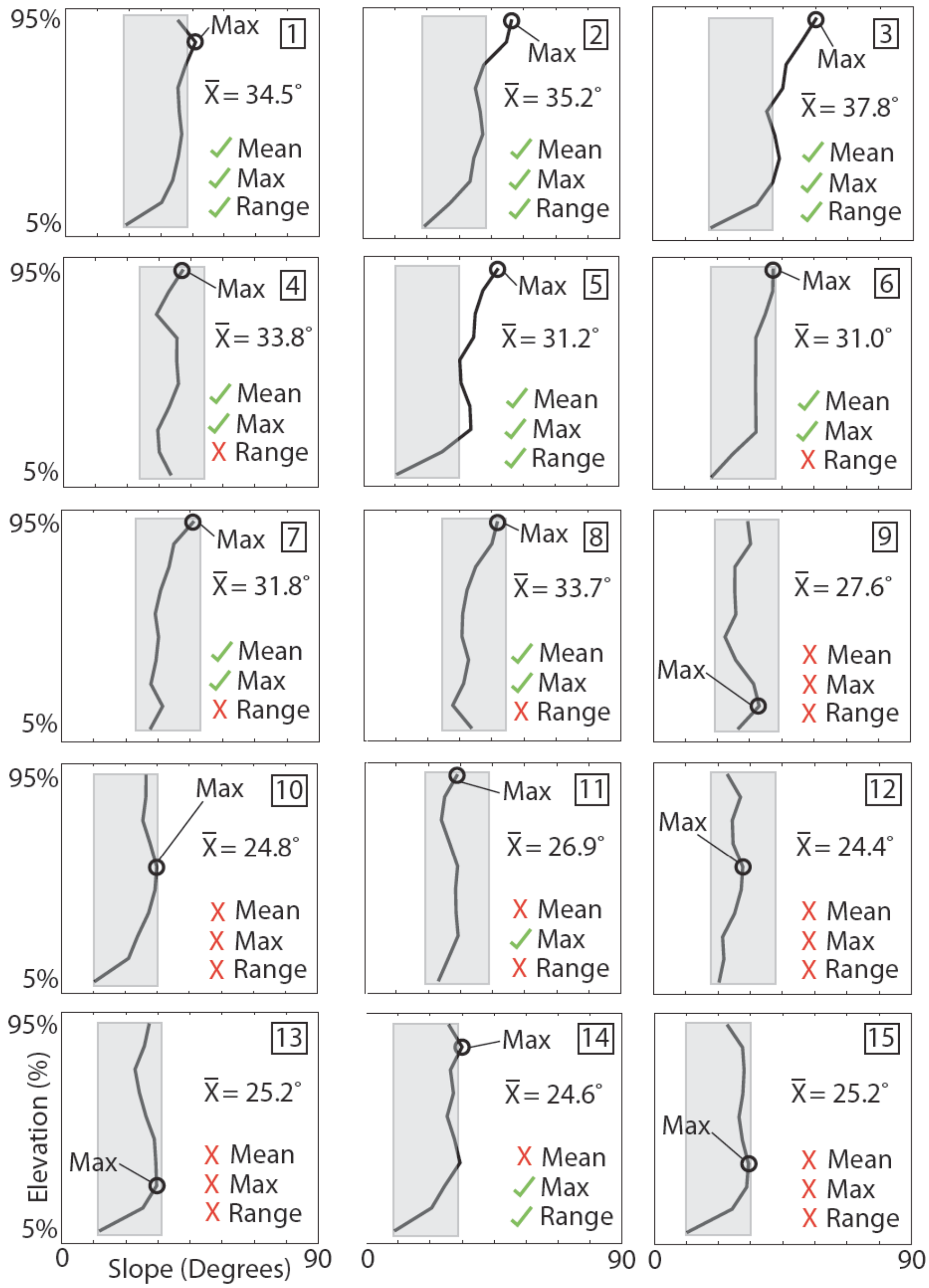


Figure 6.2: Classifications based on slope vs. elevation plots type curves for each basin in the Two Thumb Range. The 3 criteria used to determine glacial influence are: maximum value is above 80% elevation, the mean slope value is greater than 30°, and the range of slope values is greater than 20°. Basins are numbered based on glacial influence determined in Brook *et al*., 2008 with 1 being most glaciated, and 15 being the least glaciated.

Table 6.1: Classifications for basins in the Two Thumb Range based on frequency distribution and slope vs. elevation type curves.

| Basin | Slope Freq. Dist. | Slope vs. Elevation | Classification |
|---|---|---|---|
| 1 | (3/3) High Glacial | (3/3) High Glacial | (6/6) High Glacial |
| 2 | (3/3) High Glacial | (3/3) High Glacial | (6/6) High Glacial |
| 3 | (3/3) High Glacial | (3/3) High Glacial | (6/6) High Glacial |
| 4 | (3/3) High Glacial | (2/3) Mid Glacial | (5/6) High Glacial |
| 5 | (1/3) Low Glacial | (3/3) High Glacial | (4/6) Mid Glacial |
| 6 | (1/3) Low Glacial | (2/3) Mid Glacial | (3/6) Mid Glacial |
| 7 | (1/3) Low Glacial | (2/3) Mid Glacial | (3/6) Mid Glacial |
| 8 | (1/3) Low Glacial | (2/3) Mid Glacial | (3/6) Mid Glacial |
| 9 | (2/3) Mid Glacial | (0/3) Fluvial | (2/6) Low Glacial |
| 10 | (1/3) Low Glacial | (0/3) Fluvial | (1/6) Low Glacial |
| 11 | (0/3) Fluvial | (1/3) Low Glacial | (1/6) Low Glacial |
| 12 | (0/3) Fluvial | (0/3) Fluvial | (0/6) Fluvial |
| 13 | (0/3) Fluvial | (0/3) Fluvial | (0/6) Fluvial |
| 14 | (1/3) Low Glacial | (2/3) Mid Glacial | (3/6) Mid Glacial |
| 15 | (0/3) Fluvial | (0/3) Fluvial | (0/6) Fluvial |

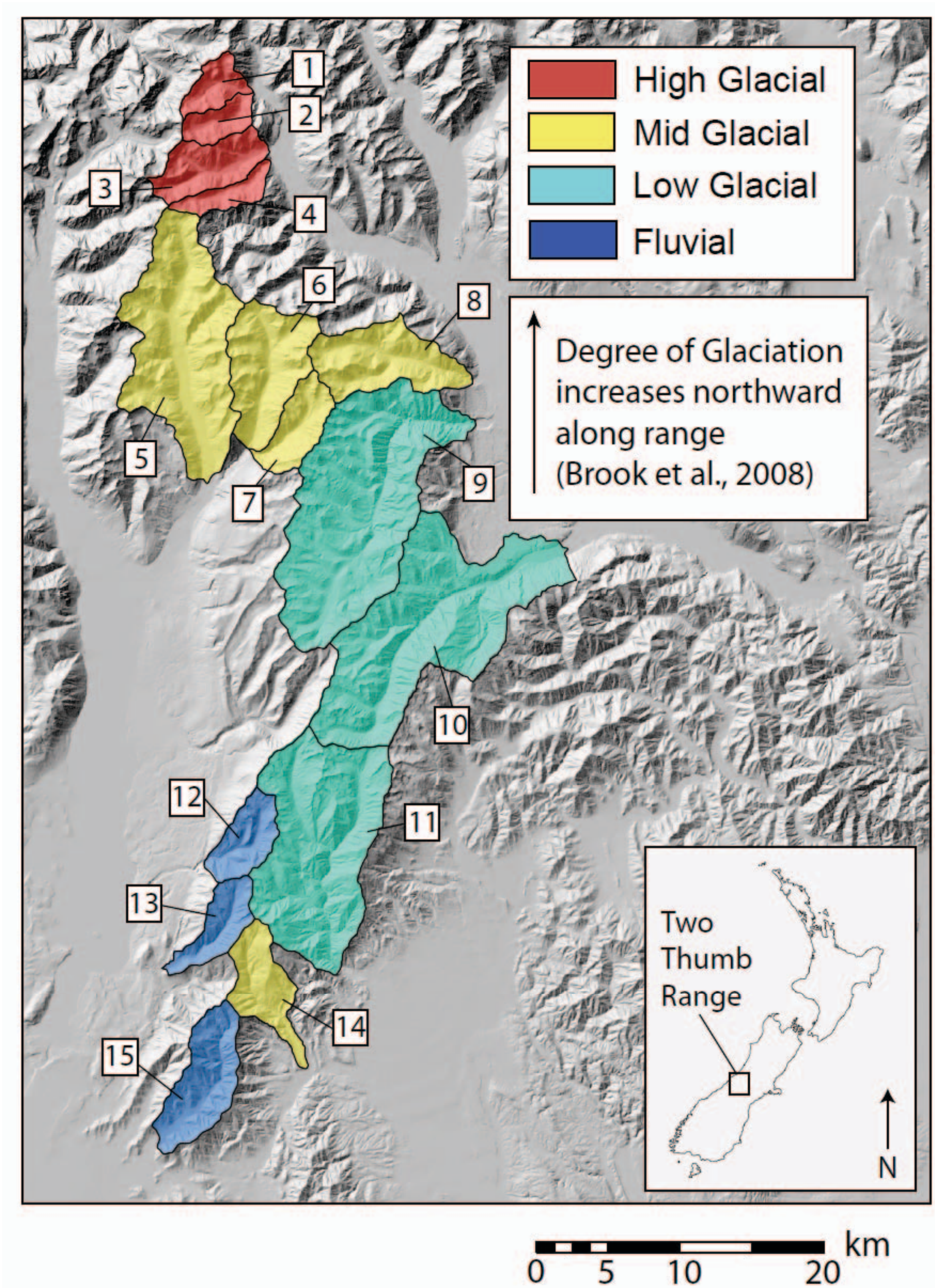


Figure 6.3: Classification of basins in the Two Thumb Range based on results from type curves (table 6.1).

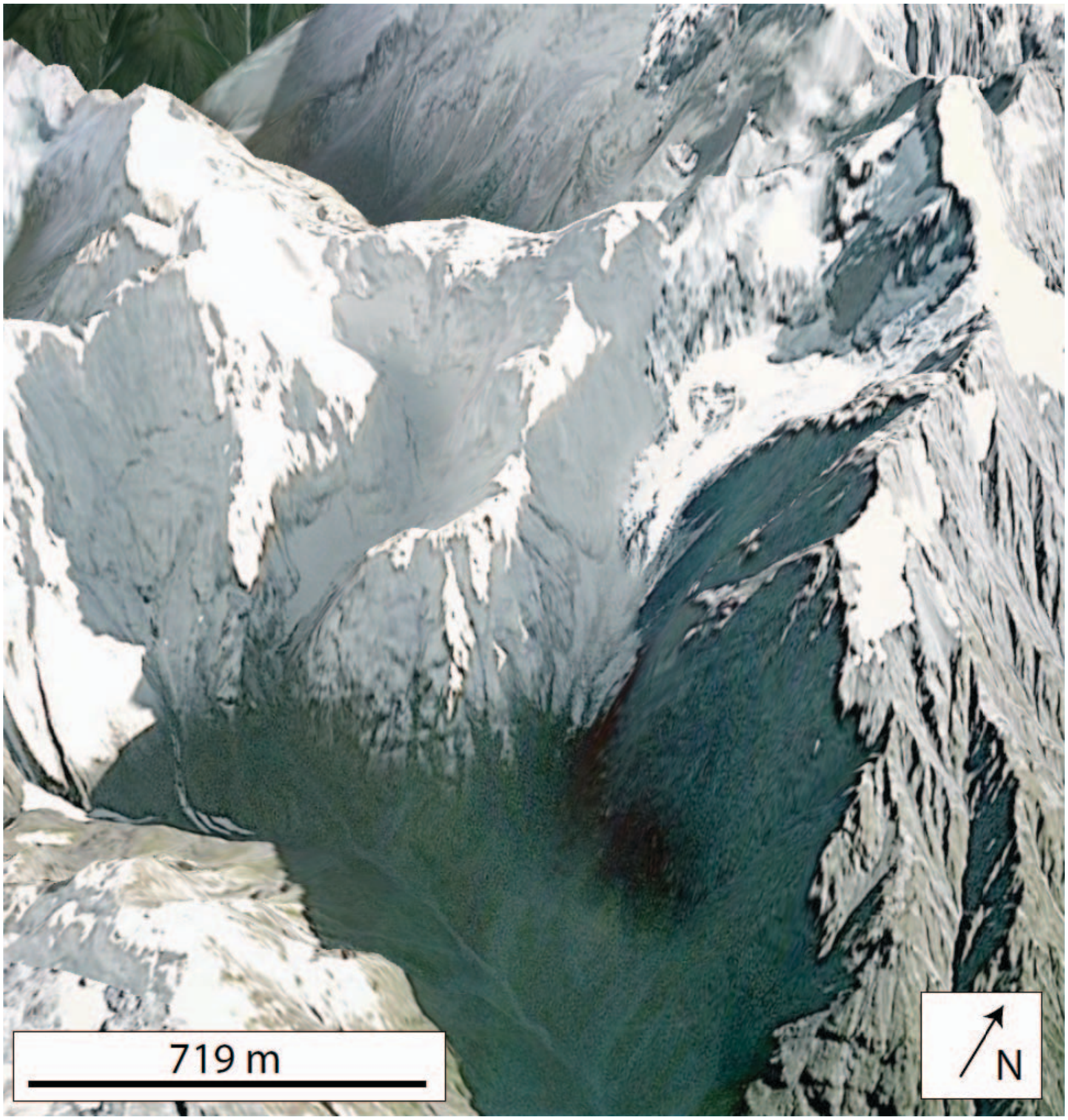


Figure 6.4: Google Earth image from the Two Thumb Range of a basin classified as high glacial. Cirques, horns, and arêtes can be seen in the landscape (43°24’09.96” S and 170° 38’52.38” E. **Google Earth**. Oct 23, 2002 – Nov 9, 2010. June 8, 2012.).

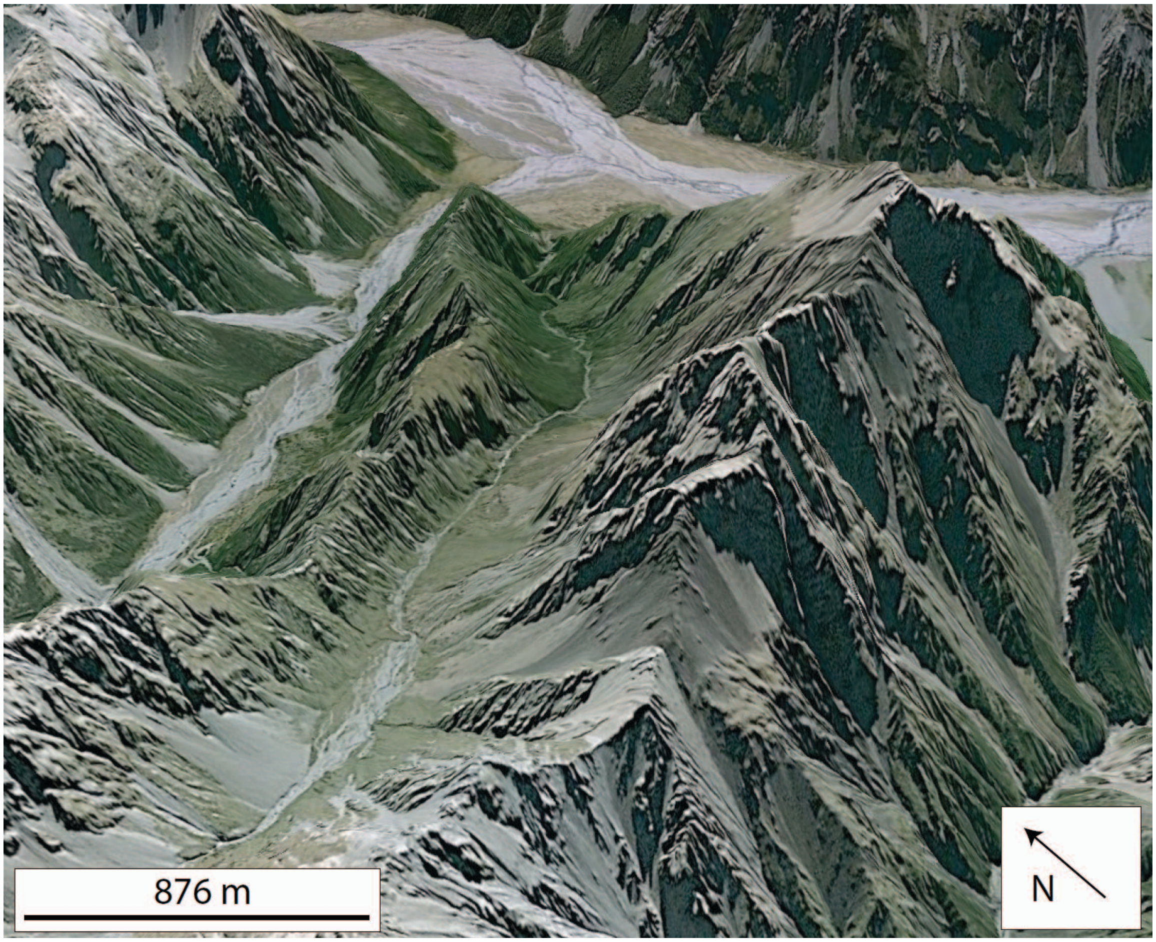


Figure 6.5: Google Earth image from the Two Thumb Range of a basin classified as high glacial. U-shaped valleys, steep slopes, and arêtes can be seen in the landscape (43°28’54.95” S and 170° 39’21.06” E. **Google Earth**. Apr 1, 2007 – Jan 18, 2008. June 8, 2012.).

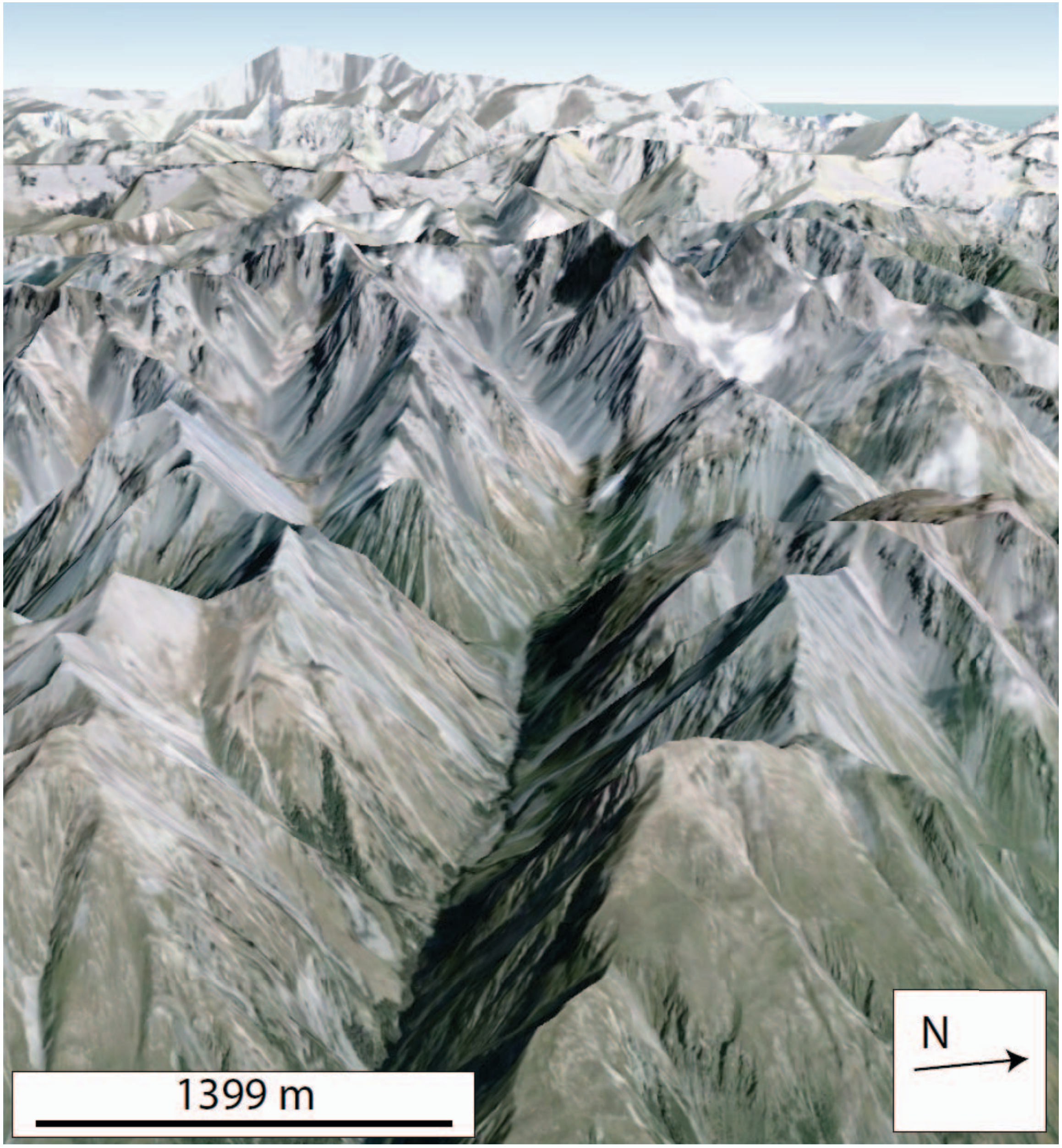


Figure 6.6: Google Earth image of a basin classified as mid glacial. This basin exhibits steep slopes and arêtes, but lacks cirques and flat valley bottoms (43°34'49.62" S and 170° 46'58.21" E. **Google Earth**. Feb 21, 2003 – Apr 15, 2010. June 8, 2012.).

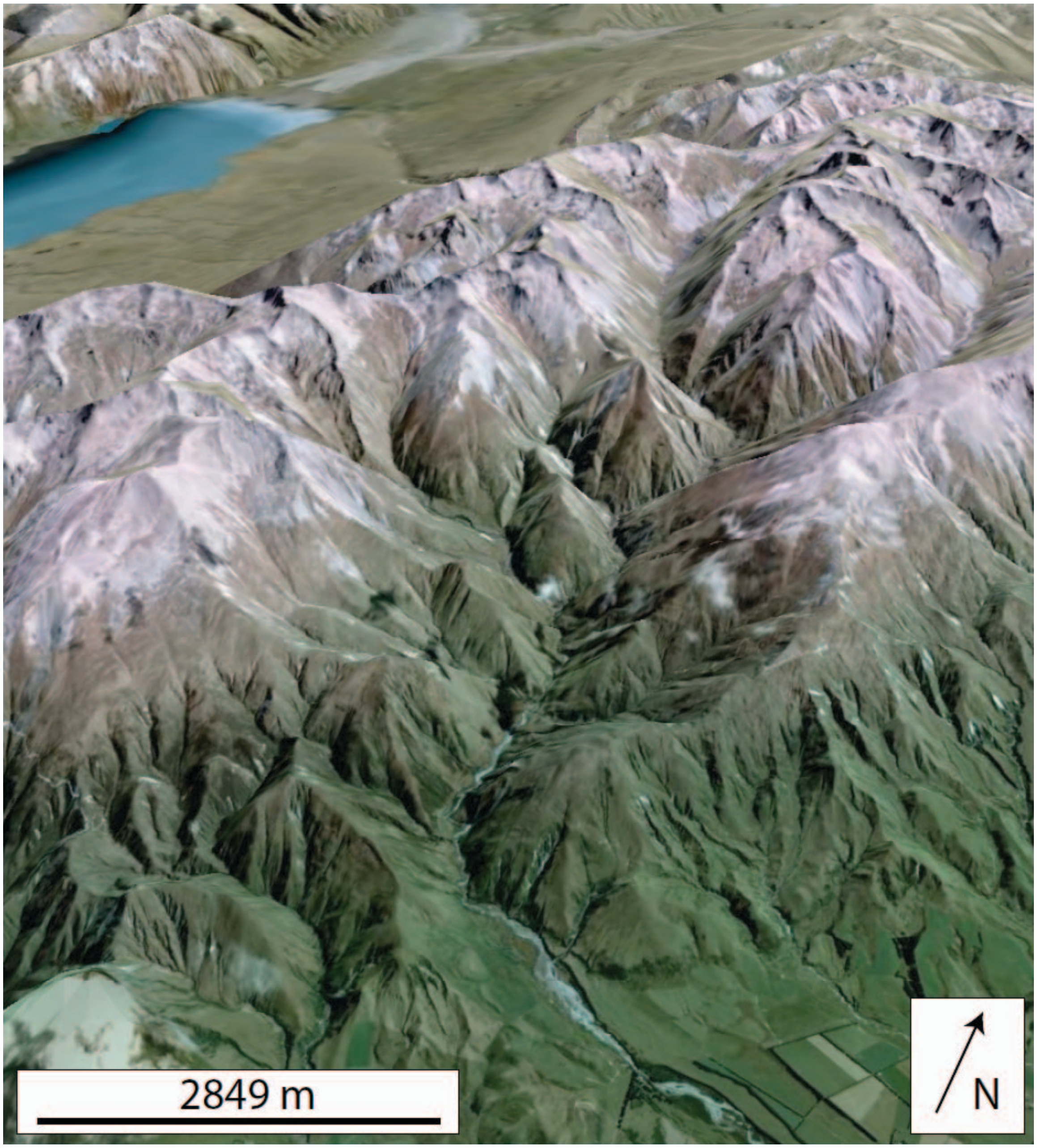


Figure 6.7: Google Earth image of basin 14, classified as mid glacial. Visual evidence shows a dendritic stream pattern and V-shaped cross-sectional geometry, consistent with fluvial basins (43°55'42.48" S and 170° 42'48.80" E. **Google Earth**. Mar 11, 2006 – Feb 26, 2011. June 8, 2012.).

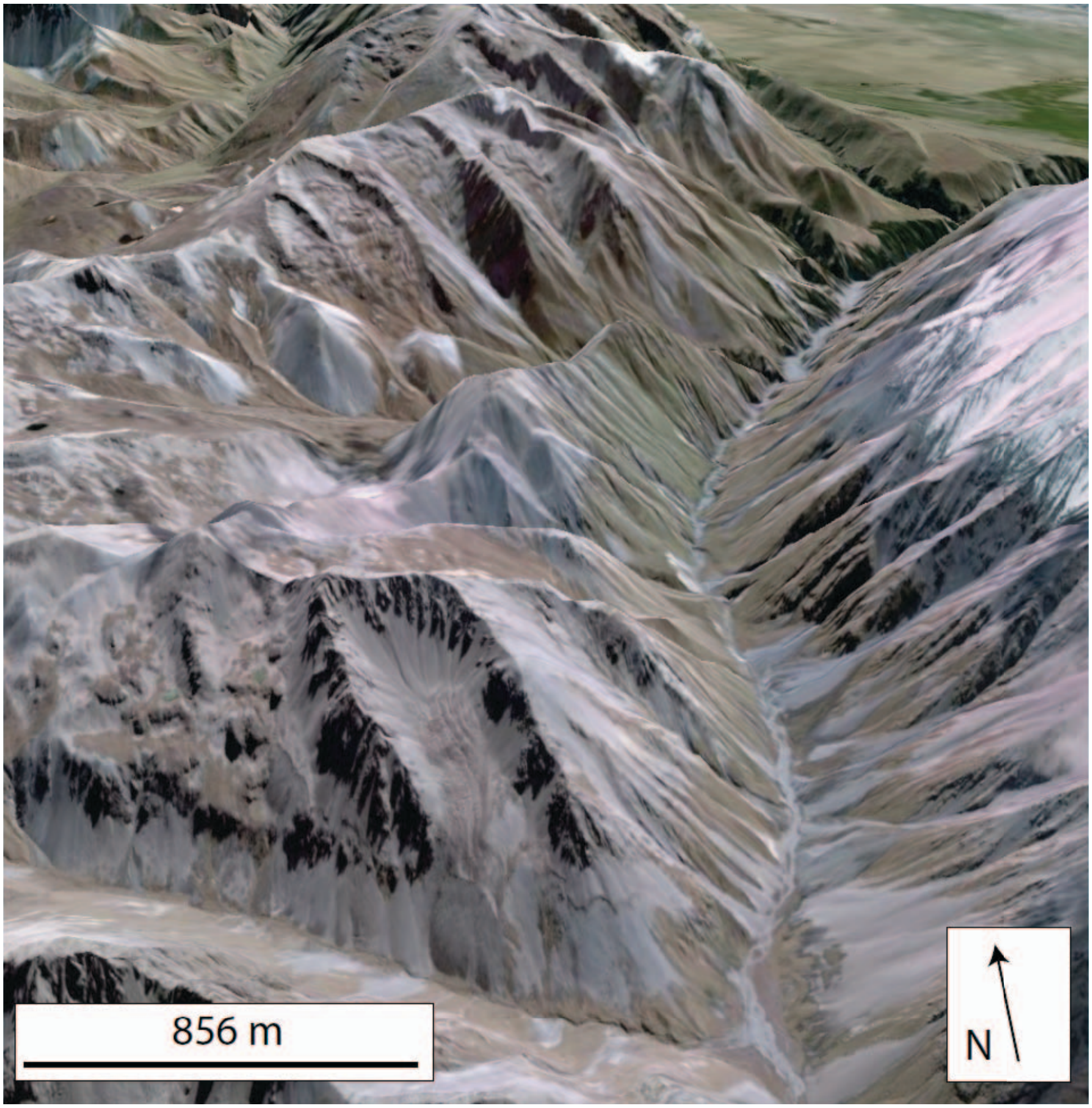


Figure 6.8: Google Earth image of a basin classified as low glacial. This basin exhibits dendritic, V-shaped stream valleys indicative of fluvial erosion, but also a few arêtes, which suggest some glacial modification (43°46’52.79” S and 170° 46’12.63” E. **Google Earth**. Feb 26, 2006 – Jan 18, 2008. June 8, 2012.).

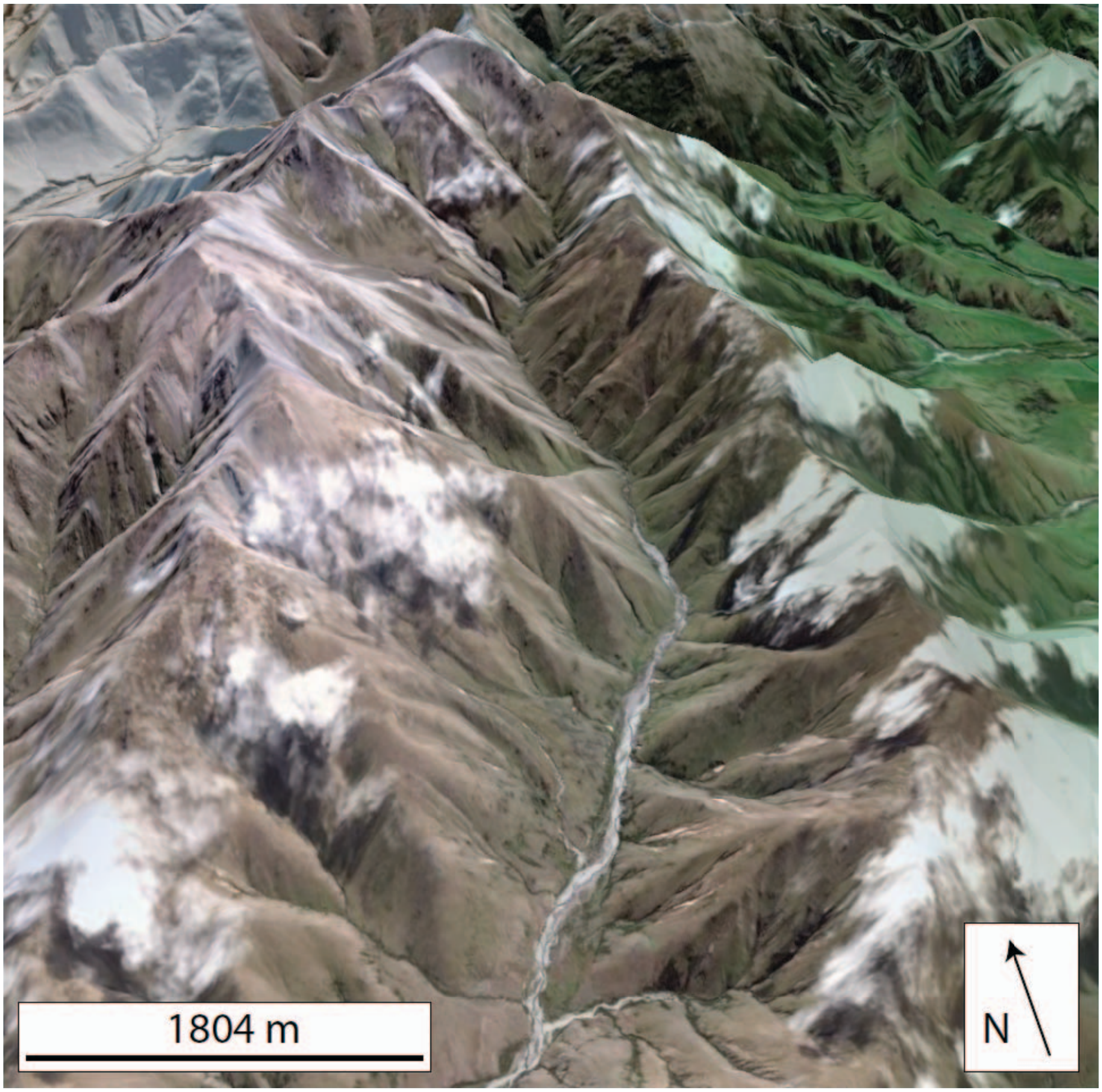


Figure 6.9: Google Earth image of a basin classified as fluvial. This basin exhibits gentle slopes with convex peaks, dendritic pattern, and V-shaped cross-section, consistent with fluvial erosion (44°01'42.12" S and 170° 36'53.01" E. **Google Earth**. Mar 11, 2006 – Feb 26, 2011. June 8, 2012.).

CHAPTER VII

# CONCLUSIONS

In mountainous areas, analysis of slope, and slope vs. elevation can be used to assess the degree of past glaciation across a landscape.

Our results show that when compared to fluvial basins, glaciated basins exhibit landforms such as cirques, arêtes, and U-shaped valleys that result in higher maximum slope values, higher frequency of slopes with low values, and higher slope values in upper elevations, and relatively low slope values in low elevations.

Results show that drainage basins with increasing glacial influence yield:

- Higher maximum slope values at high elevations
- Higher standard deviation of slope values
- Higher proportion of 0° slope values at low elevations
- Lower peak frequency of slope values
- Increasing slope values above 50°
- Range of values greater than 45° at 0.01 frequency

Slope frequency distribution plots and slope vs. elevation plots are particularly effective at determining the degree of glaciation in a landscape. In slope frequency plots, fully glaciated basins exhibit a range of slope values greater than 45° at 0.01 frequency, a significant proportion of slope values above 50°, and a peak frequency below 0.06 proportion. In slope vs. elevation plots, fully glaciated basins exhibit mean slope values greater than 30°, maximum slope values above 80% elevation, and a range of slope values greater than 20°.

## REFERENCES


Amerson, B., Montgomery, D., and Meyer, G., 2008, Relative size of fluvial and glaciated valleys in central Idaho. *Geomorphology* **93**: 537-547.

Augustinus, P. C., 1992, The influence of rock mass strength on glacial valley cross-profile morphometry: A case study from the Southern Alps, New Zealand. *Earth Surface Processes and Landforms* **17**: 39-51.

Average Annual Precipitation: Idaho. Map by Spatial Climate Analysis Service (http://www.ocs.orst.edu/prism), Oregon State University, 2000: http://www.worldatlas.com/webimage/countrys/namerica/usstates/weathermaps/idprecip.htm (accessed April 2012)

Average Annual Precipitation in Washington State. Map courtesy of www.wamaps.com: http://content.lib.washington.edu/cmpweb/resources/map-rainfall.html (accessed April 2012)

Brandon, M. T., Roden-Tice, M. K., and Garver, J. I., 1998, Late Cenozoic exhumation of the Cascadia accretionary wedge in the Olympic Mountains, northwest Washington State. *GSA Bulletin* **110**: 985-1009.

Brocklehurst, S., and Whipple, K., 2002, Glacial erosion and relief production in the Eastern Sierra Nevada, California. *Geomorphology* **42**: 1-24.

Brocklehurst, S., and Whipple, K., 2004, Hypsometry of glaciated landscapes. *Earth Surface Process and Landforms* **29**: 907-926.

Brocklehurst, S., and Whipple, K., 2006, Assessing the relative efficiency of fluvial and glacial erosion through simulation of fluvial landscapes. *Geomorphology* **75**: 283-299.

Brook, M., Kirkbride, M., and Brock, B., 2008, Temporal constraints on glacial valley cross-profile evolution: Two Thumb Range, central Southern Alps, New Zealand. *Geomorphology* **97**: 24-34.

Brozovic, N., Burbank, D. W., and Meigs, A. J., 1997, Climatic limits on landscape development in the Northwest Himalaya. *Science* **276**: 571-574.

ESRI, 2011, ArcGIS Desktop: Release 10. Redlands, CA: Environmental Systems Research Institute.

Foster, D., Brocklehurst, S., and Gawthorpe, R. L., 2008, Small valley glaciers and the effectiveness of the glacial buzzsaw in the northern Basin and Range, USA. *Geomorphology* **102**: 624-639.

Hicks, D. M., McSaveney, M. J., and Chinn, T. J. H.,1990, Sedimentation in proglacial Ivory Lake, southern Alps, New Zealand: *Arctic and Alpine Research* **22**: 26-42.

Huerta A. D., 2007, Byrd drainage system: evidence of a Mesozoic West Antarctic Plateau, in Antarctica: A Keystone in a changing World - Online Proceedings of the 10th ISAES X, edited by A.K. Cooper and C.R. Raymond *et al*., USGS Open-File Report 2007-1047, Extended Abstract 091.

Hyndman, D.W., 1983, The Idaho batholith and associated plutons, Idaho and western Montana, in, Roddick, J.A. (ed.), Circum-Pacific Plutonic Terranes, vol. 159. Geological Society of America Memoir, Boulder, Colorado; 213-240.

Katsube, K., and Oguchi, T., 1999, Altitudinal changes in slope angle and profile curvature in the Japan Alps: A hypothesis bearing on a characteristic slope angle: CSIS Discussion Paper, v. 16.

Kirkbride, M., and Matthews, D., 1997, The role of fluvial and glacial erosion in landscape evolution: the Ben Ohau Range, New Zealand. *Earth Surface Processes and Landforms* **22**: 317-327.

MacGregor, K. R., Anderson, R. S., Anderson, S. P., and Waddington, E. D., 2000, Numerical simulations of glacial-valley longitudinal profile evolution. *Geology* **28**: 1031-1034.

Mathworks Inc., 2010. MATLAB: version 7.10.0. Natick, Massachusetts: The MathWorks Inc.

McGowan, H. A., and Sturman, A. P., 1997, Characteristics of aeolian grain transport over a fluvio-glacial lacustrine braid delta, Lake Tekapo, New Zealand. *Earth Surface Processes and Landforms* **22**: 773-784.

Meyer, G. A., Fawcett, P. J., and Locke, W W., 2004. Late-Pleistocene equilibrium-line altitudes, atmospheric circulation, and timing of mountain glacier advances in the interior northwestern United States, in, Haller, K. M., and Wood, S. H. (Eds), *Geological Field Trips in Southern Idaho, Eastern Oregon, and Northern Nevada*. U.S. Geological Survey Open-File Report, Reston, VA; 64-67.

Mitchell, S., and Montgomery, D., 2006, Influence of a glacial buzzsaw on the height and morphology of the Cascade Range in central Washington State, USA. *Quaternary Research* **65**: 96-107.

Montgomery, D. R., 2002, Valley formation by fluvial and glacial erosion. *Geology* **30**: 1047-1050.

Naylor, S., and Gabet, E. J., 2007, Valley asymmetry and glacial versus nonglacial erosion in the Bitterroot Range, Montana, USA. *Geology* **35**: 375-378.

Oskin, M., and Burbank, D.W., 2005. Alpine landscape evolution dominated by cirque retreat. *Geology* **33**: 933-936.

Pelletier, J. D., 2004, Estimate of three-dimensional flexural-isostatic response to unloading: Rock uplift due to late Cenozoic glacial erosion in the western United States. *Geology* **32**: 161-164.

Schuster, R. L., Logan, R. L., Pringle, P. T., 1992, Prehistoric rock avalanches in the Olympic Mountains, Washington. *Science* **258**: 1620-1621.

Stanford, L. R., 1982. Glacial geology of the upper South Fork, Payette River, south-central Idaho. Master's Thesis, University of Idaho, Moscow, ID; 83 p.

Sternai, P., Herman, F., Fox, M. R., and Castelltort, S., 2011, Hypsometric analysis to identify spatially variable glacial erosion. *Journal of Geophysical Research* **116**: F03001, doi:10.1029/2010JF001823.

Stroeven, A. P., Hättestrand, C., Heyman, J., Harbor, J., Li, Y. K., Zhou, L. P., Caffee, M. W., Alexanderson, H., Kleman, J., Ma, H. Z., and Liu, G. N., 2009, Landscape analysis of the Huang He headwaters, NE Tibetan Plateau — Patterns of glacial and fluvial erosion. *Geomorphology* **103**: 212-226.

Tabor, R. W., and Cady, W. M., 1978, The structure of the Olympic Mountains, Washington - Analysis of a subduction zone: U.S. Geological Survey Professional Paper 1033; 38 p.

Thackray G. D., Lundeen, K. A., Borgert, J. A., 2004. Latest Pleistocene alpine glacier advances in the Sawtooth Mountains, Idaho, USA: reflections of midlatitude moisture transport at the close of the last glaciation. *Geology* **32**: 225-228.

Tippett, J. M., and Kamp, P. J., 1995, Quantitative relationships between uplift and relief parameters for the Southern Alps, New Zealand, as determined by fission track analysis. *Earth Surface Processes and Landforms* **20**: 153-175.

Upton, P., Craw, D., James, Z., Koons, P. O., 2004, Structure and late Cenozoic tectonics of the southern Two Thumb Range, mid Canterbury, New Zealand. *New Zealand Journal of Geology and Geophysics* **47**: 141-153.

# APPENDIXES

## Appendix A

### Results: Sawtooth Range, Idaho

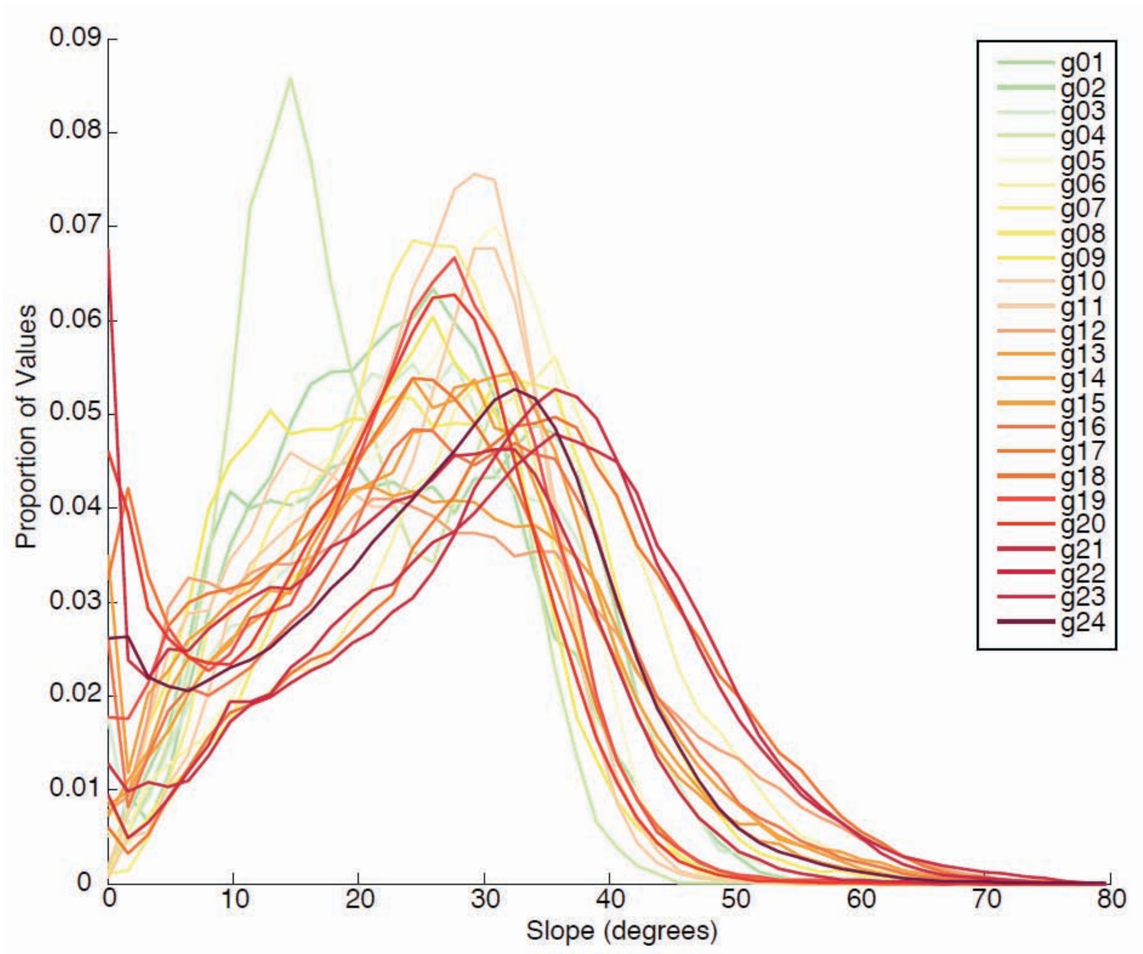


Figure A1: Slope frequency distribution curves for all glacial basins, Sawtooth Range, Idaho

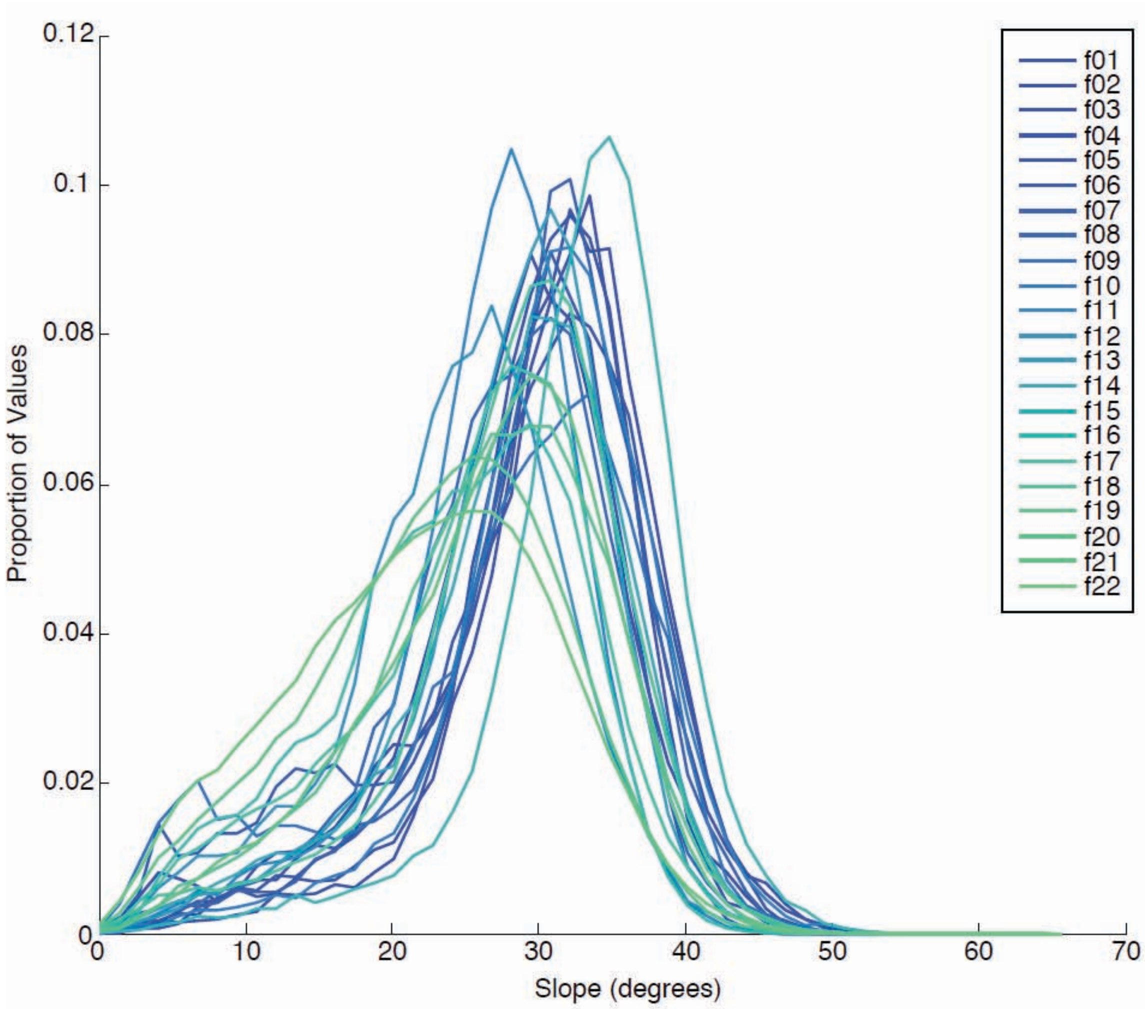


Figure A2: Slope frequency distribution curves for all fluvial basins, Sawtooth Range, Idaho

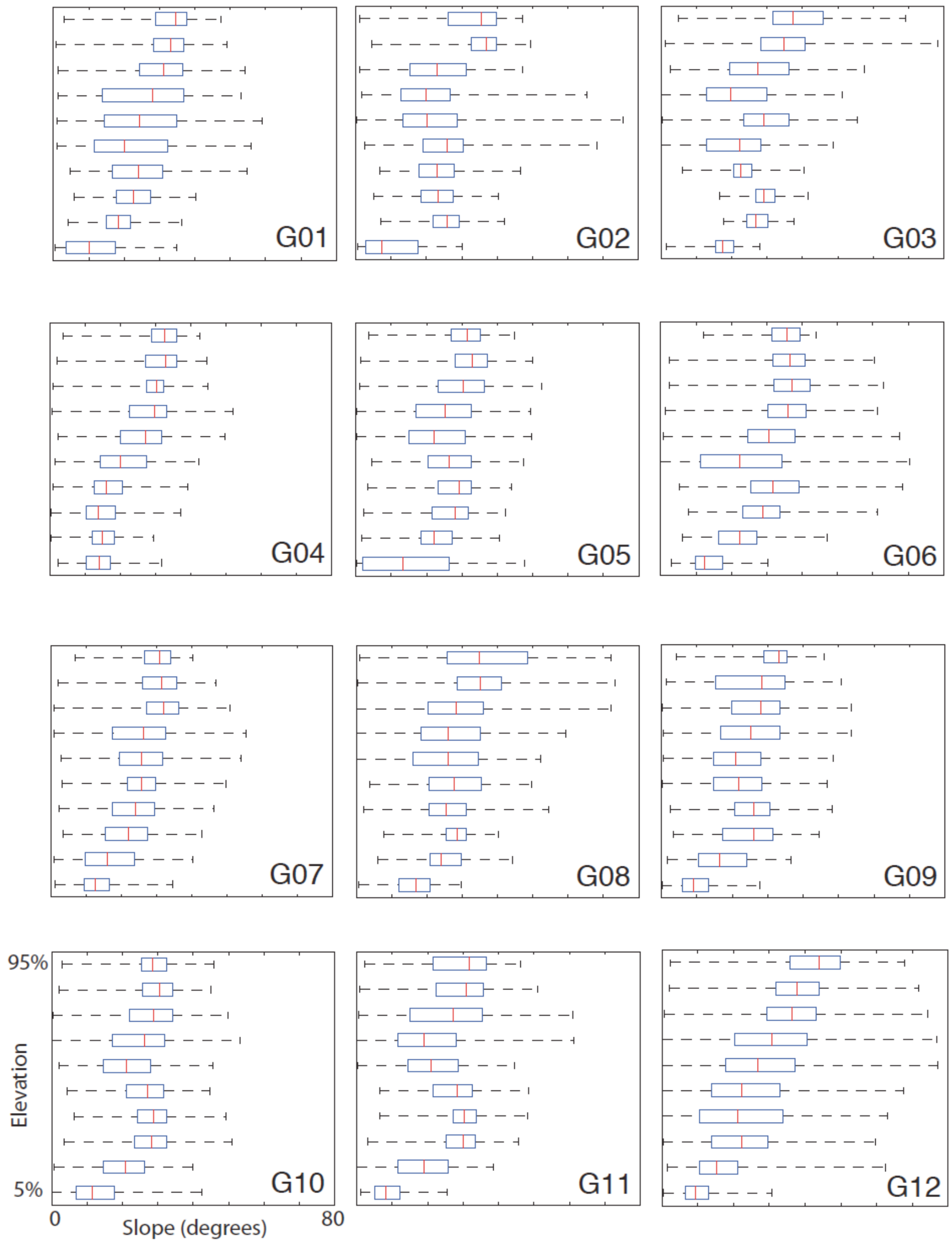


Figure A3: Slope vs. elevation plots for glacial basins G01 - G12, Sawtooth Range, Idaho

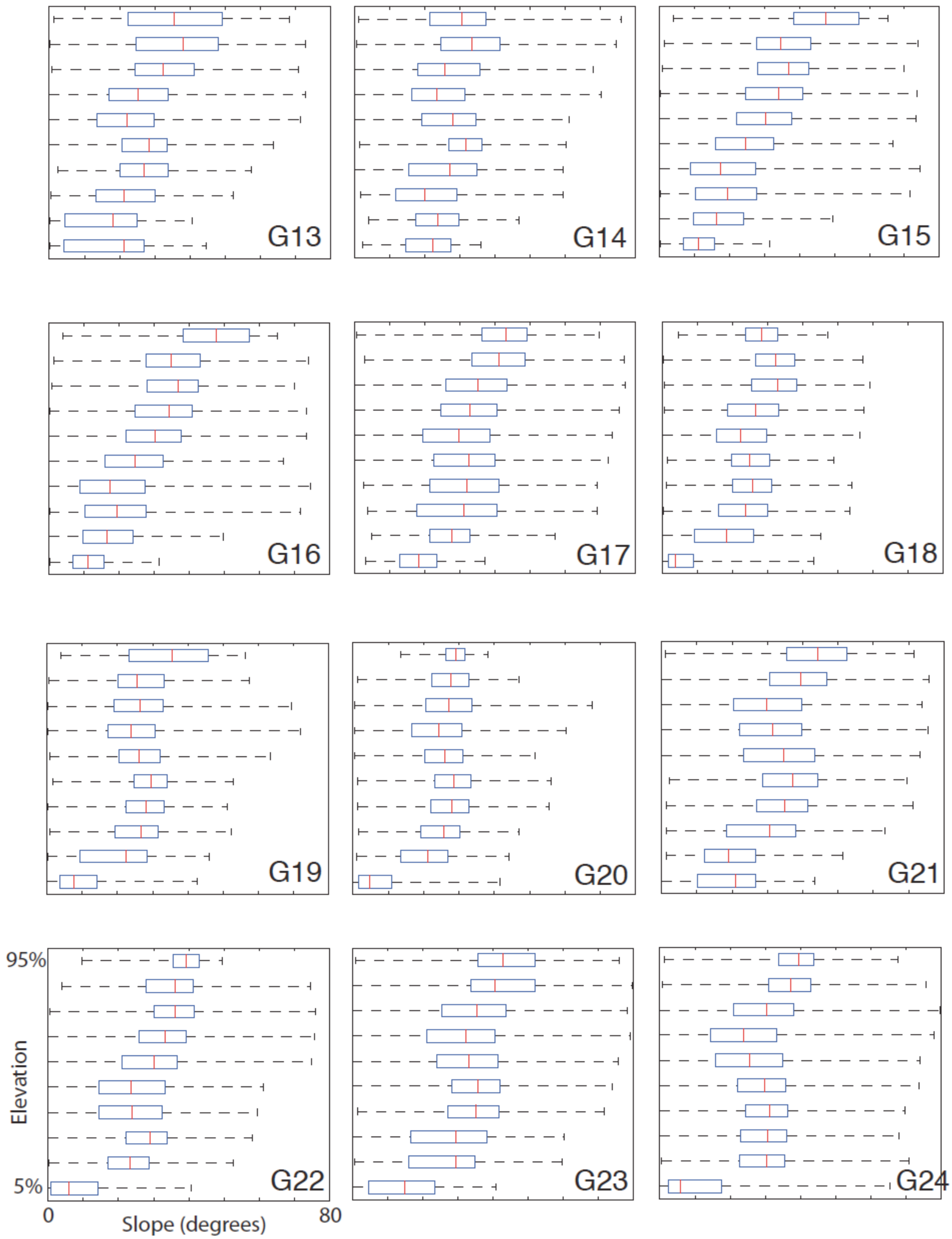


Figure A4: Slope vs. elevation plots for glacial basins G13 – G24, Sawtooth Range, Idaho


Figure A5: Slope vs. elevation plots for fluvial basins F01 – F12, Sawtooth Range, Idaho

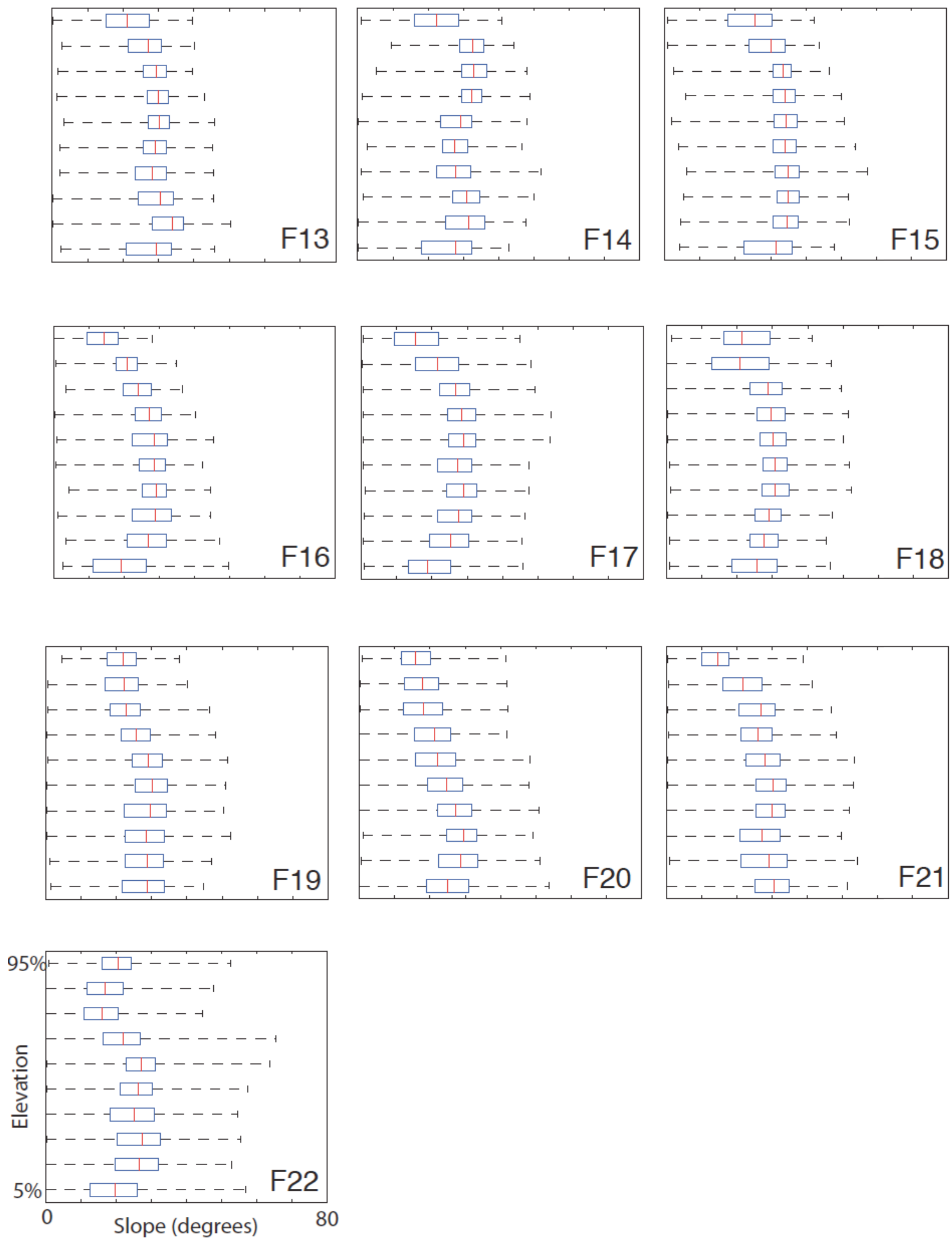


Figure A6: Slope vs. elevation plots for fluvial basins F13 – F22, Sawtooth Range, Idaho

# Appendix B

## Results: Olympic Mountains, Washington

Table B1: Slope Values for the Olympic Mountains, Washington

| Olympic Mountains, Washington: Slope Values | | | | | | |
|---|---|---|---|---|---|---|
| Erosion Type | Min | Max | Mean | Mode | Median | Std Dev |
| Glacial | 0 | 82.50 | 27.95 | 32.17 | 29.68 | 13.894 |
| Transitional | 0 | 78.29 | 28.76 | 32.10 | 29.98 | 10.723 |
| Fluvial | 0 | 72.39 | 26.36 | 29.68 | 26.89 | 9.612 |

Table B2: Planform Curvature Values for the Olympic Mountains, Washington

| Olympic Mountains, Washington: Planform Curvature Values | | | | | | |
|---|---|---|---|---|---|---|
| Erosion Type | Min | Max | Mean | Mode | Median | Std Dev |
| Glacial | -79.4 | 96.5 | 0.0232 | -0.255 | 0.058 | 1.534 |
| Transitional | -47.7 | 72.0 | 0.0189 | -1.037 | 0.066 | 1.190 |
| Fluvial | -23.9 | 23.1 | 0.0185 | 0.076 | 0.103 | 1.369 |

Table B3: Profile Curvature Values for the Olympic Mountains, Washington

| Olympic Mountains, Washington: Profile Curvature Values | | | | | | |
|---|---|---|---|---|---|---|
| Erosion Type | Min | Max | Mean | Mode | Median | Std Dev |
| Glacial | -102.7 | 93.5 | 0.0230 | 1.301 | 0.0039 | 1.971 |
| Transitional | -86.0 | 85.8 | 0.0189 | 1.627 | -0.0020 | 1.697 |
| Fluvial | -42.2 | 33.4 | 0.0185 | -0.642 | -0.0163 | 1.625 |

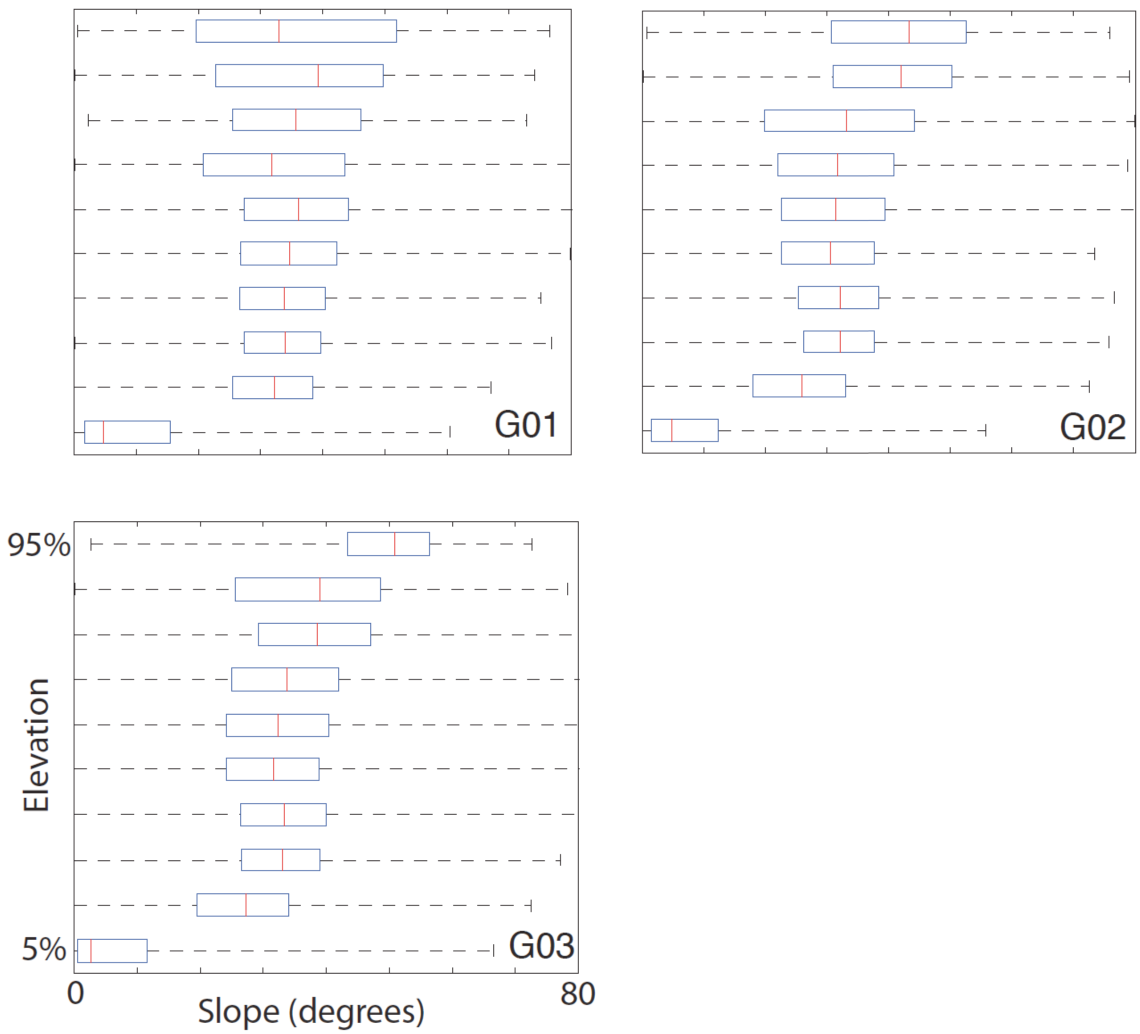


Figure B1: Slope vs. elevation plots for glacial basins, Olympic Mountains, Washington

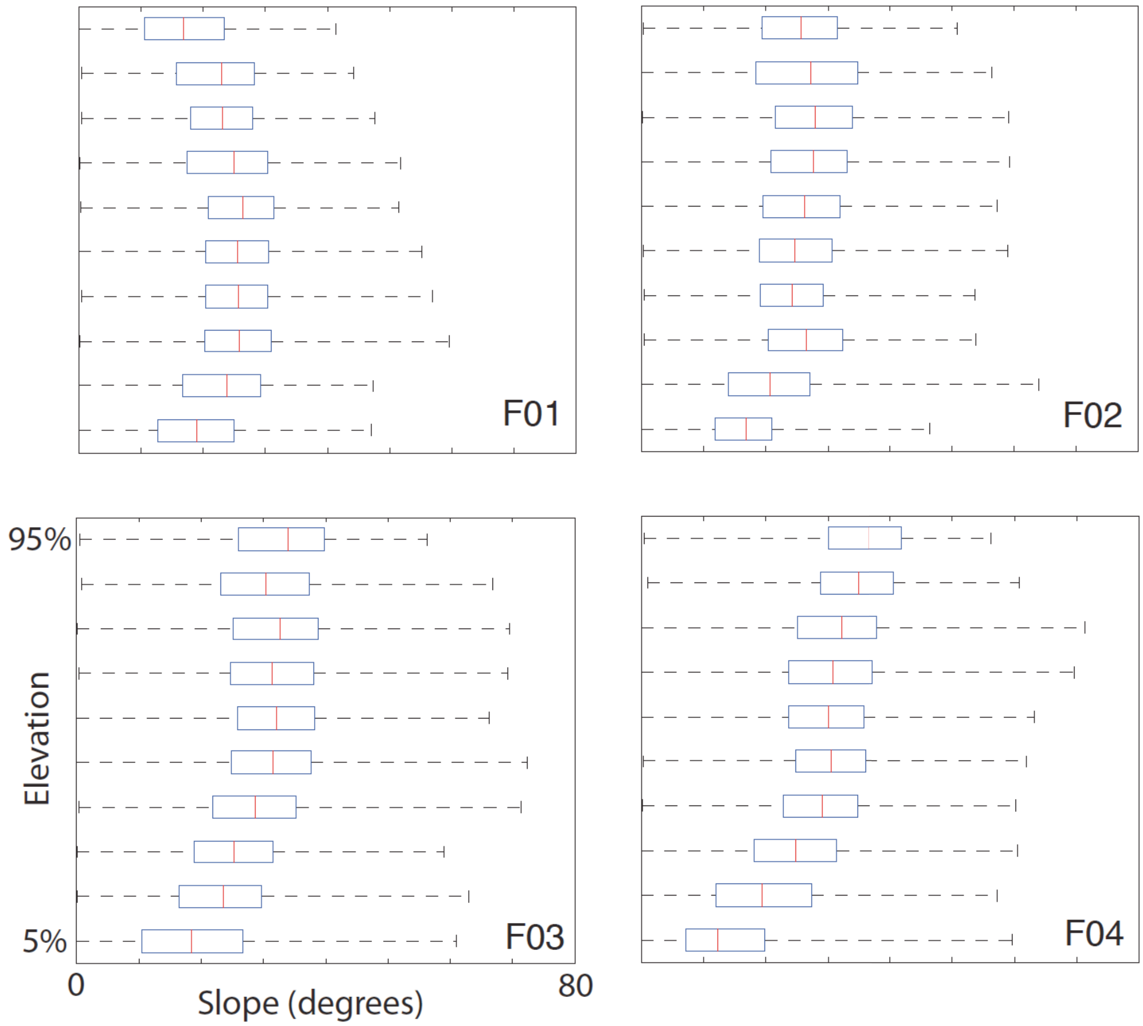


Figure B2: Slope vs. elevation plots for fluvial basins, Olympic Mountains, Washington

# Appendix C

## Results: Two Thumb Range, New Zealand

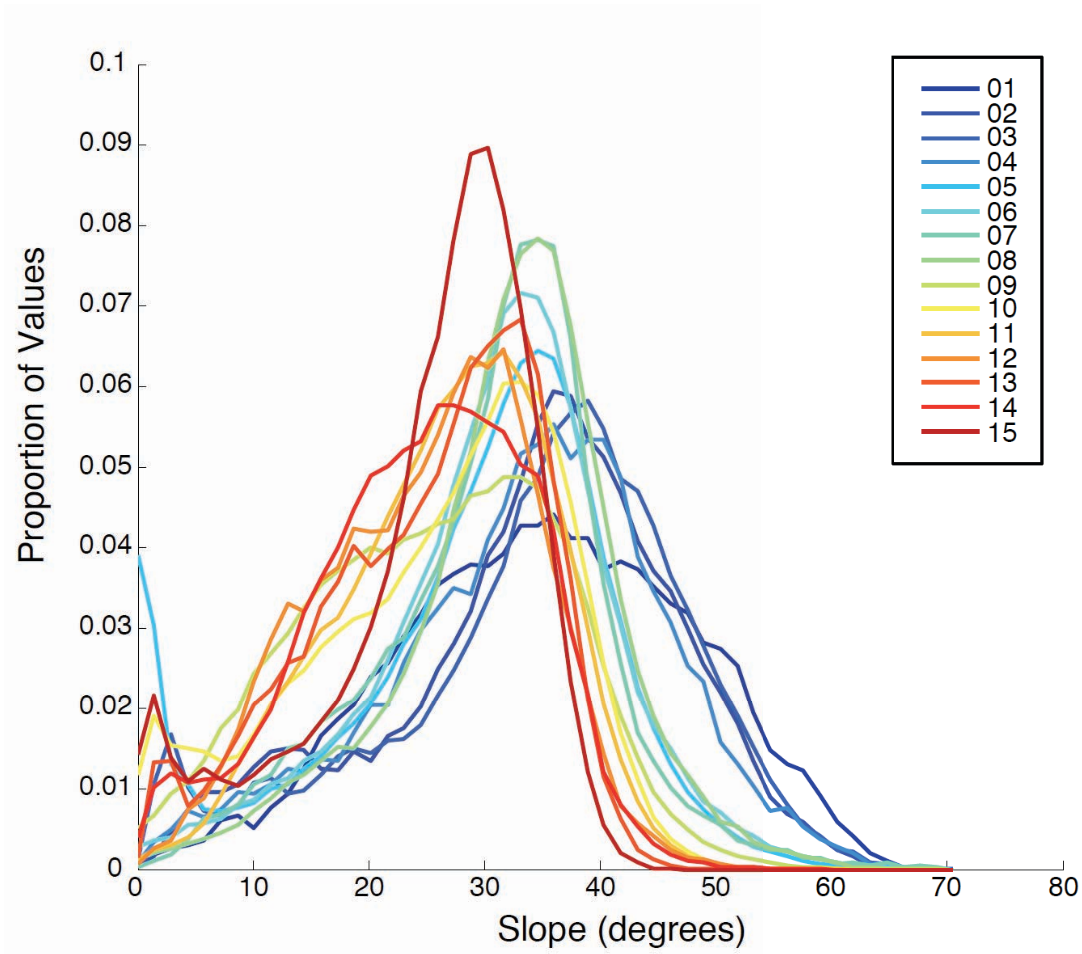


Figure C1: Slope frequency distribution curves in the Two Thumb Range, New Zealand. Basins are numbered with 01 being the northernmost (most glaciated) basin, and 15 being the southernmost (least glaciated) basin (Brook *et al*., 2008).

Table C1: Slope Values for the Two Thumb Range, New Zealand

| Two Thumb Range, NZ: Slope Results | | | | | | |
|---|---|---|---|---|---|---|
| Basin | Min | Max | Mean | Mode | Median | Std Dev |
| 1 | 0.4370 | 66.0 | 35.1 | 35.98 | 35.35 | 12.32 |
| 2 | 0.2931 | 67.2 | 34.2 | 35.98 | 35.80 | 12.02 |
| 3 | 0.4459 | 70.5 | 34.5 | 38.80 | 36.62 | 12.71 |
| 4 | 0.1185 | 64.8 | 33.6 | 35.98 | 34.82 | 11.63 |
| 5 | 0 | 64.6 | 28.6 | 34.57 | 31.37 | 12.38 |
| 6 | 0 | 68.3 | 31.0 | 33.16 | 32.13 | 9.99 |
| 7 | 0.7805 | 68.4 | 30.8 | 34.57 | 32.18 | 9.67 |
| 8 | 0 | 68.3 | 32.1 | 34.57 | 33.15 | 9.34 |
| 9 | 0 | 68.1 | 25.7 | 33.16 | 26.41 | 10.77 |
| 10 | 0 | 58.8 | 25.9 | 33.16 | 27.96 | 10.78 |
| 11 | 0 | 59.9 | 26.8 | 31.74 | 27.74 | 8.86 |
| 12 | 0.4420 | 56.6 | 25.3 | 31.74 | 26.32 | 9.07 |
| 13 | 0.1953 | 50.5 | 25.2 | 33.16 | 27.02 | 9.37 |
| 14 | 0.0716 | 58.5 | 24.8 | 26.10 | 25.60 | 9.33 |
| 15 | 0 | 46.5 | 25.3 | 30.33 | 27.66 | 9.18 |

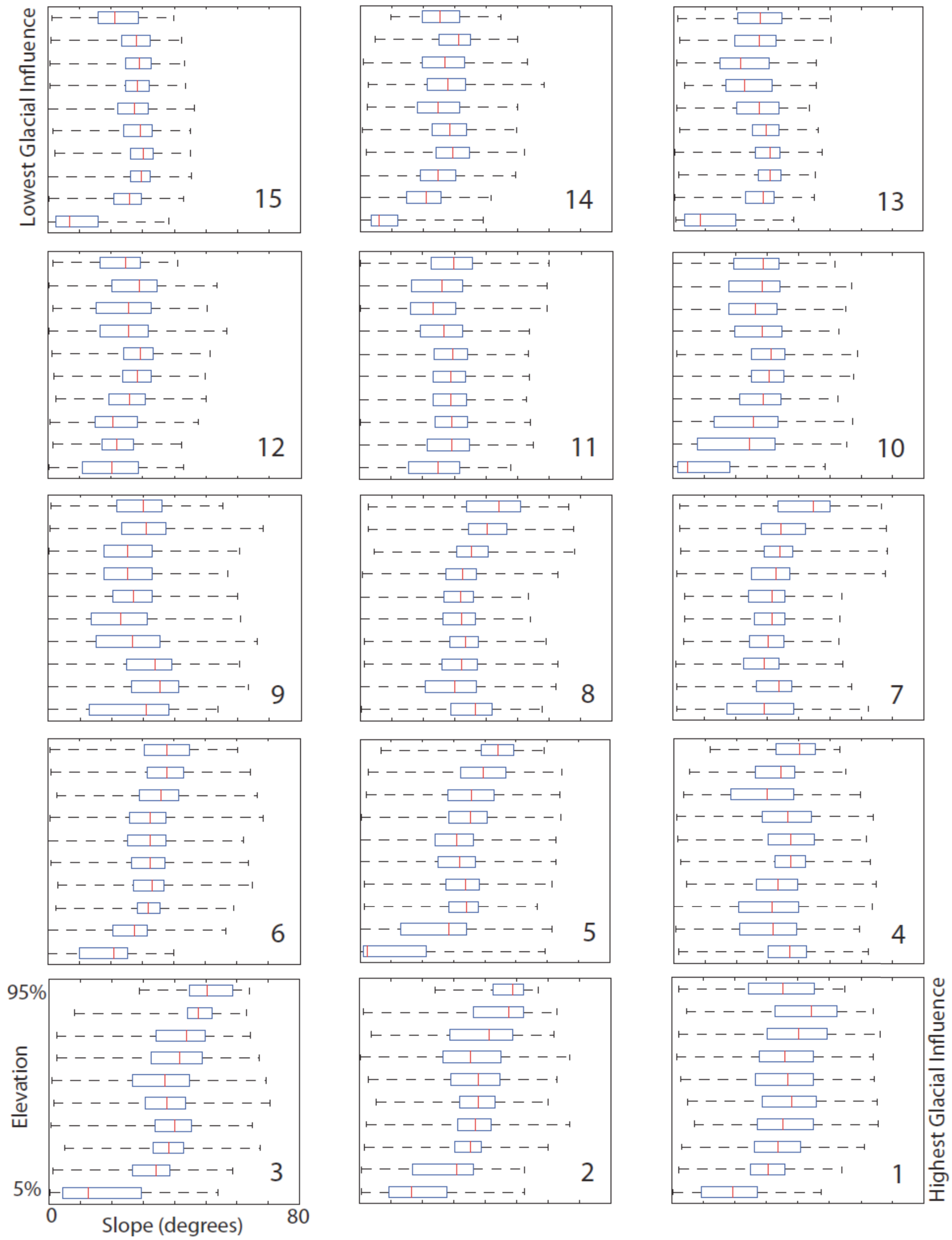


Figure C2: Slope vs. elevation plots for all 15 basins in the Two Thumb Range study area. Basins increase in glacial influence from upper left. Basin number is shown on bottom right of each plot. Slope vs. elevation results show increasing variation and stepped pattern with increasing glacial influence (Brook *et al.*, 2008).

Table C2: Planform Curvature Values for the Two Thumb Range, New Zealand

| Two Thumb Range, NZ: Planform Curvature Results | | | | | | |
|---|---|---|---|---|---|---|
| Basin | Min | Max | Mean | Mode | Median | Std Dev |
| 1 | -10.2 | 9.19 | 0.0261 | 0.085 | -0.0402 | 1.244 |
| 2 | -8.6 | 7.30 | 0.0325 | -0.160 | -0.0204 | 1.188 |
| 3 | -9.6 | 9.94 | 0.0248 | -0.027 | -0.0118 | 1.397 |
| 4 | -11.4 | 9.01 | 0.0289 | -0.179 | 0.0000 | 1.290 |
| 5 | -8.5 | 12.27 | 0.0191 | -0.006 | -0.0025 | 0.897 |
| 6 | -12.1 | 10.71 | 0.0234 | -0.027 | -0.0055 | 0.953 |
| 7 | -7.2 | 13.06 | 0.0243 | -0.106 | -0.0242 | 1.004 |
| 8 | -10.9 | 10.47 | 0.0243 | 0.013 | -0.0056 | 1.028 |
| 9 | -11.6 | 8.52 | 0.0184 | -0.143 | 0.0000 | 0.856 |
| 10 | -7.1 | 7.47 | 0.0100 | 0.045 | 0.0008 | 0.752 |
| 11 | -7.2 | 8.24 | 0.0129 | 0.057 | 0.0055 | 0.715 |
| 12 | -5.8 | 5.67 | 0.0105 | 0.034 | 0.0030 | 0.595 |
| 13 | -6.6 | 5.54 | 0.0134 | 0.086 | 0.0017 | 0.681 |
| 14 | -7.2 | 5.92 | 0.0089 | 0.001 | 0.0193 | 0.778 |
| 15 | -6.6 | 5.69 | 0.0074 | -0.067 | 0.0171 | 0.741 |

Table C3: Profile Curvature Values for the Two Thumb Range, New Zealand

| Two Thumb Range, NZ: Profile Curvature Results | | | | | | |
|---|---|---|---|---|---|---|
| Basin | Min | Max | Mean | Mode | Median | Std Dev |
| 1 | -8.78 | 8.87 | 0.0261 | 0.220 | 0.0703 | 1.227 |
| 2 | -12.00 | 7.64 | 0.0283 | -0.018 | 0.0715 | 1.089 |
| 3 | -10.04 | 9.17 | 0.0243 | 0.142 | 0.0499 | 1.136 |
| 4 | -6.63 | 11.04 | 0.0312 | -0.096 | 0.0593 | 1.148 |
| 5 | -8.91 | 6.52 | 0.0192 | -0.115 | 0.0175 | 0.850 |
| 6 | -12.71 | 7.84 | 0.0245 | 0.235 | 0.0525 | 0.928 |
| 7 | -8.98 | 7.63 | 0.0236 | 0.153 | 0.0508 | 0.952 |
| 8 | -13.01 | 8.98 | 0.0252 | -0.038 | 0.0485 | 1.004 |
| 9 | -9.15 | 11.50 | 0.0179 | 0.141 | 0.0201 | 0.826 |
| 10 | -8.54 | 8.49 | 0.0098 | 0.148 | 0.0097 | 0.774 |
| 11 | -6.67 | 6.42 | 0.0127 | 0.002 | 0.0118 | 0.714 |
| 12 | -7.07 | 4.95 | 0.0112 | 0.020 | 0.0211 | 0.668 |
| 13 | -4.79 | 4.57 | 0.0120 | -0.020 | 0.0114 | 0.637 |
| 14 | -6.09 | 7.79 | 0.0083 | -0.122 | -0.0061 | 0.721 |
| 15 | -5.05 | 5.13 | 0.0078 | -0.063 | 0.0036 | 0.591 |